Sudan University of science and Technology

College of graduate studies

Dynamic Buckling of Steel Alloy (drilling shaft) Under Different Conditions of Work Using Shot and Laser Peening Surface Treatments

الإلتواء الجانبي الديناميكي لسبائك الفولاذ (عمود الحفر) في ظل ظروف مختلفة للعمل بإستخدام المعالجة السطحية بالطلقات الكروية والليزر

A thesis submitted in partial fulfillment for the degree of
Ph.D. in petroleum engineering

By:

Ahmed M-Rachid Nakchbandi

Supervisor: Associate Professor

Cons. Eng. Dr: Ahmed Abdelaziz Ibrahim Elrayah

Co-Supervisors:

Professor Dr.: Hussain J. M. Al-Alkawi
Assistant Professor Dr.: Yousif Altahir Ahmed Bagadi

April 2021

DECLARATION

I hereby declare that the thesis based on my original work except for quotations and citations, which duly acknowledged. I also declare that it has not submitted previously or concurrently for any other degree at SUST or other institutions.

Signature: _____

Name   : Ahmed M-Rachid Nakchbandi

Date   : _____

الآيـــة

بسم الله الرحمن الرحيم

لَقَدْ أَرْسَلْنَا رُسُلَنَا بِٱلْبَيِّنَٰتِ وَأَنزَلْنَا مَعَهُمُ ٱلْكِتَٰبَ وَٱلْمِيزَانَ لِيَقُومَ ٱلنَّاسُ بِٱلْقِسْطِ وَأَنزَلْنَا ٱلْحَدِيدَ فِيهِ بَأْسٌ شَدِيدٌ وَمَنَٰفِعُ لِلنَّاسِ وَلِيَعْلَمَ ٱللَّهُ مَن يَنصُرُهُۥ وَرُسُلَهُۥ بِٱلْغَيْبِ إِنَّ ٱللَّهَ قَوِيٌّ عَزِيزٌ ﴿٢٥﴾

سورة الحديد : 25

ا

Dedication

Dear father

The Role models in my deal with the life, showing my problems, be patient on the bad time, tearing me my enjoying timer ... Give the person soho were allay teach me he can Hs for your soul.

 Dear mother

My angel, you always been with me in my bad times before the best, afraid for me, caring of me and loving me ... Hs for you.

My dear wife

Whoever inhabited my heart and shared happiness and sadness with me? Whoever pushes me forward always, to those who endure my absence and was my motivation for success … Hs for you.

Dear brothers and sisters

Who always be with me, helping me, give me some advices when I need it, corrected me when I make some mistakes ... Hs for you.

My dear children

Who have enlightened my life, who made me work, to be a role model … Hs for you.

Acknowledgment

Above all, I would like deeply to thank the Almighty, **ALLAH,** for his generosity and guidance, and without him I cannot even begin with this work. Secondly, I would like deeply to thank, beloved Prophet MUHAMMAD (peace be upon him and his family).

<div align="right">

Ahmed M-Rachid

2021

</div>

Abstract

The calculations of buckling loads are of great importance for industry. This thesis presents the description of experiments carried out on two specimen (columns) types of buckling namely, long and intermediate columns. These specimens are made from 304 stainless steel alloy which is used in many industrial applications. 32 specimens subjected to an increasing compressive load without shot peening (WSP) and with shot peening (SP).

The main objectives of the research to study the loads of columns without corrosion in oil field as well as study and evaluate the effect of corrosion. These investigated through studying the buckling behavior of solid column with fixed-pinned condition and evaluation the effect of corrosion time on the dynamic buckling behavior. The study used Euler Formula foe long columns, Johnson Formula for intermediate and short columns and Perry-Robertson as well for the three columns types.

In order to assess the critical failure an electrical Laser alarm was designed and built within the buckling test rig. At the instance when the specimen buckle reach to 1% of sample length, the electrical circuit operates immediately and the test rig stops. The buckling deflection is measured by digital dial gauge which is fixed on the side of test rig in contact within 0.7 of specimen length.

The results were obtained experimentally without any heat treatment for both cases, (without the use of shot peening (WSP) and when using the shot Peening (SP)). The results of practical experiments were compared with the theoretical formulas of Perry-Robertson, Euler and Johnson where these theories showed an overestimate of the critical flexural loads required the introduction of safety factor 1.3 and 3, respectively, to bring the experimental and theoretical results into good agreement.

The best improvement was achieved in the intermediate columns with a diameter of 10 mm and a thinness ratio of 112. Also Noticed the maximum reduction in overturning load was (28%) and (19.6%) for the long and medium columns respectively compared to the columns that have been eroded as a result of burial in the soil.

Of the desired importance, the study found the possibility of extending the life of the 304 stainless steel alloy used, which facilitates the operations inside the oil well and extends the life of the equipment used and also in a way that contributes to the economics of the various oil operations.

المستخلص

تعتبر حسابات أحمال الانثناء ذات أهمية كبيرة للصناعة ؛ تقدم هذه الرسالة وصفًا للتجارب التي تم إجراؤها على نوعين من العينات (أعمدة) من الالتواء ، وهما الأعمدة الطويلة والمتوسطة. هذه العينات مصنوعة من سبائك الفولاذ المقاوم للصدأ (304) والتي تستخدم في العديد من التطبيقات الصناعية. (32) عينة خضعت لحمل ضغط متزايد بدون ضربه بكرات الرصاص (WSP) وبضربه بكرات الرصاص (SP).

تتمثل الأهداف الرئيسية للبحث في دراسة أحمال الأعمدة الخالية من التآكل في المجال النفطي وكذلك دراسة وتقييم تأثير التآكل. تم الفحص والتقييم من خلال دراسة سلوك الانحناء للعمود الصلب بحالة مثبتة وتقييم وقت التآكل على سلوك الانحناء الديناميكي. إستخدمت الدراسة معادلات إيلر للأعمدة الطويلة ، ومعادلات جونسون للأعمدة المتوسطة والقصيرة ، ومعادلات بيري-روبرتسون أيضًا لأنواع الأعمدة الثلاثة.

من أجل تقييم نقطة الفشل الحرج ، تم تصميم وبناء إنذار كهربائي بالليزر داخل منصة اختبار الإنبعاج. ففي الحالة التي يصل فيها مشبك العينة إلى (1٪) من طول العينة ، تعمل الدائرة الكهربائية على الفور ويتوقف جهاز الإختبار. يتم قياس إنحراف الإلتواء بواسطة مقياس قرص رقمي يتم تثبيته على جانب جهاز الإختبار المتصل في حدود (0.7) من طول العينة.

تم الحصول على النتائج تجريبياً دون أي معالجة حرارية لكلتا الحالتين (بدون استخدام ضربة الرصاص (WSP) وعند استخدام الطلقة الرصاصية (SP) (Peening). تمت مقارنة نتائج التجارب العملية مع الصيغ النظرية لكل من إيلر وجونسون وبيري-روبرتسون حيث أظهرت هذه النظريات المبالغة في تقدير الأحمال الانحناء الحرجة التي معها تطلب إدخال عامل الأمان (1.3 و 3) على التوالي لتتوافق النتائج التجريبية والنظرية.

تم تحقيق أفضل تحسن في الأعمدة الوسيطة بقطر 10 مم ونسبة سُمك 112. كما لوحظ أن الحد الأقصى لخفض حمل الإنقلاب كان (28٪) و (19.6٪) للأعمدة الطويلة والمتوسطة على التوالي مقارنة بالأعمدة التي تآكلت نتيجة دفنها في التربة.

من الأهمية المرجوة ، وجدت الدراسة إمكانية إطالة عمر سبائك الفولاذ المقاوم للصدأ (304) المستخدمة مما يسهل العمليات داخل بئر النفط ويطيل عمر المعدات المستخدمة وأيضاً يساهم بشكل كبير في اقتصاديات العمليات النفطية المختلفة.

List of Contents

List of Tables

List of Figures

Symbols and Abbreviations

Symbol	Definition	Unit
σ_y	Yield stress	MPa
σ_u	Ultimate stress	MPa
$L_{eff.}$	Effective column length	mm
L_T	Total column length	mm
μm	Micron meter	-
D	Diameter of column	mm
E	Modulus of elasticity	GPa
G	Modulus of rigidity	GPa
AISI	American Iron & Steel Institute	-
δ_{in}	Initial column deflection	mm
$\delta_{cr.}$	Critical deflection	mm
P_{cr}	Critical buckling load	N
N_f	Number of machine cycles	Cycle

Chapter One

Introduction

Chapter One

Introduction

1.1 General

Calculating the stability of structures has always been an important engineering discipline. Especially the calculation of the critical buckling load of a structure which had been subject for many studies since Leonard Euler in 1744 who calculated the critical buckling load for a simply supported column. The buckling is a phenomenon, where a structure suddenly changes from one equilibrium configuration to another equilibrium configuration. The calculation of buckling loads of a structure is of great importance, due to the possibility of sudden failure of the structure, If the critical buckling load is reached. Some structures might lose stability, when the buckling load is reached, which could put operation at risk, if a roof or similar structure loses all stability (Charles E. Riley, 2003).

The current manufacturing industry emphasizes on the use of structural members, which encompass light weight with high strength and are expected to absorb high energy and carry heavy loads. These members are comprised of shell structures and shallow trusses. The shell structures have a significant advantage regarding load carrying capacity. When a load is applied to the sheath, various types of internal forces can cause any bending, torsion, transverse shear and torsion singly, jointly, or all of them (Mehmet Avcar, 2014).

One of the most important points in the design of structures and columns is to carry the maximum load endures structure or origin accurately approaching reality. This precision in the calculations rely heavily on mathematical model which is used in the analysis process and when this model is represented in the case of flexibility-plasticity, the accuracy will be the biggest in the analysis process. In structures exposed

to a single pregnancy, the accuracy can be obtained by following the traditional numerical methods to calculate the impact of a simplified plasticity. Generally, the structure or the column will fail because of when the subject material will be stressed up to its maximum limit and this is applicable to short length columns. The columns of long lengths will fail due to buckling and the buckling caused by this force is called Critical Pregnancy Load (CPL) which make this column fail abruptly. To represent this phenomenon of buckling a ruler of wood or plastic or thin rod of metal can be used and the shed force is gradually increased and then applied on a vertical column will cause it to bend. When this force removed the column will return back to the natural condition as long as the column did not reach to undergo phase, the column fail due to buckling when stress value is less than the value of yield stress of the same column. The purpose of calculating the value of buckling is to find out the value of the force or stress at which the column will be in the situation of instability and then buckling (Z. P. Bazat, 2000).

The critical buckling load is the upper limit of the allowed vertical frame loading. This load is defined by the frame configuration, cross-sections of the columns and horizontal beams as well as configuration and stiffness of the connections between them. In existing known nondestructive methods of determining the side sway frames critical load an implementation of vertical loading is technically difficult, that is especially essential at full-size tests (K. H. Al-Jubori, 2005).

As E. J. Barbero (2000) Columns are generally classified according to the type of stresses developed within the column at the time of failure, long slender columns will become unstable when the compressive stress remains elastic. The failure that occurs is referred to elastic instability. Intermediate columns fail due to inelastic instability, meaning that the compressive stress causing failure is greater than the materials proportional limit.

However, short columns sometimes called posts, do not become unstable, rather the material simply yields or fractures.

Now, it is not trivial to develop a solution that accounts for the axial loading which it is applied and distributed evenly over the cross-section of the beam or column tip. Finite element models are built for this reason and investigated to examine the buckling mode of the beam or column under a concentrated load at the exact center of the beam or column cross-section (Mott Robert L., 1996).

When the column is subjected to compressive loading, the column would start at a state of balance. Critical load is the maximum compressive load that the column can take before reaching unstable equilibrium. Any further increase in loading would result in catastrophic failure. Critical load for long and intermediate columns occurs below the elastic limits (Amir Javiddinejad, 2012).

The current study will follow the W. H. Duan (2008) to verify the miniature mechanical testing for stainless steel type 304 which is used in all commercial, industrial and domestic fields because of its good heat resisting properties and corrosion. Some applications include tanks and containers for a large variety of liquids and solids process equipment used in mines, cryogenic, chemical, food, dairy and pharmaceutical industries and drilling operations will be included.

Structure or members that carry compressive loads can be divided into two types depending on their prorated lengths and cross-sectional dimension i-e long columns and intermediate columns. When a structure is designed, it must satisfy specific length, stability, and deflection requirement. However, some structures exposed to compressive loads, and if these structures are long the loading may cause a lateral deflection for the member.

1.2 Surface treatment

Peening is broadly used to reduce or eliminate fatigue or stress corrosion cracking (SCC) within industry, with many new techniques being trialed to be competitive with currently used techniques.

They are compared in respect to a techniques cost, ease of use, surface finish, levels of plastic work, compressive residual stress intensity and depth of compressive residual stress introduced into a material. Most common peening techniques currently used in industry are shot peening and laser shock peening, both with different advantages and disadvantages.

Shot peening is most commonly used due to its low cost, however; laser peening overshadows SP with a superior surface finish, intensity of surface compressive residual stress and depth of compressive residual stress.

There are several new peening techniques, which may also be competitive with currently used techniques. At this stage in the progress of peening techniques available, it seems a comparison of current and new techniques should be made. One peening technique which has been explored, is ultrasonic impact treatment ((Charles E. Riley, 2003 and Mehmet Avcar, 2014)); however, there are sparse results on 304 austenitic stainless steel, which is a common engineering stainless steel, used in industry.

Ultrasonic impact peening can be seen as a direct impact peening treatment as is shot peening with the difference being that UIT is a thin probe used at ultrasonic frequency to introduce a compressive residual stress into the sample whilst rastering across the surface. There have been a number of research avenues taken in relation to peening and residual stress analysis, ((Z. P. Bazat, 2000) and (K. H. Al-Jubori, 2005), …, etc) however there seems to be a lack of the effect of peening with respect to new techniques

compared against currently used ones, and of the effect of these techniques on stainless steels commonly used throughout industry.

Shot peening is an effective and common mechanical surface treatment to improve metallic components' fatigue properties and corrosion resistance by means of introducing severe plastic deformation and compressive residual stresses into the near surface region ((Amir Javiddinejad, 2000), (W. H. Duan 2008), (Thomas H. K. Kang, Kenneth; 2013) and (Toe-Wan Kim, 2007)). In addition to the traditional shot peening, recent technologies, such as laser shock peening ((M. N. James, 2010) and (D. Y. Ju and B. Han, 2009)), ultrasonic peening (B. Han, D. Y. Ju and W. P. Jia; 2007), and wet shot peening (P. S. Prevey and J. T. Cammett; 2002), have been developed and used widely. In particular, the laser shock peening treatment consists of an irradiating surface of materials with nanosecond laser pulses that generate shock waves driven by plasma, which in turn lead to a certain amount of local plastic deformation (C. Yang, P. D. Hodgson, Q. Liu and L. Ye; 2008). Deep and high compressive residual stresses, limited roughening, and refined microstructure are usually the main characteristics of surfaces after laser shock peening treatment) Wei, 2020; Ahmed et. al., 2017; and Ahmed et. al., 2019) (William T. Silfvast, 2005) investigated the effects of laser shock peening on corrosion resistance of AISI 304 stainless steel in acid chloride solution and obtained the mechanism of corrosion resistance improvement by laser shock peening.

Generally, the variation of the roughness and grain refinement on the surface of metallic materials are induced by shot peening (Breck Hitz, J. J. Ewing and Jeff Hecht; 2001) Surface roughness as a crucial surface feature plays a very important role in practical application. Several studies have published indicating the significance of the roughness ((J. Dutta Majumdar and I. Manna; 2003), (Chhabra Nitish and Bhardwaj Sudeep; 2011) and

(Mohamad K. Alwan and Naseem Sabah Abrahim; 2014)). However, there is still insufficient information on corrosion properties after shot peening. Literatures on corrosion resistance after shot peening are conflicting without showing a clear trend ((R. Wathins and John Shaw; 2013), (Dongming Wei, Alejandro Sarria and Mohamed Elgindi; 2013), (Husam Al-Qablan, Hasan Katkhuda and Hazim Dwairi; 2009) and (Olumi et al., R. Wathins and John Shaw; 2013) reported that surface nanocrystallization induced by shot peening improved corrosion resistance. Nevertheless, ((Ahmed et al.; 2019, Dongming Wei, Alejandro Sarria and Mohamed Elgindi; 2013), (Husam Al-Qablan, Hasan Katkhuda and Hazim Dwairi; 2009)) found that shot peening induced higher surface roughness and reduced the corrosion resistance compared with the untreated materials.

Corrosion has many negative effects on metals. It reduces the cross-section of structural components and reduces resistance to buckling when a axial load is applied. The corrosion affects the mechanical properties and reduces the elasticity of the material and makes it structurally weak even if the structure appears stable (Thomas H. K. Kang, Kenneth A. Biggs and Chris Ramseyer; 2013).

When the column is subjected to dynamic axial load, it changes from its equilibrium state to another equilibrium state. Critical load can be defined as the maximum load the column can withstand before reaching unstable equilibrium. Any other addition to load may lead to catastrophic failure. The critical load of the columns occurs under the flexible boundary of the column (Toe-Wan Kim, 2007).

1.3 Problem Statement

Buckling is one of the important topics studied by many researchers from the mid-1940 to date. This topic is related to many mechanical parts and

structural companies and to the various forms dealt with by the subject. Also, most structures are exposed to corrosion when buried underground, which negatively affects the columns and reduces their resistance to critical loads and increases the possibility of buckling. Therefore, it is necessary to study the critical loads of long and intermediate columns without corrosion in oil field, as well as to study the effect of corrosion on these columns when it is submerged in the soil for a period of time in oil field when drilling rigs are ideal. With a choice of suitable formula to be more compatible with the experimental results and are approved in the future for engineers and researchers in petroleum filed.

1.4 Thesis Objectives

Study improving the critical loads of long and intermediate 304 stainless steel alloy columns by shot peening and leaser treatment in oil field.

The thesis objectives are:

1- Studying the elastic buckling behavior of solid column with fixed-pinned conditions.

2- Study the effect of shot peening and laser on the dynamic bending behavior.

3- Evaluating the effect of corrosion time underground on the dynamic buckling behavior.

4- Comparing the experimentally obtained results with Perry-Robertson, Euler, Johnson, and ANSYS formula, indicating which is more acceptable with the practical results.

1.5 Thesis Layout

This thesis falls in 5 chapters, as follows: -

Chapter (1) presents an introduction of the thesis and the basic reason of the study, including the purpose and objectives of this work.

Chapter (2) consists of a survey of the published works regarding the column buckling resistance and effects of corrosion. A proposal of a

modified design approach, based on the findings in literature is presented, introduces the theoretical considerations of buckling phenomenon under axial compressive load and the effect of corrosion on buckling resistance of columns. Also, buckling theories (Perry- Robertson, Euler, and Johnson) are presented.

Chapter (3) presents the experimental work regarding buckling of columns without corrosion and with corrosion are included in this work. The test layout of the specimens, measured quantities, are described.

Chapter (4) contains the experimental and theoretical results and their discussion.

Chapter (5) includes conclusions and some suggestions made for future works

Chapter Two

Literature Review and Theoretical Background

Chapter Two

Literature review and Theoretical background

This chapter presents an important pervious investigation on buckling behavior of columns using different fields i-e dry buckling, corrosion – buckling iteration and peening–buckling behavior of different materials used in the practical.

2.1 Dry Buckling Review

Kanaka and Venkateswara (2004) and M. N. James (2010) presented the expectation of the thermal post-buckling behavior of structural elements for the case of tapered columns. The simple method of predicting the thermal post-buckling behavior of tapered columns involved two steps. The first step was the evaluation of linear thermal load parameter. This was carried out using any of the methods like Rayleigh-Ritz or Finite Element Method (FEM). To predict the thermal post-buckling behavior of the columns, the next step was used to evaluate the tension developed in the columns due to large deformations. Numerical results were presented to show the accuracy of the method along with comparable FE results. It was noted that the results obtained were in close agreement with the FE results. Depth taper, as well as the diameter taper were considered. It was concluded that the column buckled with thermal load caused lateral deformations, and the method of solution was easily extended to any other configurations of structural elements and involves very little computational times.

The paper of **Al-Jubori (2005) and** also the paper of **D. Y. Ju and B. Han (2009)** Studied the critical buckling stresses of columns, solid and hallow, bending, compression, or combinations of them. An instructional computer program had been designed to find the equivalent failure stress and failure cycles for members subjected to uni and combined dynamic

loading. It was shown that compressive buckling stresses under dynamic loading are lower than those under static loading and solid columns endured are less axial compressive buckling loads than the hollow columns. Also, the buckling strength of (CK35) alloy steel was better than (CK45).

Goutam and Sajeda (2007) and the study of **B. Han et. al. (2007)** studied and presented the method of identifying the buckling load of a beam-column based on a technique named "Multi-Segment Integration Technique". This method applied to a number of problems to ascertain its soundness and accuracy. They considered a boundary-value problem for the beam-column equation, in which the boundary conditions mean that: - (i) hinged at both ends; (ii) fixed at both ends; and (iii) fixed at one end and hinged at the other end. The results obtained by finite difference method compared in order to determine the efficiency of this method. It is apparent that the approximate solutions yield very good estimates of the values obtained from both methods, and that any error is simply a function of the number of iterations used. The proposed methods therefore provide a straightforward and effective numerical technique for the problem.

P. S. Prevey and J. T. Cammett, (2002) and the work of **Jian, et. al. (2008)** established based on the geometrical nonlinear theory of large deflection elastic beams, the governing differential equations of post-buckling behavior of clamped-clamped inclined beams subjected to combined forces. When the applied force exceeded the critical value, the numerical simulation showed that the inclined beam snapped to the other equilibrium position automatically. By using an incremental displacement numerical method, the post buckling configurations of the large deflection beam at any initial inclination angle were presented, and the nonlinear stiffness of the post-buckling beam was obtained in the snap-through process. The high order mode configuration of the buckling beam did not

appear in the snap-through process in the static experiments. In addition, the beam under a transverse force did not snap until the beam tip passed a certain unstable position. The main conclusion was that the critical buckling load increased with an increasing initial angle, so did the critical displacement. This method was more suitable to solve any nonlinear post-buckling problems of inclined beams.

C. Yang et. al. (2008) and the work of **Alalkawi and Aziz (2009)** studied the Euler and Johnson theories depend on experiment tests under compressive dynamic buckling load by using 20 specimens (columns) made from two materials, 1020 Hot Rolled and 5052 Aluminum alloy. They concluded that Euler (for long columns) and Johnson (for short columns) theories can be used to estimate the dynamic critical buckling load with design factor of 3 or more.

William T. Silfvast (2005) and **Amir and Zodiac (2012)** studied the behavior of buckling an I-beam under combined pivotal and horizontal side load. It was also showed that the effective application location of the axial loading decides the buckling behavior of the long I-beam. A theoretical formula was developed to specify the critical buckling load for this combined loading configuration from the elastic static model. It was showed that this application location specifies the behavior of the buckling and the critical load of the buckling of the I-beam.

Breck Hitz et. al. (2001) and **Mohamad K. Alwan et. al. (2014)** on their work studied the buckling analysis of carbon steel columns and the carburized case for various diameters. The experimental data found that the carburization gives the columns a high tensile strength and hardness and critical buckling load compared with the as-received columns that have low carbon (without carburized). The experimental data showed good

compatibility with the FEM results, while the compatibility was reduced by increasing the diameter of the column.

J. Dutta Majumdar and I. Manna (2003) and **Avcar (2014)** discussed the influence of the boundary cases, cross-sections and slenderness ratios on the buckling load of the steel column. Two different boundary conditions such as Fixed-free (F - F) and pinned-pinned (P - P) with three various cross-sections area, such as square, rectangle and circle cross sections were used. Finite element model (FEM) has been performed and compared with numerical computations. They found that the buckling load of fixed-free (F – F) column was less than pinned-pinned (P – P) column.

R. S. Khurmi and N. Khurmi (2017) on their work a strut is defined as a structural member that subject to an axial compressive load, a strut may be inclined, horizontal or even vertical called column. The columns used in frames and buildings. The first attempt to study the stability of the long column was made by Euler. The equation that Euler derived it for the critical buckling load of long columns based on bending stress. The direct stress in long columns is negligible as compared to the bending stress. Therefore, the Euler formula cannot be used in the case of the short columns because direct stress cannot be neglected.

Aead I. H. (2015) tested stainless steel samples under compression buckling load and it was obtained that the maximum (SF) for unpreened samples is (1.7) and for laser penned is (1.7) and he recommended that the (SF) may be not less than (2).

Ahmed A. Ibrahim, Husain J. Alalkawi and Ahmad M-Rachid Nakchbandi (2017) this study showed that buckling plays a very important role in the design of slender columns. When the members are long, the loading, which is lower than yielding, may be large enough to cause the

member to deflect laterally. It is well established that the mechanical surface treatments, e.g., shot peening, plasma peening and laser peening are effective method to enhance the resistance of metallic material. In this work, the main aim is to estimate the optimum improvement of dynamic behavior of medium carbon steel alloy due to shot peening experimentally. The behavior of rotating arcular column buckling of steel alloy under compression loading showed significant improvement due to shot peening time (SPT) at 25 mints. Which gave higher resistance against buckling and increasing the buckling time, after that the improvement tends to be reduced?

2.2 Corrosion-Buckling interaction Literature reviews

V. Azar et. al. (2010) investigated the influence of shot peening treatment on hardness, fatigue and corrosion behavior of 316L stainless steel in Ringer's solution, hardness, fatigue and electrochemical tests were performed on each specimen before and after shot peening treatment. The concluding remarks observed that shot peening treatment increases the surface hardness and fatigue resistance.

Sidharth (2009) and the work of **Mohamad K. Alwan et. al. (2014)** studied the effect of pitting corrosion on the mechanical properties and dimensions of the plate. Pitting corrosion width, depth, length Degree of Pitting, (DOP) was the main factor which reduced the ultimate strength of the plates. (FEM) was used to evaluate the corrosion impact on the plate. It was found the existence of doubler on the plates has a large influence on the buckling resistance of the plate. The buckling strength tended to increase for great doubler thickness. The buckling resistance was reduced when the thickness of the doubler is less than the thickness of corrosion feature on the plate.

R. Wathins and John Shaw (2013) and the work of **Oszvald and Dunai (2012)** studied the influence of corrosion on the buckling behavior and resistance of corroded steel angle section members. Buckling tests were executed on 24 steel angle section specimens. The influences of the corrosion location and the reduction of the cross-section were studied by experimental investigations where the corrosion was modeled by artificial thickness reduction. It was found that the buckling resistance was reduced by corrosion in different rates: different corrosion locations, cross-section, and volume reduction causes large scatter in the buckling resistance reduction.

Fridman (2014) and the work of **Dongming Wei and Alejandro Sarria (2013)** demonstrated the optimal design of compressed columns with a circular cross section under axial compressive forces and exposed to a corrosive environment. The initial volume of the structure is taken as an optimal parameter. The main constraint is the buckling of a loaded column at the final time of its operation. Gutman-Zaynullin's exponential stress corrosion model adopted for the analysis. Analytical and numerical results derived for optimal variation of the cross-sectional area of the bar along its axis. The corrosion model by Dolinsky allows one to get a sufficiently accurate optimization problem for bars under axial compression in a corrosive environment.

Kashani et. al. (2016) and the work of **Husam Al-Qablan et. al. (2009)** calculated the effect of corrosion on the resistance of buckling. Corrosion has negative effects on the elasticity of the column. The numerical model developed in this study is capable of responding to the linear bending of the reinforced concrete until the total collapse. The obtained results showed that it is unsuitable to suppose that corrosion only impacts the main vertical strengthening in the column.

Uwiringiyimana et. al. (2016) and the work of **M. Arif Gurel and Murat Kisa (1995)** summarized the effect of inhibitors on the corrosion of stainless steels and aluminum alloys in various media. The degeneration in stainless steels and aluminum alloys materials happened because of the exposure to corroding environments. Inhibitors are used to reduce the corrosion of these alloys in deferent corrosive media and increase their durability.

Hussain J. Al-alkawi, Samih K. Al-najjar (2018) in this work Corrosion buckling interaction behavior of AISI 304 stainless steel circular columns was investigated. Long and intermediate columns diameter of (6 mm) are tested in as received and corroded condition. Corroded columns are tested after embed in soil for different periods of time. Rotating buckling machine test was used to evaluate the critical buckling load (pcr) under dynamic compression loads. By using Perry Robertson formula, experimental work results compared. The results showed that increasing in corrosion time (embedding time), reduction in critical buckling load increases also. Maximum reduction of buckling load value was (2.28% and 1.37%) for long and intermediate column respectively as compared with as received condition.

Katalin Oszvald and László Dunai (2012) in which the aim of this work is to study the effect of corrosion on the buckling behavior and resistance of corroded steel angle section members. The influences of the corrosion location and the loss of cross-section are studied by experimental investigations, where the corrosion is modelled by artificial thickness reduction. Compressive buckling tests are carried out on twenty-four specimens. Different corrosion damages are modelled, like uniform, pitting and local corrosion in the specimens. The buckling behavior and the

relationship of the corrosion reduction and the resistance decrease are determined.

Ahmed A. Ibrahim, Al- Alkawi H. J, Al Nagshabandi A. M. Rachid, Samih K. Al-najjar (2019) this paper investigates the dynamic behavior of buckling on AISI 304 stainless steel and AISI 304 corroded and as received were tested under dynamic compression buckling condition columns. Maximum reduction in buckling load was (28%) and (19.6%) for long and intermediate soil corroded columns respectively as compared with as received condition. Perry-Robertson equation was used to compare with the experimental results of buckling load.

2.3 Peening-Buckling behavior Literature reviews

Al-Alkawi et. al. (2015) and the work of **Chhabra Nitish and Bhardwaj Sudeep (2011)** explained the comparison of column buckling behavior between experimental results of median carbon steel CK35 and Hong model**.** Columns are tested under dynamic buckling without and with shot peening**,** where the comparison presented a good conservative correlation for the columns. The comparison includes initial imperfection, load period and slenderness ratio of columns. It shows that the Hong model was able to estimate the dynamic buckling behavior of Ck35 columns.

G. H. Majzoobi et. al. (2016) used a numerical simulation; which was LS-DYNA finite element code; the modelling of shot peening process was accomplished by simulation of multiple shot impacts on a target plate at different velocities, the results showed that, residual stress distribution was highly dependent on impact velocity and multiplicity, impact velocity significantly influenced the residual stress profile, and the increase of velocity improved the residual stress distribution up to a particular point. On the other hand, they showed that the increase in the velocity may reduce

the maximum residual stress. Also showed that when reducing the shooting velocity, the peek residual stresses reduce.

Donzella et. al. (2011) proposed the effect of shot peening treatment on Sintered steel plates were analyzed in terms of micro-structural, mechanical properties, residual stress profiles. Residual stresses after the treatment were measured by means of the hole drilling technique and correlated to the mechanical properties and the surface densification of both steels in order of varying the nominal density. The obtained results showed presence of the principal residual stresses for each specimen as expected in shot-peened components.

Ali Yousuf et. al. (2017) studied the improving of mechanical properties of aluminum alloy 2017A-T3 due to utilized ultrasonic peening. Three types of ultrasonic peening were conducted, oneline (1UP), two lines (2UP) and three lines (3UP) on the surface of the samples. All three types of UP improved the mechanical properties, but the best enhancement has obtained at (1UP).

Al-Alkawi and Saad T. Faris (2017) in which the aim of this work is to investigate the effect of soil corrosion on the critical buckling load of circular columns made of 2014-T4 aluminum alloy. In this work, 24 specimens were used and buried in the soil for 120 days. The samples divided into two groups (12 columns with corrosion before shot penning (SP) and ultrasonic impact treatment (UIT), and 12 columns with corrosion after combined surface treatments (SP+UIT)). The experimental results revealed that the corrosion negatively affects the mechanical properties of the material, and the reduction percentage (R%) for ultimate tensile strength (UTS) and yield strength (YS) was 1.95% and 4.57% respectively. After combined surface treatments (SP+UIT) for the corroded columns, the ultimate tensile strength (UTS) and yield strength (YS) were improved with

(2.42%, and 2.87%) respectively. Perry-Robertson, Rankine, and ANSYS used to estimate the critical buckling load (Pcr) and compare it with the experimental results. Rankine and Perry's formulas achieved a good agreement with the experimental without and with (1.5) factor of safety respectively. While ANSYS gave satisfactory prediction with a safety factor before and after (SP+UIP) of (2.2 and 2.7) and (1.9 and 2.7) for long and intermediate columns respectively.

Ahmed Naif Al-Khazraji (2014), this paper model and optimize the fatigue life and hardness of medium carbon steel CK35 subjected to dynamic buckling. Different ranges of shot peening time (STP) and critical points of slenderness ratio which is between the long and intermediate columns, as input factors, were used to obtain their influences on the fatigue life and hardness, as main responses. Experimental measurements of shot peening time and buckling were taken and analyzed using (DESIGN EXPERT 8) experimental design software which was used for modeling and optimization purposes. Mathematical models of responses were obtained and analyzed by ANOVA variance to verify the adequacy of the models. The resultant quadratic models were obtained. A good agreement was found between the results of these models and optimization with the experimental ones with confidence level of 95 %.

H. J. M. Al – Alkawi, F. A. K. Fattah and A. I. Hussain (2016), the purpose of this paper design and manufacture the electrical laser alarm system to assess the buckling failure of 304 stainless steel column and to estimate the critical buckling load (Pcr) under increasing compressive load without shot peening (WSP) and with shot peening (SP). The evaluation of the critical buckling load (Pcr) was done experimentally and theoretically for long and intermediate pinned – fixed columns. The experimental results revealed that 25 min. shot peening time (SPT) improved the critical

buckling load (Pcr) by 13.3% - 15.39% improvement percentage (IP) for long columns while 18.51% -23.07% for intermediates. Also, it was observed that reducing the effective length (Leff) resulted in increasing the effect of 25 min. shot peening time (SPT) and kept constant when effective length (Leff) larger than 200mm. The difference percentage (DP) obtained between theoretically and experimentally comparison showed the critical buckling load (Pcr) was 33.33 to 41.18 for non-shot peening and 23.07 to 33.34 for 25 min. shot peening time (SPT) based on Euler and Johnson theories for both long and intermediate columns. Also, it was revealed that increasing the slenderness ratio (S.R) resulted in reducing the critical buckling load (Pcr) for both columns and both conditions of testing without shot peening (WSP) and shot peening (SP).

P. Peyre and al (2014), the influence of laser peening (LP) on the electrochemical behavior of AISI type 316L stainless steel in a saline environment was evaluated. Surface modifications were investigated as they might have beneficial effects on the corrosion behavior. Low residual stress and work hardening levels were found, when compared with a conventional shot-peening (SP) treatment, mainly because of the absence of martensite transformation in the case of LP. Surface changes were accompanied by small roughening effects and a global preservation of the surface chemistry after treatment. Therefore, electrochemical tests performed on samples after LP and SP treatments showed increases in remain potentials, reductions of passive current densities and anodic shifts of the pitting potentials evidenced by a stochastic approach of pitting. The better pitting resistance was observed after LP treatment, which seems to reflect a reduction or an elimination of active sites for pitting at lower potentials. Even though the deleterious surface state of shot peened surfaces possibly counterbalances the beneficial influence of residual

stresses, a beneficial influence of mechanical surface treatments has been demonstrated regarding the localized corrosion properties.

2.4 Remarks and lessens to learn

Brief review of the previous studies that summarized above highlights the most important observations that comes as follows:

1- Several studies were found on the effect of different types of loading on the buckling resistance and strength of columns, and that served as a solid base for this research study.

2- Some of the previous studies offered analytical methods, and only a little of them consider analytical and practical results. However, this study will do both analytical and practical approach.

3- Most of the preceding studies focused on determining the critical buckling load of various materials statically. Meanwhile, this study focuses on 304 stainless steel alloy and do determine the critical buckling loads using analytical models and well compared to practical lab investigation.

4- Studies had thoroughly investigated the buckling phenomenon by applying increasing-dynamic loading experimentally as this study did.

5- Studies investigated thoroughly the buckling failure for different slenderness ratios of columns as this study did.

6- Previous studies not focused heavily on the study of the effect of underground corrosion on the buckling of columns. So, the present work will study the effect of corrosion time underground on critical buckling load of columns.

7- Most previous studies used the Euler formula for long columns and the Johnson formula for intermediate and short columns. In the current work, the formula of Perry-Robertson used in addition to the two previous formulas

8- Lack of sufficient studies in the field of petroleum Drill pipe buckling is a nasty thing. When a tubular (casing or drill string) buckles, it can become useless - or worse, it may cause other problems, like parting the string with time consuming fishing operations and costly repairs (one of the main aims of this study is to avoid such problems).

2.5 Theoretical and Numerical Consideration

There are several ways to determine the failure of structures such as type of structure, kind of load and the nature of the materials. For example, an axle in a car may unexpectedly breakdown from the refined cycles of loading. This leads the structure to lose its ability to complete its intended function. The best solution to avoid these types of failures is through structures designed to remain within the limits of maximum stress which can be tolerated. Thus, the strength and stiffness are significant factors in this design. In addition, buckling is another type of failure resulting from structural instability as a result of axial compressive on the structural member (Al-Alkawi H. J. M. and Al-Khazraji A. N., Z. F; 2015).

Buckling is one type of failure that leads to a sudden breakdown in structures when column is exposed to axial compressive stress. When a column of a structure is loaded with a small axial pressure, it is distorted with a noticeable change in geometry. At the point of critical load value, the structure unexpectedly experiences a large distortion and may lose its stability to carry the load. This stage is the buckling stage (Nashwa Abdul – Hammied Saad and Aathraa Husian Hashim; 2014).

In the beginning the loads of the shaft are stable and with the addition of a load that exceeds the buckling it becomes unstable; it is also possible to say that the least deviation of the column from its straight form leads to buckling. The point at which the buckling occurs is called the point of

bifurcation (Ali A. Ali, Esam A. Ebrahim, Mohammed H. Sir and Barazan A. Hamah; 2013).

The column is part of the structure being exposed to carrying axial compressive load and it may break by buckling. The purpose of column analyses procedures is to predict the level of load and stress when the column is unstable and buckle (D. Y. Ju and B. Han; 2009).

The slenderness ratio has a major role in determining the column's ability to carry the axial load. The fact that the column is a slender compression member may fail when the level of stress exceeded the elasticity of the metal. As well as, the failure of most columns occurs at a level below the strength of the materials of the column. Because most of them are slender (ratio of column length to cross section area) and the columns may collapse because of buckling (lateral instability). Instability is a change in the shape of the column due to the large axial load and may cause column failure and thus lead to a collapse (Al-Alkawi H. J., Al-Khazraji A. N. and Essam Zuhier Fadhel; 2013).

Buckling is the unwanted lateral displacement of the column through which the column cannot carry any additional stresses. Buckling is the unexpected lateral displacement of the column through which the column cannot carry any additional stresses. Buckling may be of a totalitarian nature, but may also be of a concentric type. The concentric buckling occurs due to the compressive stresses or maybe because of the combined compression, and bending buckling and totalitarian buckling caused by the loss of resistance of the cross-section. A structure or a member in a balanced case under a compressive load may become unstable and the structure acquires a new equilibrium state or a new trend of behavior (Al-Alkawi H. J., Talal A. A., Safaa H. A., Selman B. A. and Khengab A. Y; 2012).

Columns are vertical elements subjected to axial compressive stress (Y. Fouad, Mostafa M. Elmetwally, 2011). Columns are divided into two, or rather three categories (short, intermediate and long columns of length). The ratio of the length of a column to the least radius of gyration of its cross section is called the slenderness ratio (S.R). All formulas used in the analysis of the column contain the slenderness ratio. It is the ratio that determines the column type to be long, intermediate or short. However, the way the column type is mended similarly affects its behavior. Therefore, the long-term in the slenderness ratio must be adjusted to determine the effective length. The effective column length can be defined as the length of an equivalent pin ended column having the same load-carrying capacity as the member under consideration, then the effective slenderness ratio is:

$$S.R = \frac{KL}{r} = \frac{L_e}{r} \quad \dots\dots\dots\dots\dots\dots\dots\dots\dots\dots\dots\dots\dots\dots\dots\dots\dots\dots\dots\dots \text{(2-1)}$$

Where

K: end factor

L_e: effective length, taking into account the manner of attaching the ends

r: smallest radius of gyration the cross section of gyration, defined as

$$r = \sqrt{\frac{I}{A}} \dots\dots\dots\dots\dots\dots\dots\dots\dots\dots\dots\dots\dots\dots\dots\dots\dots\dots\dots\dots\dots \text{(2-2)}$$

I: moment of inertia.

A: cross section area.

The slenderness ratio is the main indicator of the way of failure that could be predictable for a column under the axial load. Lower slenderness ratios led to the higher critical stresses, as offered in Figure (2-1) (Al-Alkawi H. J. M., Al-Khazraji A. N., Z. F; 2015).
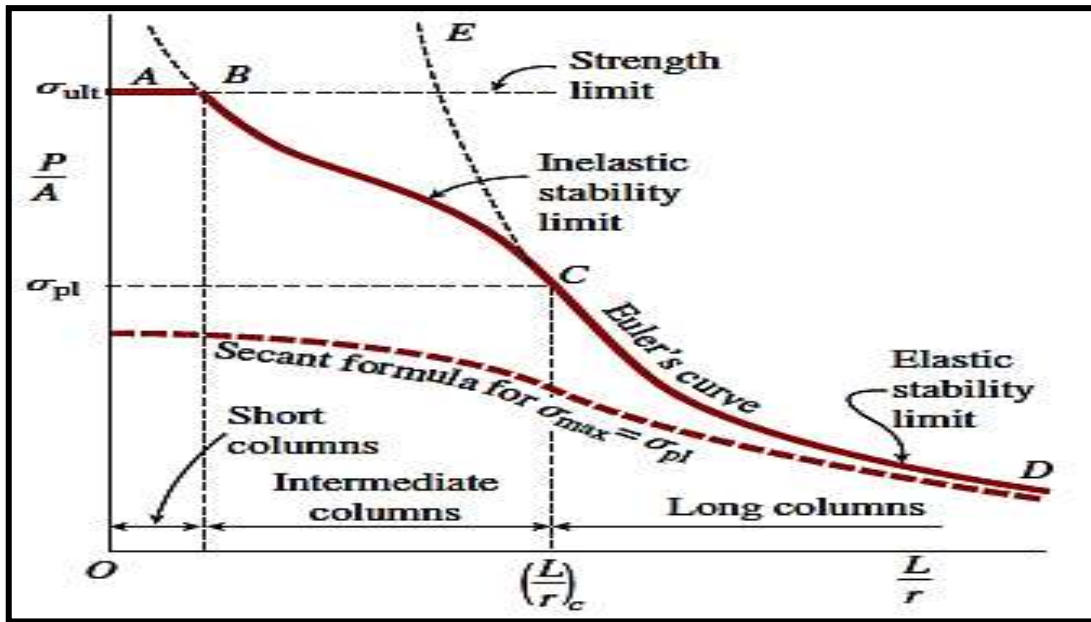
Figure (2-1): Relation between Compressing Stress and Slenderness Ratio (Al-Alkawi H. J. M., Al-Khazraji A. N., Z. F; 2015).

The amount of K is based on the end conditions of the column, as shown in Figure (2-2). It should be noted that the values listed for K are based on the expected shape of the deflected column when buckling takes place.
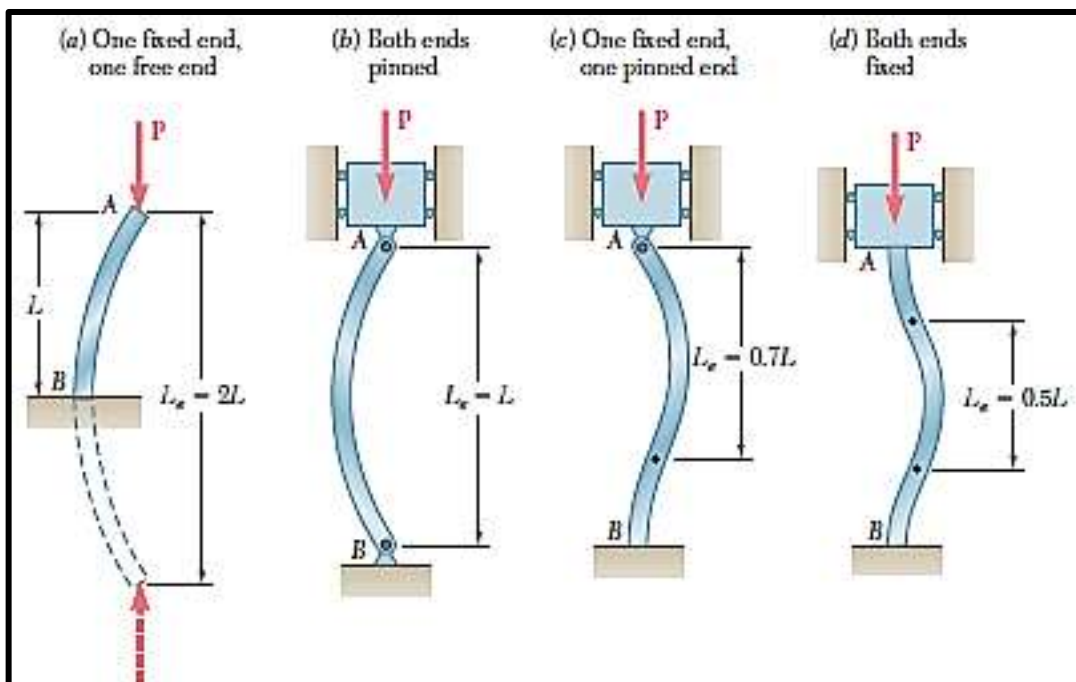
Figure (2-2): Values of K for effective length, L_e=KL for different connections (Jorge H. B. Sampaio Jr. and Joan R. Hundhausen; 1998).

The value of (L_e/r) which determines whether the column is long or short is found by equating the transition slenderness ratio formula (column constant formula). (Uros Zupanc and Janez Grum; 2010)

$$C_c = \sqrt{\frac{2\pi^2 E}{\sigma_y}} \dots\dots\dots\dots\dots\dots\dots\dots\dots\dots\dots\dots\dots\dots\dots\dots\dots\dots\dots\dots\dots\dots \text{(2-3)}$$

E: module of elasticity.

σ_y: yield strength.

If the slenderness ratio (Le/r) is greater than (C_c), then the column is long, and the Euler formula, defined in the next section should be applied to deal with this column type. When the slenderness ratio (Le/ r) is less than (C_c), the column is short or intermediate column type (long, intermediate, and short) can also be determined based on the following Table (2-1).

Table (2-1): Different materials columns slenderness ratio (S.R= L_e/r) (Arnold Mukuvare, 2013).

Material	Short column (strength limit)	Intermediate column (Inelastic stability limit)	Long column (Elastic stability limit)
Structural steel	S.R.<40	40< S.R.< 150	S.R.>150
Aluminum Alloy AA6061 -T6	S.R. <9.5	9.5 < S.R.< 66	S.R. > 66
Aluminum Alloy	S.R.<12	12< S.R.<55	S.R. > 55
Wood	S.R.<11	11< S.R.<(18-30)	(18-30)<S.R.<50

The corrosion of the buried metals in the soil is one of the biggest engineering and economic problems. The corrosion in the soft wet soils is more violent than corrosion in dry soils, because of the presence of moisture and oxygen together, this type is called wet corrosion. While, dry corrosion occurs at high temperatures, such as oxidation, and the different layers of corrosion are formed on the surface in terms of chemical and physical properties, and these layers vary by changing the mean corrosion air (Jorge H. B. Sampaio Jr. and Joan R. Hundhausen; 1998).

Corrosion is the deterioration of the base material properties as a result of a chemical or electrochemical environment reaction, which is applied to the medium of corrosion and not as a result of a mechanical process such as the friction in the machines. Metal structures and pipes are corroded by contact with soil or water. Iron surfaces of metal structures, pipes, and steel equipment are generally corroded when their surfaces are affected by soil

or water due to chemical reactions accompanied by the flow of electrons (i.e., flow of electricity). It can be said that the process of corrosion is an electrochemical process that results in the loss of parts of metal (Rekha M. Bhoi and L. G. Kalurkar; 2014).

Several important factors in the makeup of a soil affect underground corrosion: moisture content, degree of aeration, concentration of soluble salt and hydrogen ion concentration. These factors cause difference in solution potential that stimulate electrochemical corrosion at the anodic areas. Corrosion underground may also be accelerated by the presence of the stray electrical currents or by galvanic currents which result from connecting the structure with more cathodic metals (Y. Pekbey, A. Ozdamar and O. Sayman; 2007).

2.6 Euler Buckling of Columns

The first formula for the analysis of the buckling column was presented early by the Euler world in 1744. This classical theory is still valid in the present time and is likely to remain so. The slender columns have a variety of constraints. Euler's equation discusses the small elastic deflection of ideal columns (Arnold Mukuvare, 2013).

In this case, the Euler load was derived for a column that is fixed-pinned condition as shown in Figure (2-3) by derivation of differential equation deviation curve. When the column is exposed to axial compressive load, it leads to its buckling as shown in Figure (2-4).

A reactive moment M_0 develops at the base because there can be no rotation at that point (Al-Alkawi H. J. M. and Al-Khazraji A. N., Z. F.; 2015).

$$M_0 = R\,L \quad \text{...} \quad (2\text{-}4)$$

M_0: reactive moment.

R: reaction force.

L: length of column.

The bending moment of buckling column through distance X from the fixed end is

M=M₀-PV-RX=-PV+R(L-X)..(2-5)

V: lateral displacement

P: reaction force at pinned end

X: axial displacement.

And, hence, the differential equation become

$$EIv''=M=-PV+R(L-X) \quad\quad\quad\quad (2\text{-}6)$$

E: module of elasticity

I: moment of inertia

By exchange $k^2 = P$ /EI and rearranging, the equation become

$$v'' + k^2 v = \frac{R}{EI}(L-X) \quad\quad\quad\quad (2\text{-}7)$$

V=C₁ sin KX + C₂ cos KX + $\frac{R}{P}$ (L-X)...(2-8)

The first two idioms on the right-hand part comprise the homogeneous solution and the other term is the particular solution .The solution can be established by substitution until the differential equation (2-6).

As the solution has three anonymous values (C1, C2, and R), there are boundary cases. $V(0) = 0,$ $\quad v'(0) = 0$ and $\quad V(L) = 0$
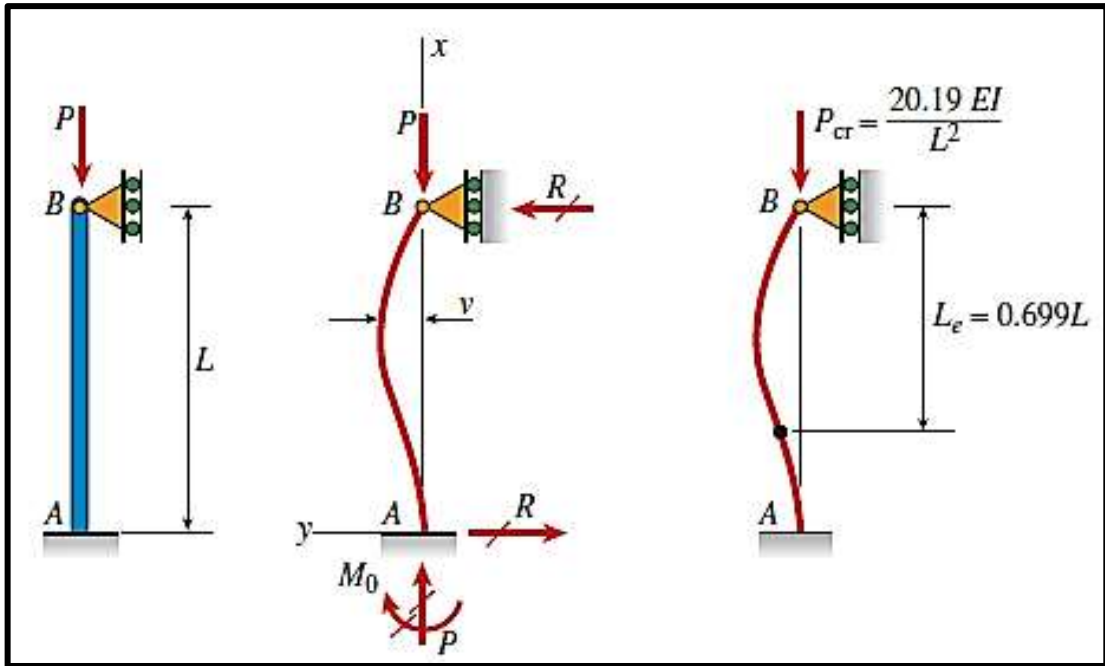
Figure (2-3): (fixes-pinned) Column condition (Nashwa Abdul – Hammied Saad and Aathraa Husian Hashim; 2014).

Using these conditions in equation (2-8) yields

$$C2 + \frac{RL}{P} = 0 \text{ ... (2-9)}, \quad C1K - \frac{R}{P} = 0 \text{ ... (2-10)}, \quad C1\tan KL + C2 = 0 \text{ ...(2-11)}$$

C1 = C2 = R = constant c

If $C_1 = C_2 = R = 0$, where the fiddling solution and the deflection is zero.

If all three equations are satisfied → In such a situation, the accepted solution and the deflection become zero.

To take out the solution for buckling, the equations (2-9), (2-10) and (2-11) should solved in a widely general way. One method of solution is to remove R from the first two equations, which yields

$$C1KL + C2 = 0 \text{ or } C2 = -C1KL \text{ .... (2-12)}$$

Then substituting 2 into Equation (2-9) and buckling equation could be found:

$$KL = \tan KL \text{ ....(2-13)}$$

The solution of this equation supplies the critical load as shown in Figure (2-3). The conformable critical load is

$$Pcr = \frac{20.19E\,I}{L^2} = \frac{2.046\pi^2 EI}{L^2} \qquad \ldots\ldots\ldots\ldots\ldots\ldots\ldots\ldots\ldots\ldots\ldots\ldots\text{(2-14)}$$

The column effective length could be obtained using the following equation.

$$Le = 0.699L \simeq 0.7L \qquad \ldots\ldots\ldots\ldots\ldots\ldots\ldots\ldots\ldots\ldots\ldots\ldots\text{(2-15)}$$

The column effective length was shown in Figure (2-3).

The lowest critical buckling loads and identical effective lengths for other support conditions columns are summarized in Figure (2-4).
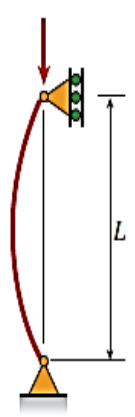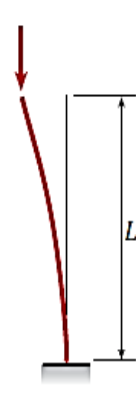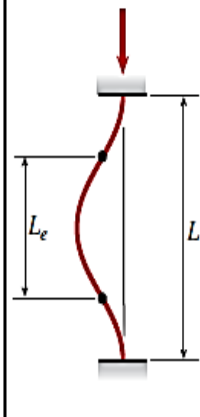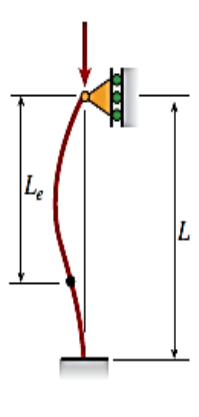
(a) Pinned-pinned column	(b) Fixed-free column	(c) Fixed-fixed column	(d) Fixed-pinned column
$P_{cr} = \dfrac{\pi^2 EI}{L^2}$	$P_{cr} = \dfrac{\pi^2 EI}{4L^2}$	$P_{cr} = \dfrac{4\pi^2 EI}{L^2}$	$P_{cr} = \dfrac{2.046\,\pi^2 EI}{L^2}$
$L_e = L$	$L_e = 2L$	$L_e = 0.5L$	$L_e = 0.699L$
$K = 1$	$K = 2$	$K = 0.5$	$K = 0.699$

Figure (2-4): The critical buckling load and the effective length for ideal columns (Al-Alkawi H. J. M., Al-Khazraji A. N. Z. F.; 2015).

Euler's equation displays the relevance between characteristics of the column and critical buckling load of pinned end column. The critical load that leads to buckling can be estimated as follows (2-16) (R. C. Hibbler, 2005).

$$\text{Pcr} = \frac{EI\pi^2}{L^2} \quad \dots\dots\dots\dots\dots\dots\dots\dots\dots\dots\dots\dots\dots\dots\dots\dots\dots\dots\dots\dots\dots\dots\text{(2-16)}$$

Pcr: critical buckling load

E: module of elasticity

I: moment of inertia

Also, the critical stress (σ_{cr}) for a column P_{cr}/A, which will be always applicable as long as the material limits are not exceeded (Toe-Wan Kim, 2007).

$$\sigma_{cr} = \frac{\pi^2 Er^2}{L_e^2} = \frac{\pi^2 E}{(L_e/r)^2} \quad \dots\dots\dots\dots\dots\dots\dots\dots\dots\dots\dots\dots\dots\dots\dots\text{(2-17)}$$

Euler – Johnson Formula

The Euler formula can only be applied to long columns where the slenderness ratio is greater than the column constant. It is also possible to say that the Euler equation does not depend on the mechanical properties of the metal except the elasticity model participated into the calculation.

The slenderness ratio is based only on the dimensions of the column. A column that is long and slender will have a higher slenderness ratio SR, than column constant Cc and therefore a low critical stress, Euler equation can be used to evaluate the critical load. The critical load Pcr is depending on the dimensions of the columns. The material strength is not involved in the above formula. A column that is intermediate or short and squat have a lower slenderness ratio S.R. than a column constant Cc and will buckle at a

high stress, and Johnson formula can be applied. This formula may be written as

$$P_{cr} = A\sigma_y \left[1 - \frac{\sigma_y (\frac{Le}{r})^2}{4\pi^2 E} \right] \dots\dots\dots\dots\dots\dots\dots\dots\dots\dots\dots\dots\dots(2\text{-}18)$$

σ_y: yield of strength

The critical load P_{cr} is directly affected by the mechanical properties in addition to its modulus of elasticity (H. A. Hussein, 2010). Thus, column buckling analysis should be performed as soon once one known that buckling failure mode occurs. Computation of the slenderness ratio of the column and the slenderness ratio at the dividing line between Johnson formula, and Euler, which will specify a formula suitable for finding critical load, as shown in Figure (2-5).
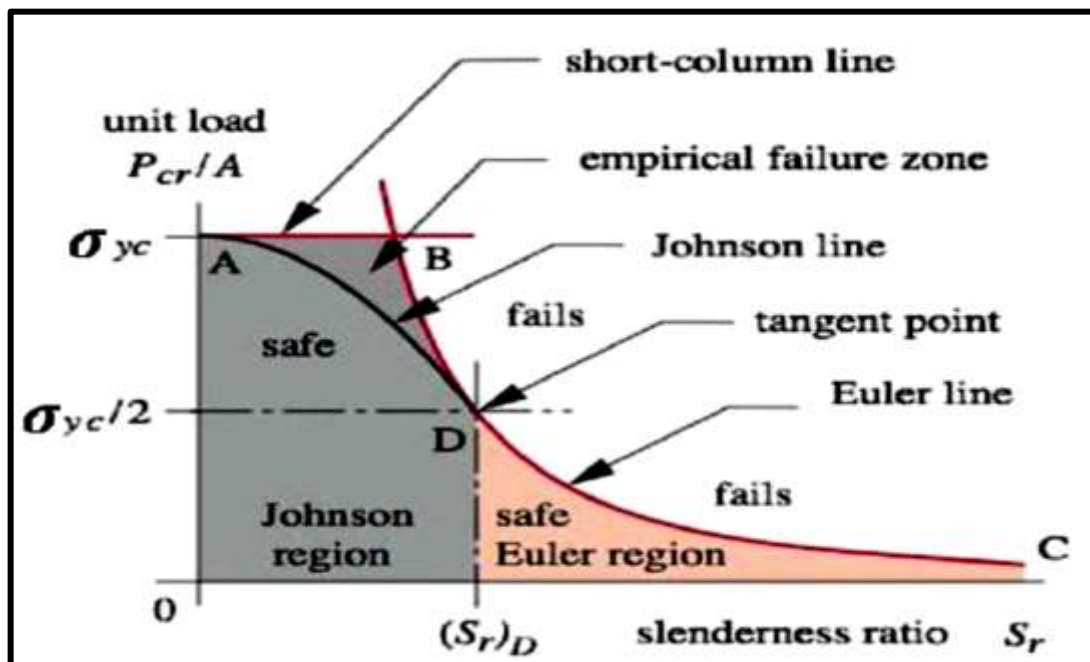
Figure (2-5): Construction of column failure line (Nashwa Abdul – Hammied Saad and Aathraa Husian Hashim; 2014).

2.7 Perry-Robertson formula

The Perry-Robertson formula was improved to take into account the shortcomings of the Euler equation for long columns as well as the Johnson equation for intermediate and short columns. This formula was developed from the assumption that all practical failures could be represented by a hypothetical initial curvature of the column. The Perry-Robertson formula depends on the hypothesis that any failure in the column during improper industry or eccentricity or material of loading can be allowed to the maximum strut of an initial curvature result of below equation.

$$y_o = C_o cos\frac{\pi X}{L}.$$

For the sake of calculation, this is supposed to be a cosin curve, in spite of the actual shape supposed to have a very small influence on the result. Consequently, the strut AB of Figure (2-6) of L is pin-connected at the ends. The initial curvature y_o at each distance X from the center is then specified by Timoshenko S. P. and Gere, J. M (1961) (James M. Gere, Barry J. Goodno, 2009).
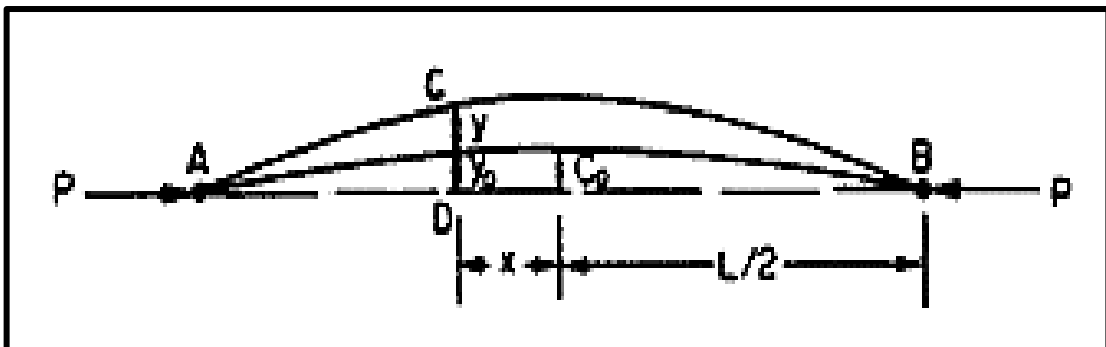
Figure (2-6): Column with initial bending (James M. Gere and Barry J. Goodno; 2009).

When a compressive load (P) is applied at the column end, the buckling will be increased to $y_o + y$

$$BM_c = EI\frac{d^2y}{dx^2} = -P\left(y + C_o\cos\frac{\pi X}{L}\right)$$

$$\frac{d^2y}{dx^2} + \frac{P}{EI}\left(y + C_o\cos\frac{\pi X}{L}\right) = 0 \dots\dots\dots\dots\dots\dots\dots\dots\dots\dots\dots\dots \text{(2-20)}$$

So, the solution will be:

$$y = A\sin\sqrt{\left(\frac{P}{EI}\right)}X + B\cos\sqrt{\left(\frac{P}{EI}\right)}X + \left[\left(\frac{PC_o}{EI}\cos\frac{\pi X}{L}\right)/\left(\frac{\pi^2}{L^2} - \frac{P}{EI}\right)\right] \dots\dots\dots\text{(2-21)}$$

A and B are the constants.

When $x = \pm L/2$, $y=0$, then $A = B = 0$

$$y = \left[\left(\frac{PC_o}{EI}\cos\frac{\pi X}{L}\right)/\left(\frac{\pi^2}{L^2} - \frac{P}{EI}\right)\right] = \left[\left(PC_o\cos\frac{\pi X}{L}\right)/\left(\frac{\pi^2 EI}{L^2} - P\right)\right] \dots\dots\dots\text{(2-22)}$$

subsequently dividing out of, numerator and denominator, by A

$$y = \left[\left(\frac{P}{A}C_o\cos\frac{\pi X}{L}\right)/\left(\frac{\pi^2 EI}{L^2 A} - \frac{P}{A}\right)\right] \dots\dots\dots\dots\dots\dots\dots\dots\dots\dots\dots\text{(2-23)}$$

But $P/A = \sigma$ and $(\pi^2 E I/L^2 A) = \sigma_e$ (The Euler stress for pin-ended columns)

$$\text{Then} \quad y = \frac{\sigma}{(\sigma_e - \sigma)}C_o\cos\frac{\pi X}{L} \dots\dots\dots\dots\dots\dots\dots\dots\dots\dots\dots\dots\text{(2-24)}$$

subsequently, total buckling at any point is specified by

$$y + y_o = \left[\frac{\sigma}{\sigma_e - \sigma}\right]C_o\cos\frac{\pi X}{L} + C_o\cos\frac{\pi X}{L}$$

$$= \left[\frac{\sigma_e}{\sigma_e - \sigma}\right]C_o\cos\frac{\pi X}{L} \dots\dots\dots\dots\dots\dots\dots\dots\dots\dots\dots\dots\dots\text{(2-25)}$$

$$\text{Maximum deflection (when x= 0)} = \left[\frac{\sigma_e}{\sigma_e - \sigma}\right]C_o \dots\dots\dots\dots\dots\dots\text{(2-26)}$$

C_o = central deflection

Maximum B.M. $= P\left[\dfrac{\sigma_e}{\sigma_e - \sigma}\right] C_o$ ....(2-27)

B.M = bending moment

The maximum stress that causes buckling is

$$\dfrac{M\,y}{I} = \dfrac{P}{I}\left[\dfrac{\sigma_e}{\sigma_e - \sigma}\right] C_o h \ \dots\dots\dots\dots\dots\dots\dots\dots\dots\dots\dots\dots\dots\dots\dots \ (2\text{-}28)$$

Where h is the distance of the outside flipper from the neutral axis (N.A) of the column. Therefore, the maximum stress owing to combined bending and thrust is given by:

$$\sigma_{max} = \dfrac{P}{I}\left[\dfrac{\sigma_e}{\sigma_e - \sigma}\right] C_o h + \dfrac{P}{A}$$

$$= \dfrac{P}{PAK^2}\left[\dfrac{\sigma_e}{\sigma_e - \sigma}\right] C_o h + \dfrac{P}{A} = \sigma\left[\dfrac{\eta\sigma_e}{\sigma_e - \sigma} + 1\right] \text{ where } \eta = \dfrac{C_o h}{k^2} \ \dots\dots\dots\dots(2\text{-}29)$$

If $\sigma_{max} = \sigma_y$ the compressive yield stress for the material of the column, the above equation when solved for gives

$$\sigma = \left[\dfrac{\sigma_y + (1+\eta)\sigma_e}{2} - \sqrt{\left(\dfrac{\sigma_y + (1+\eta)\sigma_e}{2}\right)^2 - \sigma_y\sigma_e}\right]\dots\dots\dots\dots\dots\dots\dots(2\text{-}30)$$

This is the Perry-Robertson formula required, But $P = A\sigma$

Then

$$P = A\left[\dfrac{\sigma_y + (1+\eta)\sigma_e}{2} - \sqrt{\left(\dfrac{\sigma_y + (1+\eta)\sigma_e}{2}\right)^2 - \sigma_y\sigma_e}\right]\dots\dots\dots\dots\dots\dots(2\text{-}31)$$

Where η is a constant depending on the material.

For a brittle material, $\eta = 0.015 \ L/k$

For a ductile material, $\eta = 0.3\left(\dfrac{L_e}{100r}\right)^2$

Le = effective length of pinned end strut (= 0.7 L of fixed ends strut. & = 2.0 L of strut with one end fixed)

r = radius of gyration

σ_y= yield stress

σ_e= Euler stress

A= cross section area of column

2.8 Numerical Analysis

As known, the finite element method (FEM) is the quickest, most reliable and effective method for the solution of complicated problems of mechanics with the assistance of computers. This method can handle problems with complex geometry, while it has the ability to take under consideration the material and geometric nonlinearities (J. M. Gere, 2004).

The FEM is used in the critical buckling analysis of the column with more than one condition, which is one of the most accurate numerical methods (J. M. Gere, 2004).

The FEM has been used extensively to simulate many applications in structural dynamics (J. M. Gere, 2004) The objective of this module is to provide the adequate theoretical and practical background to analyze dynamic problems through numerical simulations based on the FEM with ANSYS package (Barry Dupen, 2012). The FEM consists of five essential states (D. Y. Ju and B. Han; 2009):

1. Definition of the FEM mesh.
2. Selecting a displacement model.
3. Formulate the discrete equation.
4. Solving the stiffness equation.
5. Determining element stresses and strains

The FEM of the problem is a very important step for checking accurate information. For the EFM, a computer program called ANSYS has been used. Beam element is used in the modeling and FE mesh of column is modeled using appropriate nodes and elements based on length and cross-section of the column with sizing and bias factor (J. Dutta Majumdar and I. Manna; 2011).

ANSYS is a general-purpose FM modeling package for solving numerically a wide variety of mechanical problems. These problems include static, dynamic, structural analysis (both linear and nonlinear), heat transfer, and fluid problems, as well as acoustic and electromagnetic problems (Barry Dupen, 2012).

ANSYS provides two methods of modeling which are the solid and direct modeling. With solid modeling, geometrical boundaries of the model are described, controls over the size and desired shape of the selected element are established, and then the ANSYS program is instructed to generate all the nodes and elements automatically. In contrast with the direct generation method, the location of every node and the size, shape, and connectivity of every element are determined by the user prior defining these entities in the ANSYS model. The solid modeling is generally more appropriate for large or complex models, allows working with a relatively small number of data items as well as many other advantages (E. Z. Fadhel, 2014).

ANSYS 17 (APDL) was used to carry out the FE analysis in this work. ANSYS is used to analyze the critical buckling load on 304 stainless steel alloy columns. Therefore, it can predict the theoretical buckling strength of an ideal elastic structure. It computes the structural characteristics for the given system loading and constraints.

Chapter Three

Practical and Experimental Work

Chapter Three
Practical and Experimental Work

As previously reported, most researchers have adopted a theoretical safety factor of 2.5 to 3.5 when using the Euler-Johnson and Perry theories. This experimental work aims to obtain the optimal safety factor after comparisons between the experimental, theoretical and computational outputs.

3.1 Experimental Work

The experimental work is necessary to study some factors that are very difficult to attain by theory. Mechanical properties for 304 stainless steel alloy are presented and the testing description is given by using a Test-Rig which mainly consists of testing system (compression, torsion). The experimental work plan can be summarized as follows:

1- Selecting the material.
2- Testing the chemical composition and mechanical properties.
3- Using two groups of buckling specimens. Group (1) as received (without corrosion). Group (2) corroded specimens; they were embedded in soil for (60) days.
4- Applying buckling test of column under increasing dynamic load on the specimens.
5- Measuring initial static deflection using digital dial gauge.
6- Using laser alarm system to scale and gauge the critical deflection.

The experimental procedures are shown in the flowchart of work plan as given in Figure (3-1).
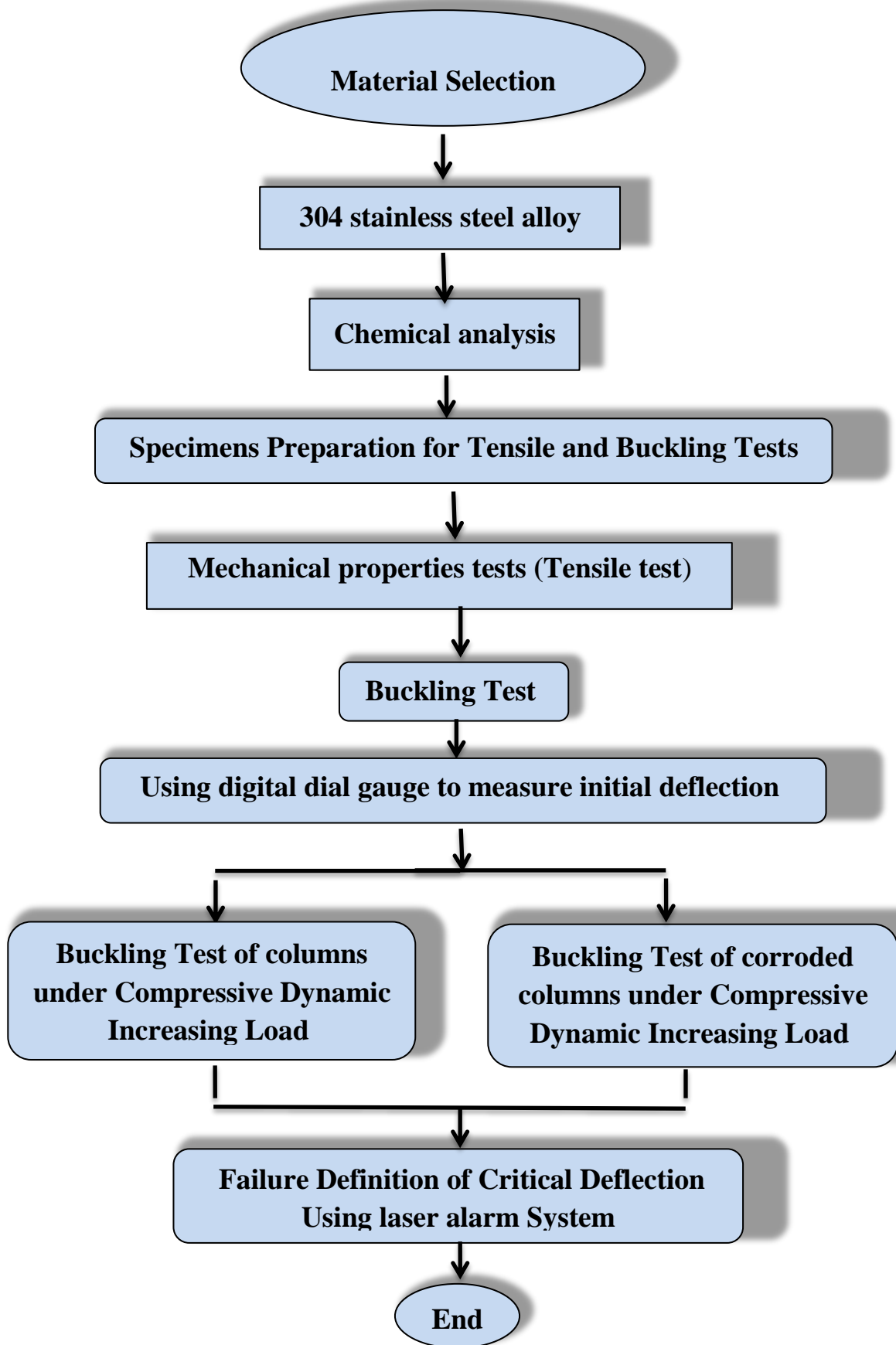
Technical path of experimental work procedure.

3.2 Material selection

The material used in the current work is 304 stainless steel alloy. This material is widely used in chemical equipment, coal hopper linings, cooking equipment, cooling coil, cryogenic vessels, nuclear vessels, dairy equipment, evaporators, flatware utensils, feed water tubing, flexible metal hose, food processing equipment, hospital surgical equipment, hypodermic needles, marine equipment and drilling operations.

The 304 stainless steel is the most widely used of all stainless steels because of the chemical and mechanical properties with weld ability and corrosion/oxidation resistance which provide the best all round performance stainless steel at relatively low cost. All the material was obtained from the State Company of Mechanical Industries, AL-Ascandarya and tested to determine its chemical composition of the steel alloy in Company State for Inspection and Rehabilitation Engineering (SIER). Results are listed in the table (3-1), while the mechanical properties shown in table (3-1) were obtained using the test machine WDW-200E at University of Technology-Material Engineering Department (Iraq), and carried out at room temperature (25°C).

Table (3-1): Chemical composition of 304 stainless steel (wt %).

304 stainless steel	C% Carbon	Mn% Manganese	P% Phosphorus	S% Sulfur	Si% Silicon	Cr% Chromium	Ni% Nickel	N% Nitrogen	Fe% Iron
Standard ASTM A240 [10]	0.08 Max	2.00. max	0.045. max	0.030 Max	0.75 Max	18.0- Max	8.0- Max	0.10 max	Balance
Experimental	0.026	1.72	0.016	0.021	0.66	18.9	9.6	0.07	Balance

3.3 Mechanical Properties

The tensile test was completed using the (WDW-200E) tensile testing machine with a capacity of 200KN offered as in Figure (3-1). The testing machine is located in the Materials Engineering Department-University of Technology. Then, the mechanical properties of the (304 stainless steel) are obtained according to American Society for Testing and Materials (ASTM A370) Tablet (3-2). Tensile sample dimensions are listed in Figure (3–2).

Figure (3–1): Tensile test instrument.
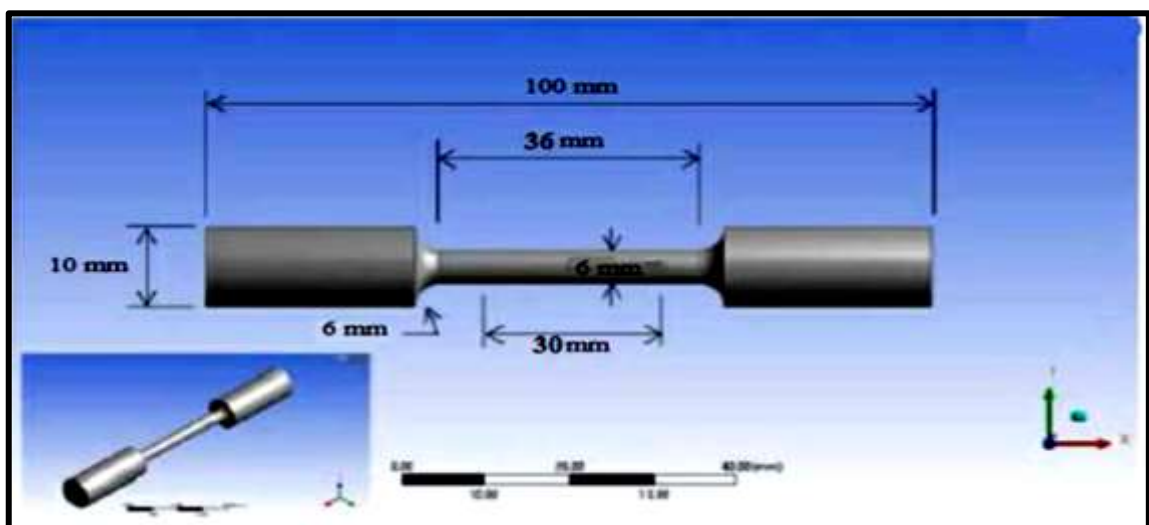
Figure (3–2): Tensile test sample with dimensions according to ASTM.

Table (3-2): Mechanical properties of 304 stainless steel.

304 stainless Steel	δu (Mpa)	δy(Mpa) 0.2%proof Stress	E (Gpa)	G (Gpa)	μ Poi-ratio	ε % Elongation
Standard ATM A304 [10]	621	290	193-200	74-77	0.30	55
Experimental (dry)	628	311	200	75	0.31	51
Experimental (corrosion)	591	288	198	74	0.29	58
Experimental (corrosion)+sp	599	301	199	76	0.29	53

Initial Deflection Measurement

Digital dial gauges are essential instruments that are used to measure accurately very small and diminutive liner distances. Analog and digital dial gauge models according to specific applications (Robert L. Mott, 2004). The advantages of digital dial gauge are:

- High sensitivity up to $0.025\mu m$ (1μ in), precision, and good response.
- Ease of using and Human error reduction.
- Reading of data that can be offered in different formats.

The digital dial gauges shown in Figure (3-4) works when the spindle touches the sample and changes its displacement. This change in displacement is converted into digital readings (Robert L. Mott, 2004).

Figure (3-3): Testing machine digital dial gauge (Robert L. Mott, 2004).

Laser Security System

LASERS are devices that amplify or increase the intensity of light to produce a highly directional, high intensity beam that typically has a very pure frequency or wave length. They come in sizes ranging from approximately one tenth the diameter of a human hair to that of a very large building (Hussain Abdulziz A., H. J. M. Al–Alkawi; 2009).

The word of LASER is an acronym that stands for "light amplification by stimulated emission of radiation". In a fairly unsophisticated sense, a laser is nothing more than a special flashlight. Energy goes in, usually in the form of electricity, and light comes out. But the light emitted from a laser differs from that from a flashlight (Robert D. Cook and Warren C. Young, 1985).

LASER is essentially a coherent, convergent and monochromatic beam of electromagnetic radiation with wave length ranging from ultra-violet to infrared. Laser can deliver very low ($\sim$ mW) to extremely high (1–100 kW) focused power with a precise spot size/dimension and interaction/pulse time (10^{-3} to 10^{-15} s) on to any type of substrate through any medium. Laser is distinguished from other electromagnetic radiation mainly in terms of its coherence, spectral purity and ability to propagate in a straight line (A. L. D. Ricardo, 2005).

LASER has many industrial, scientific uses, and military, including welding, fiber optics, microscopic photography, target detection, surgery, measurement devices, etc. (M. Kobayashi, T. Matsui and Y. Murakami; 1998).

LASER-Ray passes through long distance without scattering effect and the ray is almost invisible. Only the radiation point and incident point are visible. So, by this security project can make an invisible boundary of a

sensitive area. There are two parts of the system. One is transmitter and other is receiver. The actual system coupled with the buckling test rig is shown in figure (3-5).
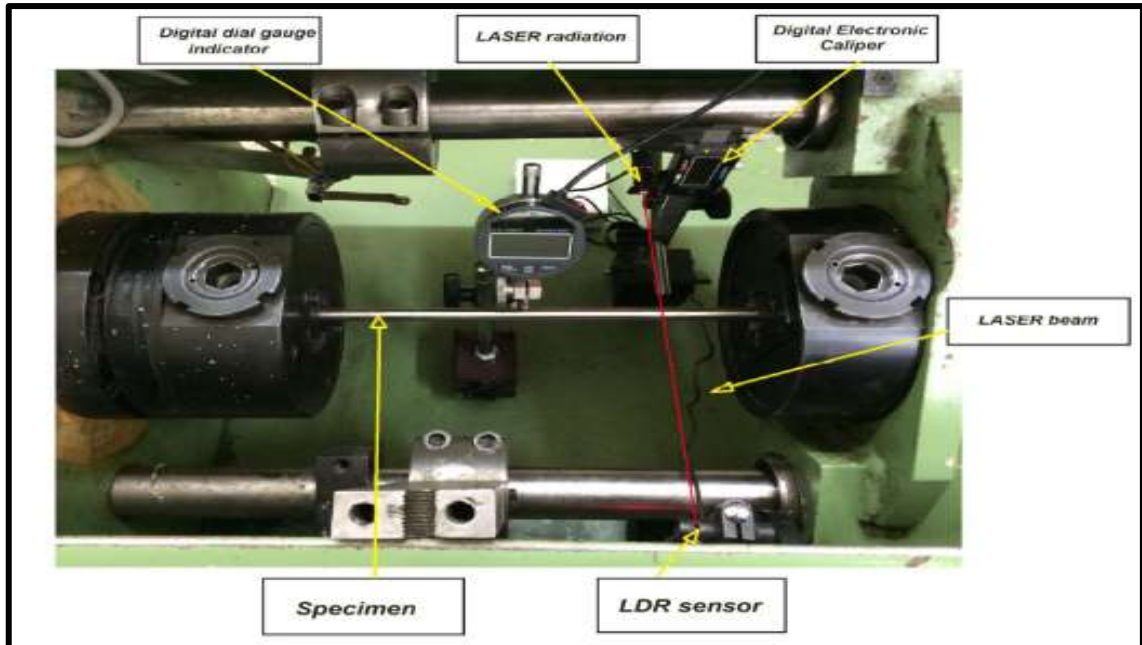
Figure (3-4): Actual Electrical Laser Alarm System Coupled with Buckling Test Rig Machine.

The transmitter part is built with a LASER radiator, a pair of dry cell batteries, an on-off switch and a stand to hold on digital electronic caliper. In the receiver side, there is a focusing Light Depending Resistor (LDR) sensor to sense the LASER continuously. The LDR sensor been mounted on a stand and is connected to the main driver circuit. The circuit has two parts. One is to filter the signal of discontinuity ray and others is for alarm circuit. When anybody crossover the invisible ray the main circuit sense the discontinuity by sensor and turn on the alarm circuit. If once the alarm circuit is on it will continue ringing. There is duration of ringing depends on preset timer. The system has built with low cost and high performance. The power consumption of the system is very low (S. H. Alokaidi, 2012).

3.4 Buckling Specimen Design

Two types of buckling specimens were prepared, long and intermediate. The material was received as columns of (10 mm) in diameter (d). The dimensions of the specimens used are shown in Figure (3-6). The specimens used in the testing of buckling were received in the form of rods of (304 stainless steel alloy), in different lengths of submitted samples.
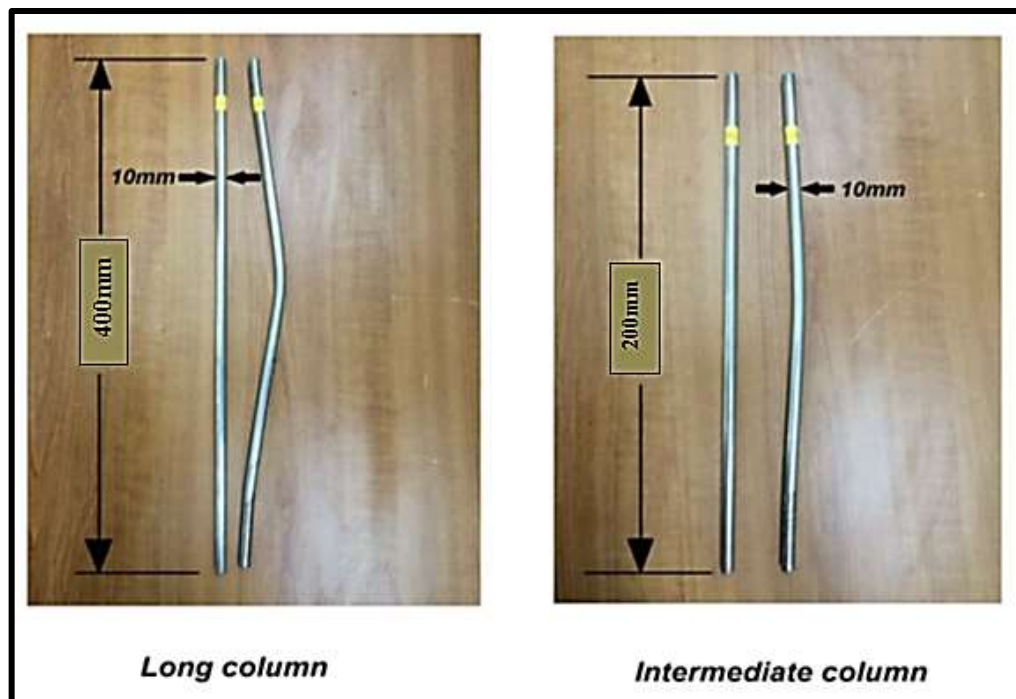
Figure (3-5): Buckling specimen for long and intermediate columns.

Table (3-3): Buckling specimen for different lengths and daimeters.

No.	Lt (mm)	Le(mm)	D(mm)	A(mm^2)	I(mm^4)	Type of column
1	400	280	10	78.539	490.87	Intermediate
2	380	266	10	78.539	490.87	Intermediate
3	330	231	10	78.539	490.87	Intermediate
4	340	238	10	78.539	490.87	Intermediate
5	500	350	10	78.539	490.87	long
6	480	336	10	78.539	490.87	long
7	430	301	10	78.539	490.87	long
8	440	308	10	78.539	490.87	long

Different specimen lengths exist to get different slenderness ratios (L_e/R) in order to simulate the long and intermediate samples buckling behavior; results are shown in tablet (3-3) and (3-4).

Table (3-4): Slenderness ratios for buckling specimens.

Item	L t (mm)	L (mm)	S.	Type of column
1	500	350	140	Long
2	480	336	134.4	Long
3	430	301	120.4	Long
4	440	308	123.2	Long
5	400	280	112	Intermediate
6	380	266	106.2	Intermediate
7	330	231	92.4	Intermediate
8	340	238	95.2	Intermediate

There are two groups of buckling specimens used in this study. Group (1) as received (without corrosion). Group (2) corroded specimens, which embedded in soil Figure (3-7) for (60) days and then subjected to increased buckling load. The chemical analysis of the soil was conducted in Iraq Geological Survey Authority, where the test results were (SO_3= 0.20 %), (PH= 8.25) and (T.D.S = 0.4%).

Figure (3-6): Specimens in soil.

3.5 Buckling Tests - Rig

The buckling test-rig shown in Figure (3-8) was used in the work. Figure (3-9) shows the schematic diagram. The Test-Rig consists of the following parts:-

1- Torsion system.
2- Compression system.

Figure (3-7): Machine of buckling test-rig used in this work
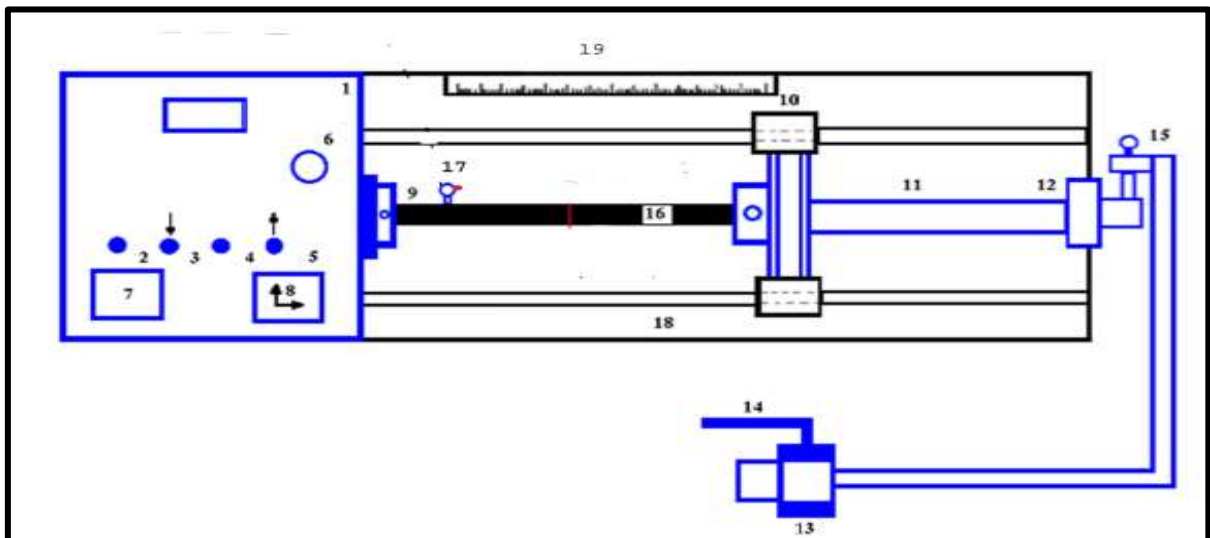
Figure (3-8): Diagram of buckling test-rig used.

Buckling test-rig Components consist of:

1- Control panel for torsion system

2- Power motor indicator

3- The engine rotation is clock wise direction

4- Manually start the engine

5- The main engine operation platform

6- Power and power cut platform

7- Engine speed indicator

8- Two-speed switch

9- Holding gripe

10- Specimen location mechanism

11- Compression screw shaft

12- Flange

13- Hydraulic pump

14- Hydraulic pump lever

15- Pressure gauge

16- Buckling specimen

17- Digital dial gauge indicator

18-Compressive conjunction tool

19- Specimen length measurement rule

The bucking test-rig contained a torsion system: Consists of an electrical motor of (0.5 KW), operating at two different speeds, low speed (17 r.p.m) and another high-speed (34 r.p.m) and when the electrical motor starts, it causes movement in two different directions clockwise and counterclockwise. A cycle-counter indicator (indicates the number of cycles), is fixed in the front of the control panel. The register digits are (99999.9), it refers to the number of cycles during the test. Figure (3-10) shows the torsion system of the test-rig.
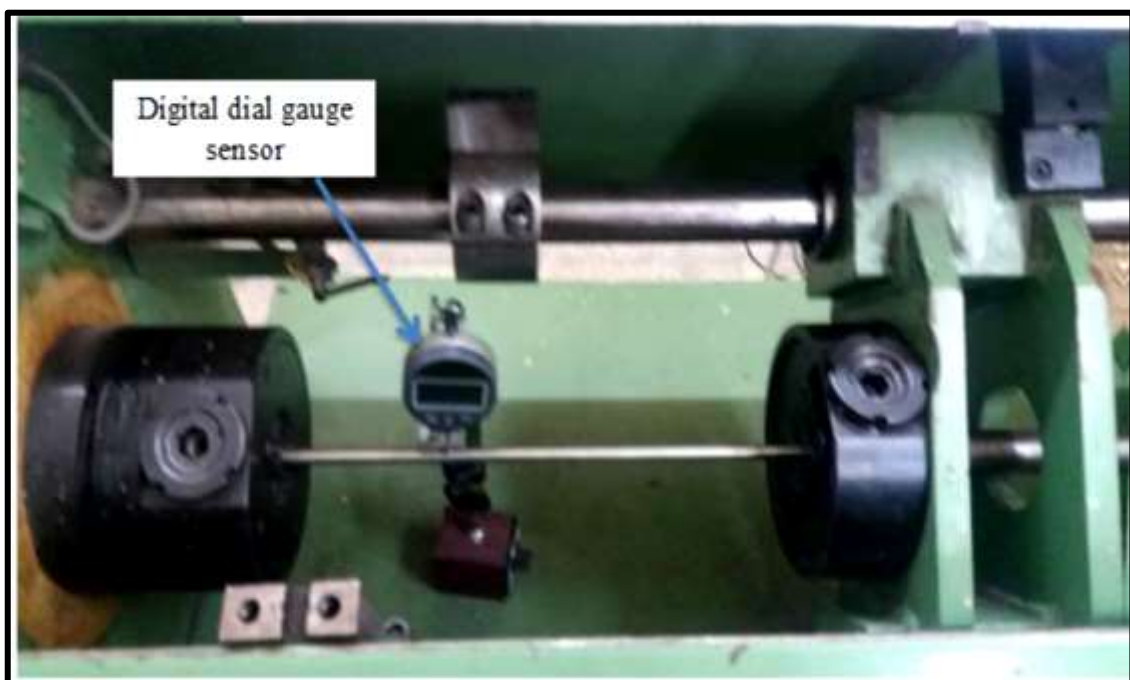
Figure (3-9): Torsion system of the test-rig.

The torque applied in this system can be found from the motor power using the following procedure:

$$P = \omega.T \quad \text{...(3-1)}$$

P: power (watt)

ω: angular velocity (rad/s)

$$\omega = \frac{2\pi N}{60} \quad \text{...(3-2)}$$

N: number of cycle (rpm)

The system of compression includes manual hydraulic pump connected to an analog gauge of maximum pressure up to (315 bar). It uses the shaft screw to transfer pressure from the pump in the jaw that supports the sample. Figure (3-11) displays the compression system.
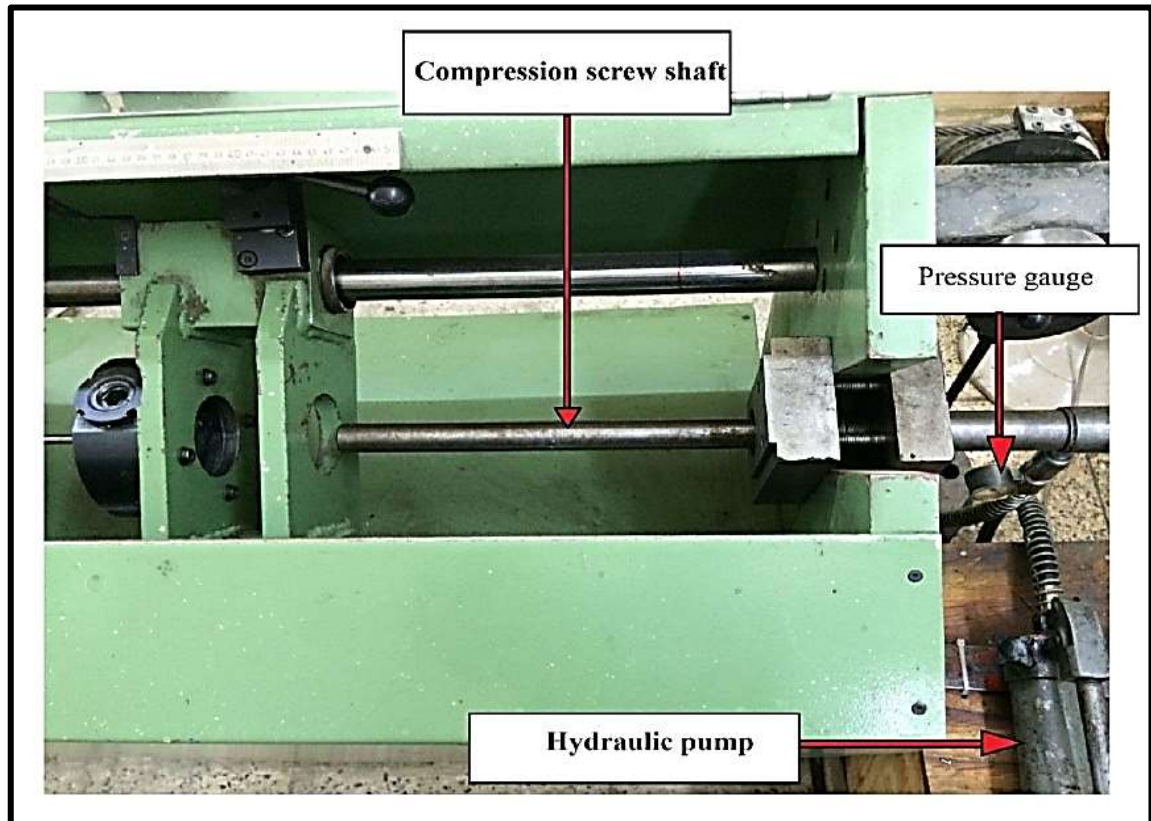
Figure (3-10): Compression system sections

When lateral deflection reaches 1% of the total length column then the test stops automatically using alarm leaser system. Pest on previous works done use this value failure definition. This is called the critical buckling of the columns. When lateral deflection exceeds this ratio (1%L), the sample fails (K. H. Al-Jubori; 2005).

Shot Peening Treatment

Shot peening is a cold working process where the worked material is peened with spherical shots to introduce compressive residual stresses, hardening and remove surface layers. Shot peening improve the mechanical properties such as stress corrosion cracking. Shot peening is widely used in

many industries such as automobile, aircraft and machines (Robert L. Mott, 2004). Shot peening is used to create residual compressive stresses on the surface of materials and these residual compressive stresses stay in the material whether the load affected on the member or not. The residual stress induced by the shot peening process is the function of material and mechanical conditions. Shot peening process is impacting a surface of material with shot (metallic cast steel balls, ceramic particles, glass) with adequate force to make plastic deformation. It operates by the technique of plasticity, each particle functions as a ball-peen hammer. The magnitude of the residual compressive stress induced and the depth of induced layer depend greatly on the peening intensity. Peening intensity is defined as a measure of the kinetic energy within a stream of peening media (shot). Peening intensity depend on the (shot size, shot speed, shot hardness, impact angle, shot flow rate, coverage, etc.). Shot peening application is in (Axles, drive shafts, gears, Turbine blades, Aerospace industry, Heavy load applications, and Components subjected to a cyclic stress) (Hussain Abdulziz, 2009)

Shot peening treatment are conducted by using centrifugal wheel system. Diameter of wheel 590 mm, and operating speed 1435 r.p.m. The shot flow rate is varied to obtain various shot peening intensities. In the current work Shot blasting Machine (model STB-OB) as shown in Figure (3-11).
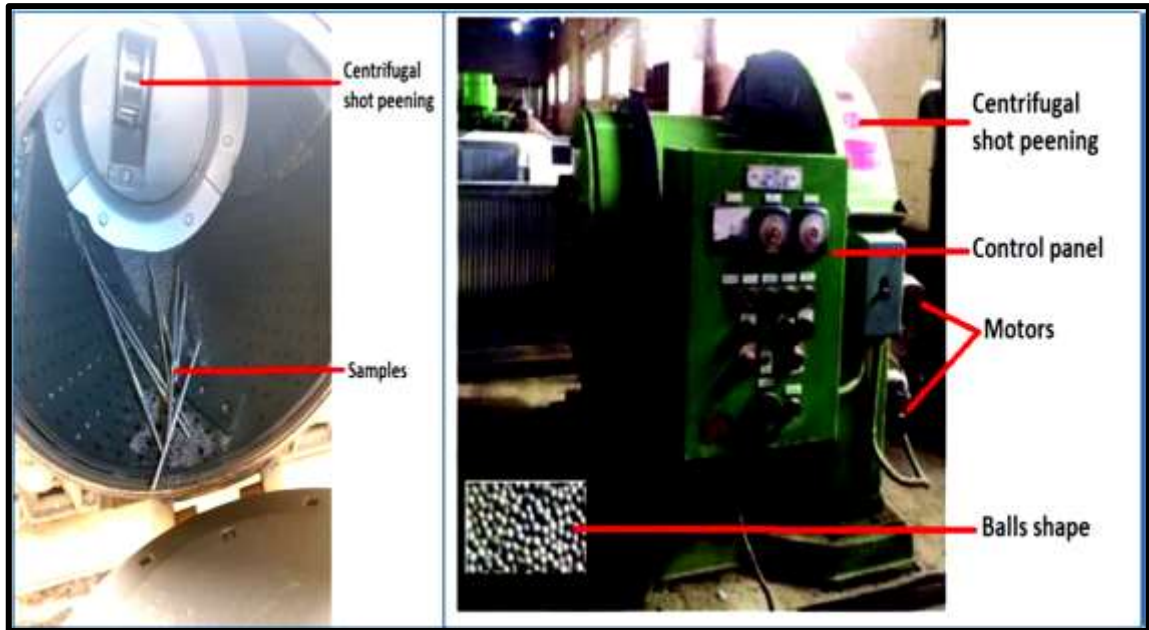
Figure (3-11): Shot peening machine.

3.6 Operation of laser alarm system

Laser used as an essential component in an electrical circuit system. Laser ray radiate through long distance without scattering effect and the ray is almost invisible. Only the radiation point and incident point are visible. Through this type of insurance and security, the border can be made invisible to legitimate sensitive areas. There are two parts of the system. One is transmitter and other is receiver. Where the transmitter is installed on the electronic digital caliper device held within the buckling test rig machine. The receiver part is a sensitive type of LDR is held within the buckling test rig, and in turn, it is part of the transmitter, in exchange for part of the sender and perpendicular to the test specimen samples.

After the test specimen is installed in the test-rig and the pointer of the dial gauge indicator is located at distance 0.7 of the effective length from the fixed end, the initial deflection was read and recorded.

When operated the laser system for the transmitter part installed on the electronic digital caliper device at a distance of 0.7 of the effective length

of the fixed end too. So as to make the laser beam comes into contact with the test specimen surface. Then raise the laser beam by the electronic digital calipers amount of initial deflection plus 1% of the effective length of the test specimen, were this represents a critical buckling load.

When the test start operating the electric motor with a low speed (17r.p.m.), an axial dynamic compressive pressure gradually applied under control load on the specimen by a hydraulic pump system. When the lateral buckling deflection reaches to the laser beam level, the test specimen will cut off the laser beam path, and here begin the electrical system working through a sound buzzer to alert that the test specimen has reached the amount of the critical lateral buckling deflection, which generated by the critical buckling load, then the electrical motor is switched-off manually.

Without this electrical system cannot determine the critical load with high accuracy, which proven that the electric laser system as a safety for critical loads. The system aims to reduce the side effects of the deformation as a result of high loads.
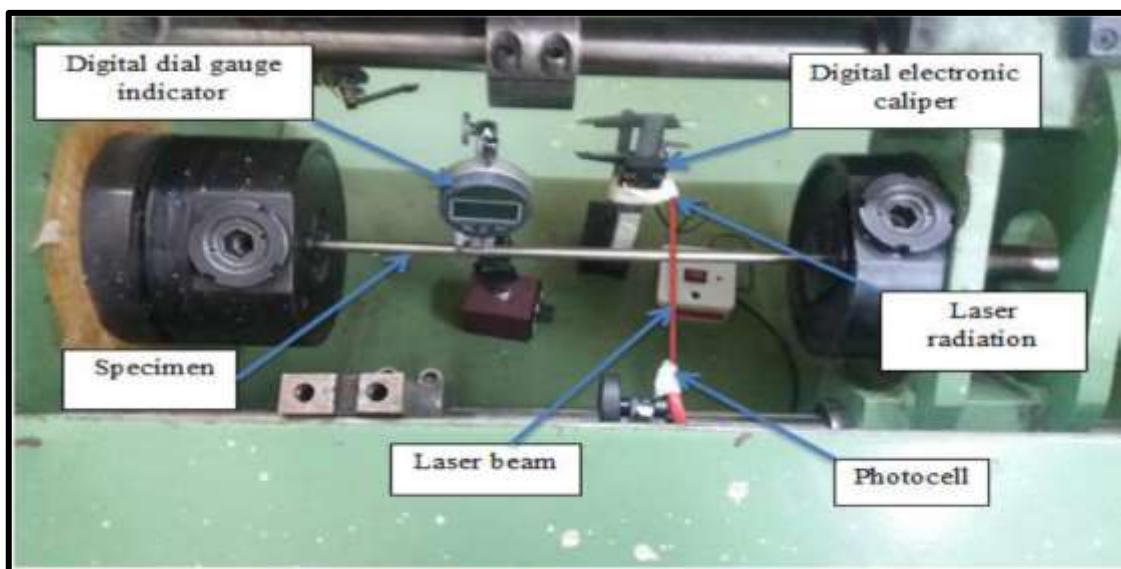

Figure (3-12): Laser alarm system.

Chapter Four

Results and Discussion

Chapter Four
Results and Discussion

The following results contains analysis of the obtained (experimentally and theoretical) data and discussions for both cases of the dry buckling and buckling corrosion interaction for 304 stainless steel alloy. The theoretical results introduced to Perry-Robertson theory, Euler and Johnson formulas, and the resulted data of these tests will be utilized in ANSYS program used to investigate buckling by numerical analysis.

4.1 Mechanical properties testing (tensile test)

The results for mechanical properties were made by using the WDW-200E tensile rig. Table (4-1) shows results of the tensile test for dry and corrosion state of 304 stainless steel alloy column specimens. The results listed are an average of three readings.

Table (4-1): Mechanical properties Results for columns without corrosion and Columns with 60 days corroded.

304 stainless Steel	δu (Mpa)	δy(Mpa) 0.2%proof Stress	E (Gpa)	G (Gpa)	μ Poi-ratio	ϵ % Elongation
Standard ATM A370 Thomas H.K.Kang,Kenneth (2014)	621	290	193-200	74-77	0.30	55
Experimental Dry	628	311	200	75	0.30	51
Experimental Corrosion	591	288	198	74	0.29	58
Experimental Corrosion+sp+l	599	305	199	76	0.31	53

It can be seen in table (4-1), that corrosion treatment reduces the mechanical properties of the above alloy surface, because of corroded weakens of surface and decreasing its hardness and increasing roughness. It was clear that the results of corroded specimens were lower than that of un-

corroded members. Increasing a corrosion time tend to reduce the mechanical properties. The specimens [3 specimens] of 2 months corroded has approximately 2.53 % reduction in ultimate forces compared to a un-corroded specimens. (Hussein. F. A. and Jack Champaigue, 2001) had found that a reduction in ultimate strength of 3061 Al-alloy was 2.7% due to corrosion time in soil of 60 days.

4.2 Dynamic Buckling Load

(24) Specimens were tested under increasing compressive dynamic loading. The machine has only two speeds (17r.p.m) and (34r.p.m.). The speed of (17r.p.m.) was adopted because the buckling phenomenon is not obvious in high speeds, uncontrollable and besides the designing lives factors can not be controlled. The specimens were prepared with different slenderness ratios, for testing under increasing loads. Table (4-2) shows the results for the specimens tested under increasing compressive dynamic loads for long columns (304 stainless steel alloy).

Table (4-2): specimens tested results under increasing compressive dynamic loads for long columns (304 stainless steel alloy)

SP NO.	L mm	L_{eff} mm	D mm	A mm^2	S.R	P_{cr} N	δin mm	Δcr mm 1% of L
1	500	350	10	78.539	140	5236	0.33	5
2	480	330	10	78.539	134.4	5818	0.3	4.8
3	460	322	10	78.539	128.8	6649	0.22	4.3
4	440	308	10	78.539	123.2	6981	0.24	4.4

It is clear from table (4-2) that increasing in slenderness (SR) resulting in reducing the critical buckling load. This finding agreed well

with the provirus work done in this field. While table (4-3) gives the results of dynamic buckling under increasing compressive load for intermediate specimens (304 stainless steel alloy).

Table (4-3): dynamic buckling results under increasing compressive load for intermediate specimens (304 stainless steel alloy)

Sp NO.	L mm	Leff Mm	D Mm	A mm^2	SR	Pcr N	δin mm	δcr mm 1%of L
1	400	280	10	78.539	112	6723	0.28	4
2	380	266	10	78.539	106.2	7480	0.3	3.8
3	360	252	10	78.539	100.8	7812	0.21	3.3
4	340	238	10	78.539	95.2	8311	0.18	3.4

From table (4-2) and (4-3), it is noticed that the specified load for failure decreases whenever the columns were changed from intermediate to long columns. The intermediate columns within the inelastic region need more stress to reach failure, so, whenever the slenderness ratio approaches intermediate columns, failure stress is more, and when the value of slenderness ratio increases, the failure stress decreases. So, the control system ensures safety when access lateral buckling to the extent is known by shut down the test-rig automatically. Also, it is observed that the initial shaft deflection has an important effect on the critical dynamic compressive stress and also when increasing the initial deflection reduces the critical torsional load.

When the axial load is gradually increased, it reaches the stage where the column begins to buckle. The load that causes the column buckle is called buckling load or possible to be called critical load and here it is possible to say that the column is under an elastic instability. Referring to figure (4-1)

the value of buckling load is low for long columns, and relatively high for intermediate columns.
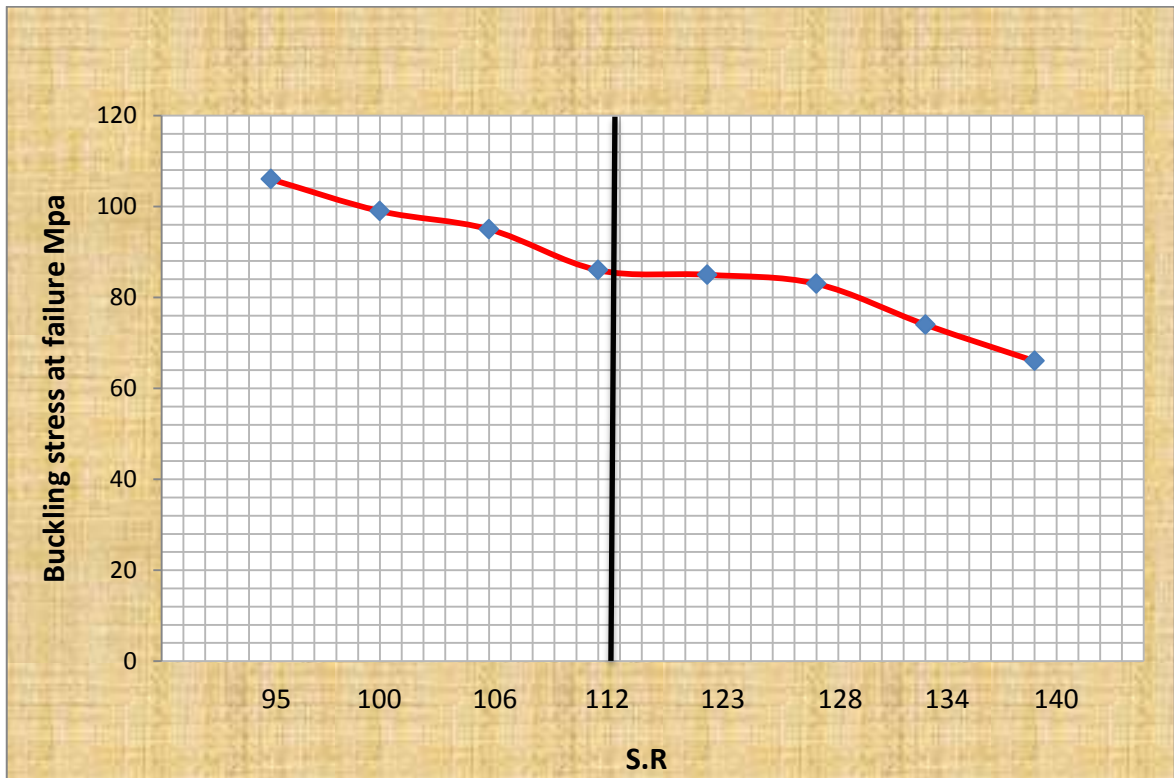

Figure (4-1): Dynamic compression buckling stress for (304 stainless steel alloy) columns

4.3 Corroded Columns Buckling Test Results

Tables (4-4) and (4-5) present the experimental results of dynamic buckling test of (304 stainless steel alloy) for long and intermediate column specimens without corrosion effect (as received). They also, show the experimental results of buckling test of corroded columns (group 2). It can be seen from tables ((4-4) and (4-5)), corrosion underground leads to the reduction in critical buckling load. The buckling life (cycle) of pre-corroded column specimens decreased compared with that of as reserved specimens. The reason for this finding is that the obstruction of column corroded surface to ensure the buckling load. It appears that the corrosion condition at 60 days gives a small reduction of dynamic buckling resistance

for the specimen of (group 2) compared with non-corroded columns specimen (group 1).

Table (4-4): Corrosion-buckling interaction for long columns (fixed-pinned)

SP NO.	AS received Group(1)			60 days corrosion Group(2)			Reduction in critical buckling load %
	Pcr (N)	δin mm	δcr mm	Pcr (N)	δin mm	δcr mm	60 day
1	5236	0.33	5	4837	0.65	5	7.62
2	5818	0.3	4.8	5581	0.48	4.8	4.06
3	6649	0.22	4.6	6521	0.31	4.6	1.92
4	6981	0.24	4.4	6754	0.4	4.4	3.25

Table (4-5): Corrosion-buckling interaction for intermediate columns (fixed-pinned)

SP NO.	As-received Group(1)			60 days corrosion Group(2)			Reduction in critical buckling load %
	Pcr (N)	δin mm	δcr mm	Pcr (N)	δin mm	δcr mm	60 day
1	6723	0.28	4	6409	0.61	4	4.67
2	7480	0.3	3.8	7271	0.38	3.8	2.79
3	7812	0.21	3.6	7555	0.4	3.6	3.29
4	8311	0.18	3.4	8128	0.22	3.4	2.2

The effect of corrosion can be clearly noted that the effect done by the dynamic buckling loads as reported in the tables ((4-4) and (4-5)). The value of these buckling properties is reduced by about 1.92% to 7.62% for

60 days for long corroded columns respectively and from 2.2 % to 4.67 % for 60 days for the intermediate corroded columns. Figure (4-2) illustrates the values of buckling load reduction due to 60 days corroded in soil.
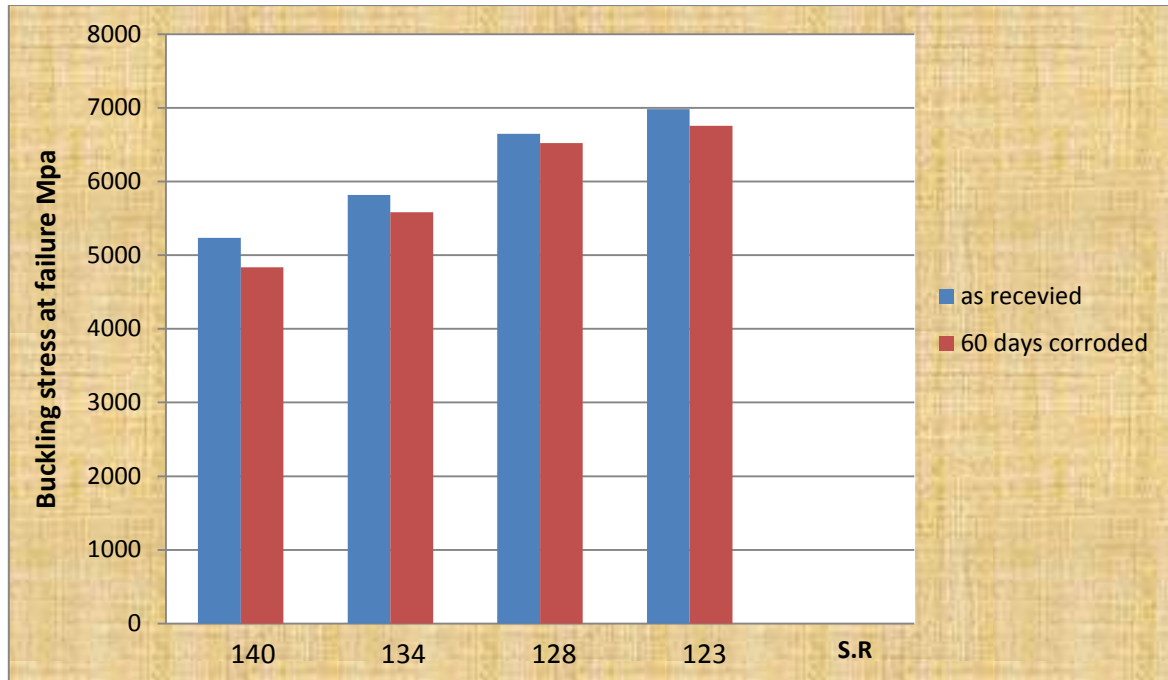

Figure (4-2): Corrosion-buckling interaction for long columns.

While figure (4-3) presents the reduction in buckling load for intermediate column due 60 days corrosion in soil.
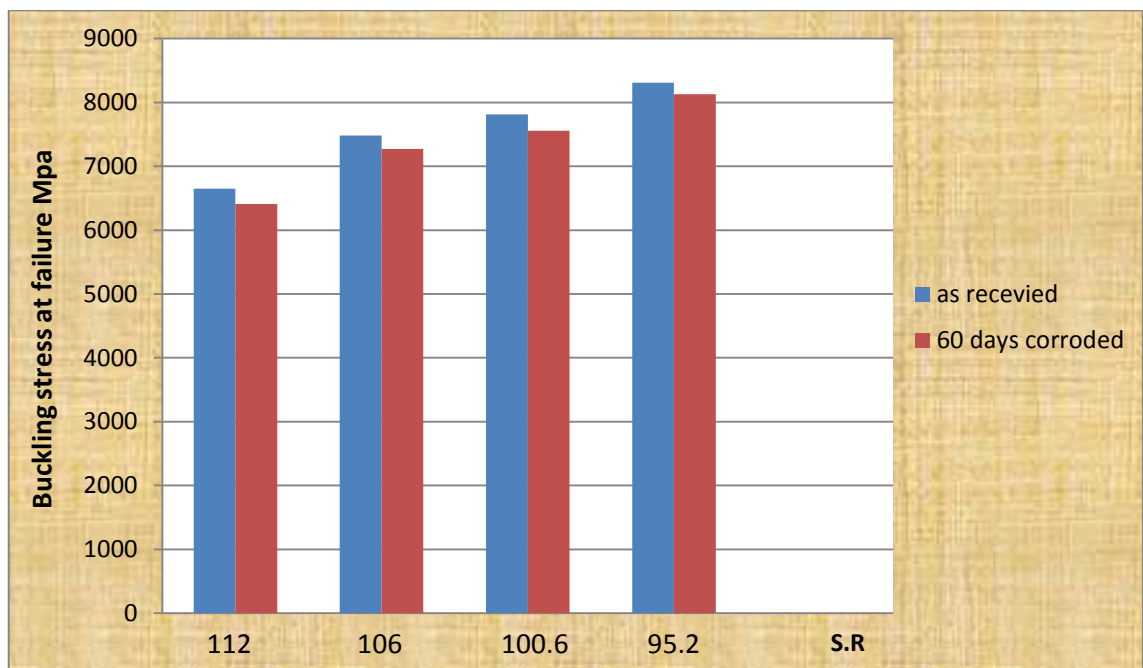

Figure (4-3): Corrosion-buckling interaction for intermediate columns

The corrosion phenomena strongly affect buckling behavior of columns subjected to a dynamic increase compression load. On the basis of the experimental results, it has to be remarked to show the importance of corrosion effects on the critical buckling loads, see Figures (4-2) and (4-3).

4.4 Application of Perry- Robertson formula

When comparing the Perry-Robertson results with the experimental critical load value in the two cases (no wear, and with corrosion) the prediction of Pcr due to Perry-Robertson (PR) does not match the experimental results. After arithmetic verification and estimation of Pcr under dynamic loading by Perry-Robertson, the formula is multiplied by a factor (1.3) to match the experimental results.

Table (4-6): Comparison between Perry-Robertson results with experimental critical load value for long columns.

Sp No	L	D	P_{cr} EXP		P_{cr}(N) *Perry-Robertson*		P_{cr}(N) *Perry-Robertson* with S.F of 1.3	
	mm	mm	As-received	60 days	As-received	60 days	As-received	60 Days
1	500	10	5236	4837	6294.9	6166.5	4842.2	4743.4
2	480	10	5818	5581	7021.2	6869	5400.9	5283.9
3	460	10	6649	6521	7345	7181.5	5650.6	5524.2
4	440	10	6981	6754	7963.9	7776.9	6126	5982.2

Table (4-7): Comparison between Perry-Robertson results with experimental critical load value for intermediate columns.

Sp No	L	D	P_{cr} EXP		P_{cr}(N) Perry-Robertson		P_{cr}(N) Perry-Robertson with S.F of 1.3	
	mm	mm	AS received	60 days	AS received	60 days	AS received	60 days
1	400	10	6723	6409	9432.767	9181.2	7255.974	7062.4
2	380	10	7480	7271	10301.75	10005	7924.425	7696.2
3	360	10	7812	7555	11272.18	10918	8670.905	8398.5
4	340	10	8311	8128	12349.52	11922	9499.631	9170.8

For S.R. greater than 112 the column may change to become long column. The value equal to 52MPa can limit the type of column, i.e. greater than 52MPa columns are said to be long and less than this value are called intermediate columns.

Figure (3-13) displays the relation of stress at failure and slenderness ratio as presented by Perry-Robertson formula for a long and intermediate columns compared with experimental results made (304 stainless steel alloy) with one end pinned and the other fixed (K = 0.7), having a yield strength of = 300 MPa
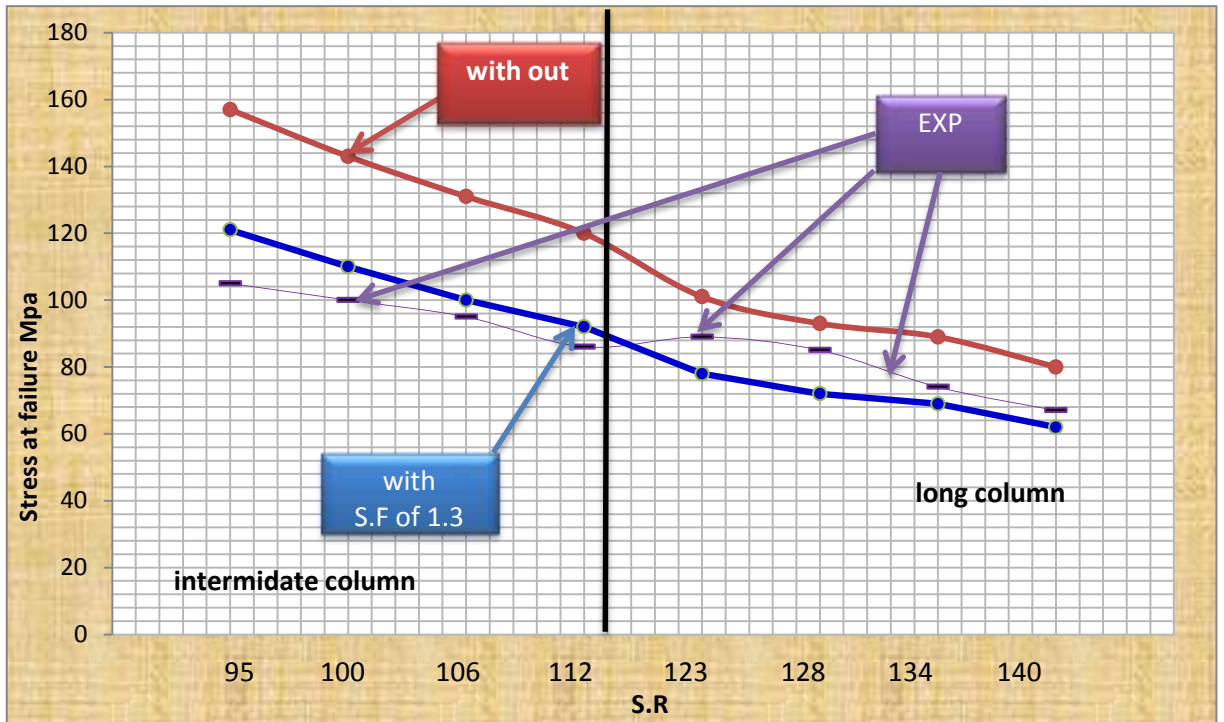
Figure (4-4): Perry-Robertson curve with the experimental results for 304 stainless steel alloy.
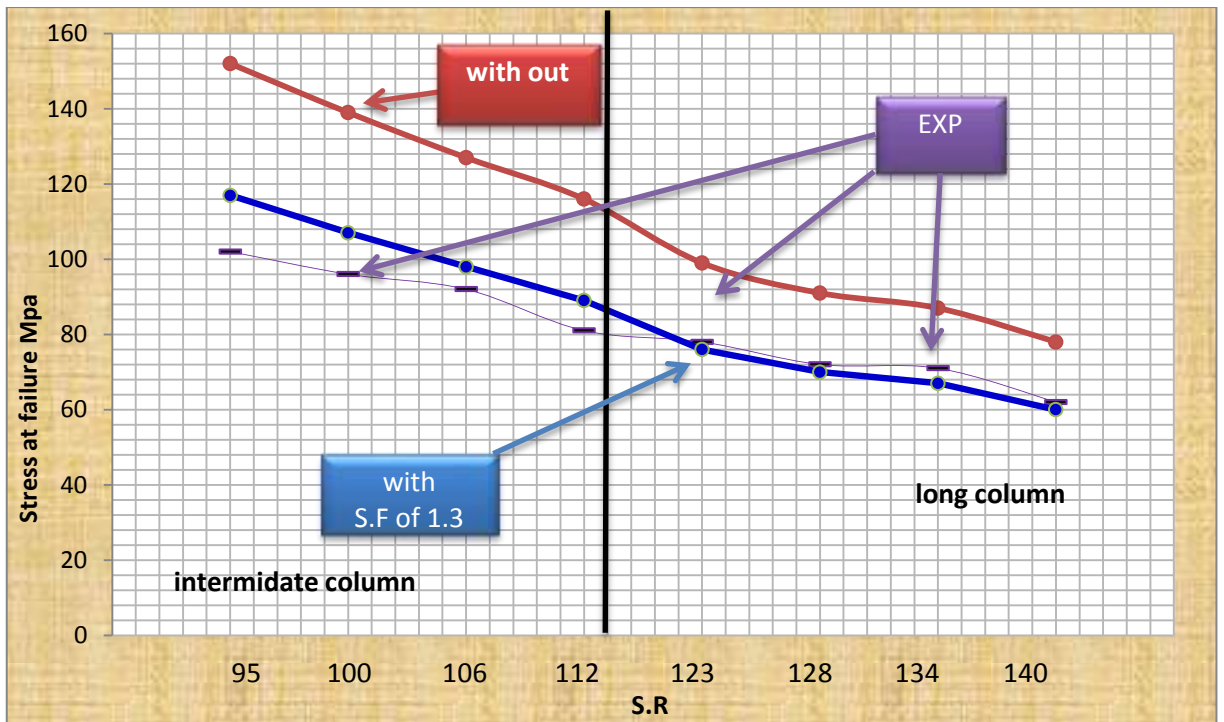

Figure (4-5): Perry-Robertson curve with the experimental results for 304 stainless steel alloy (corrosion).

4.5 Euler and Johnson Application to Experimental Data

Euler's and Johnson's theories can be used for estimation of critical buckling stress, and it can be useful in the early stages of the design process. This study divides members into intermediate and long length, where Johnson's equation is valid with intermediate length and Euler's equation is valid for long members. The tangent point between Euler curve and Johnson curve for 304 stainless steel alloy member with a yield stress of 300MPa is (S.R. = 112). Intermediate columns are defined by the minimum slenderness ratio, and for 304 stainless steel alloy, the value is equal (S.R. = 52) both defined as long members, i.e. Euler equation can be used but it should be noted that they are also within Johnson validations area. Johnson's equation estimates the critical buckling stress for the test parts to be lower than the critical buckling stress estimated with Euler's equation. The estimation of P$_{cr}$ according to above theories can be listed in tables (4-8) and (4-9).

Table (4-8): Comparison between Euler results with experimental critical load value for long columns.

Sp No	L	D	P_{cr}(N) EXP		P_{cr}(N) Euler		P_{cr}(N) Euler with S.F of 3	
	mm	mm	AS received	60 days	AS received	60 days	AS received	60 Days
1	500	10	5236	4837	7909	7830.6	2636.5	2610.2
2	480	10	5818	5581	8897.5	8808.5	2965.8	2936.1
3	460	10	6649	6521	9345.1	9251.6	3115	3083.8
4	400	10	6981	6754	10213.9	10111.8	3404.6	3370.6

Table (4-9): Comparison between Johnson Formula results with experimental critical load value for intermediate columns.

Sp No	L	D	$P_{cr}(N)$ EXP		$P_{cr}(N)$ Johnson		$P_{cr}(N)$ Johnson with S.F of 3	
	mm	mm	AS received	60 days	AS received	60 days	AS received	60 days
1	400	10	6723	6409	23202.8	21560	7734.2	7186.6
2	380	10	7480	7271	23330.3	21670.4	7776.7	7223.4
3	360	10	7812	7555	23435.1	21761.2	7811.7	7253.7
4	340	10	8311	8128	23542.1	21853.9	7847.3	7284.6

Figure (4-5) displays the relation of stress at failure and slenderness ratio as presented by Euler and Johnson formulas for a column made of (304 stainless steel alloy) with one end pinned and the other fixed (K = 0.7), having a yield strength of σy = 300MPa
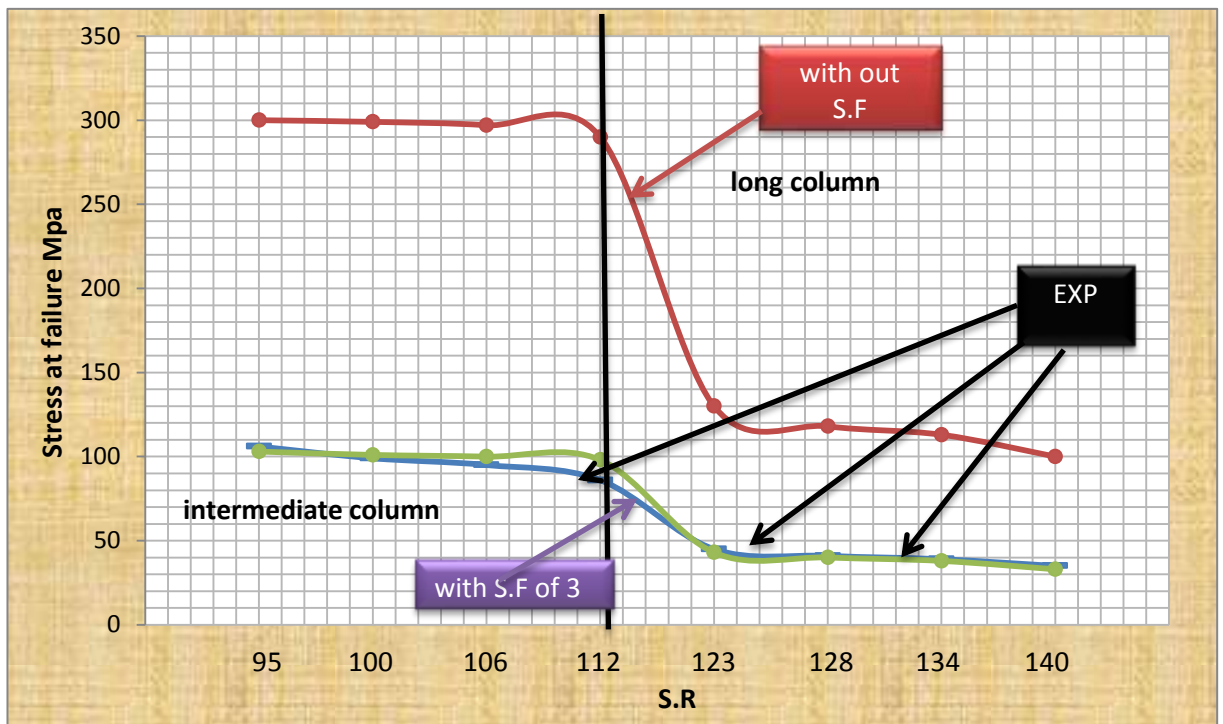

Figure (4-6): Johnson-Euler curve with the experimental results for 304 stainless steel alloy.
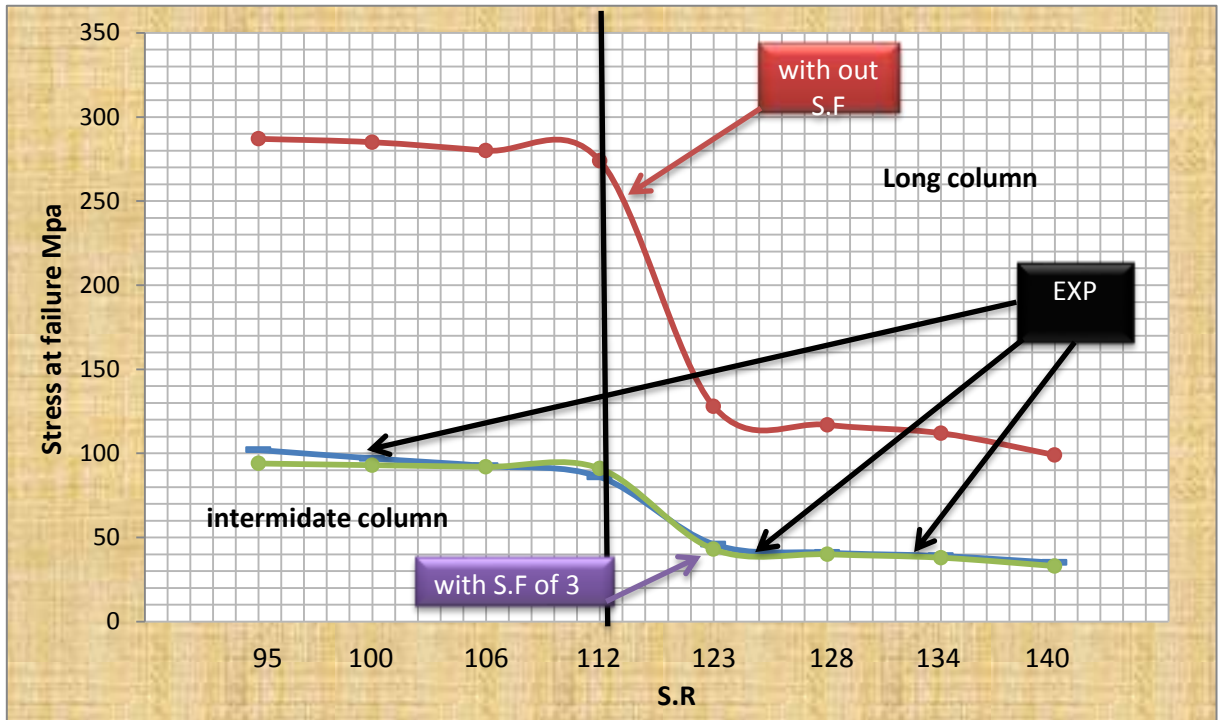
Figure (4-7): Johnson-Euler curve with the experimental results for 304 stainless steel alloy (corrosion).

4.6 Comparison between ANSYS17 and Experimental

Numerical model using ANSYS package were employed and compared with the experimental results. Tables (4-10) and (4-11) showed the numerical results of critical buckling under dynamic increasing load without factor of safety (F.S). If a factor of safety of (2) has to be taken. The table (4-10) below gives the percentage discrepancy between the experimental and numerical results. The difference might be attributed to the fact that, due to the assumption made in the ANSYS package and the difficulties to control the measurement in the experimental work and some error may occur in reading the experimental data.

Table (4-10): Comparison between ANSYS results with experimental critical load value for long columns

Sp No	L	D	P_{cr}(N) EXP		P_{cr}(N) ANSYS		P_{cr}(N) ANSYS with S.F of 2	
	mm	mm	AS received	60 days	AS received	60 days	AS received	60 days
1	500	10	5236	4837	11237	10216	5712	5107
2	480	10	5818	5581	12389	11262	6194	5631
3	460	10	6649	6521	13727	12479	6863	6239
4	440	10	6981	6754	14295	12995	7147	6497

Table (4-11): Comparison between ANSYS results with experimental critical load value for intermediate columns

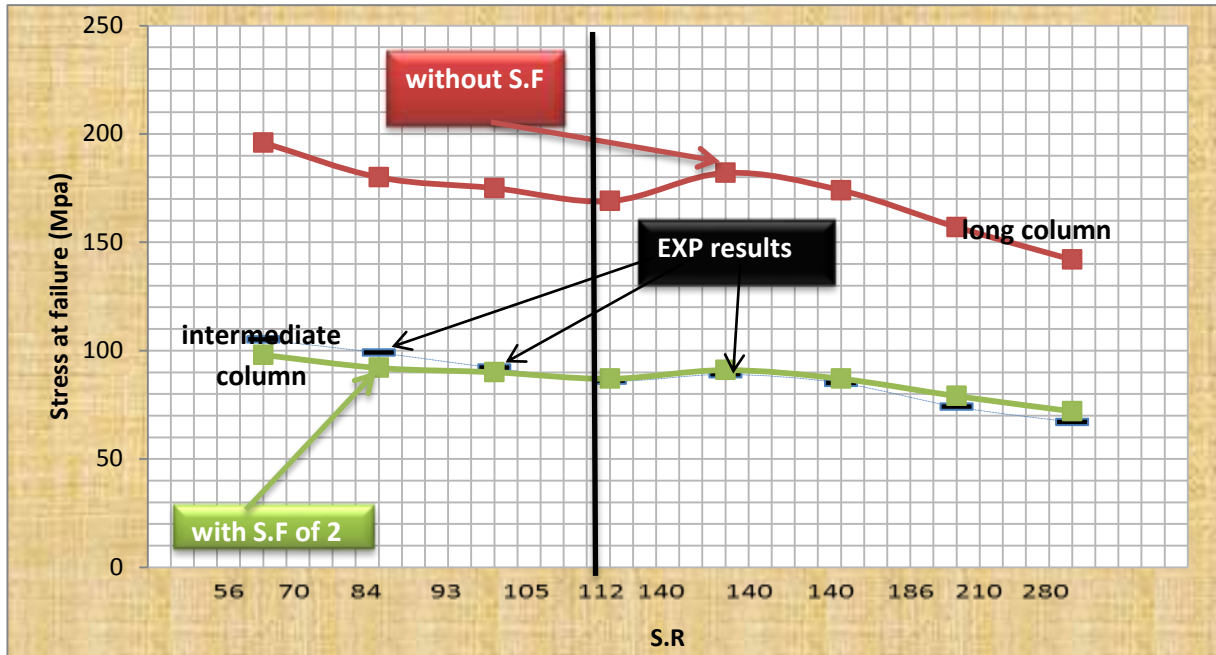| Sp No	L	D	P_{cr}(N) EXP		P_{cr}(N) ANSYS		P_{cr}(N) ANSYS of 2	
	mm	Mm	AS received	60 days	AS received	60 days	AS received	60 days
1	400	10	6723	6409	13289	12080	6645	6040
2	380	10	7480	7271	15190	13809	7595	6904
3	360	10	7812	7555	15472	14065	7736	7032
4	340	10	8311	8128	16967	15424	8483	7713

Figure (4-8A): Presents the prediction of long and intermediate columns using ANSYS package17 without and with 2 safety factors.
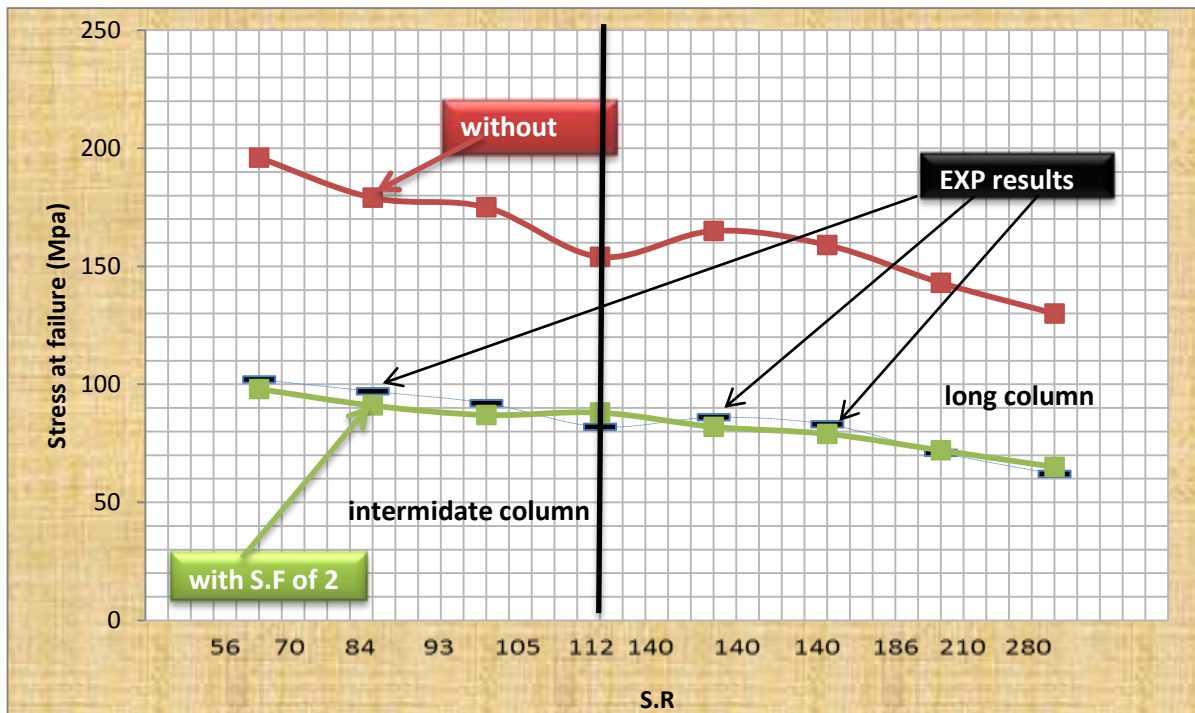

Figure (4-8B): ANSYS curve with the experimental results for 304 stainless steel alloy steel alloy (corrosion).

Figures (4-9), (4-10), (4-11) and (4-12) show the numerical results of critical buckling under dynamic increasing load without safety factor (F. S.). If a factor of safety (2) has to be applied then figures (4-9), (4-10), (4-

11), (4-12) and appendix (1) rustles give synonymous between the Stress, total deformation, Equivalent elastic strain and strain.

the ANSYS package outcomes are displaying the relation of stress at failure and the Equivalent Stress, total deformation, Equivalent elastic strain and strain energy of 304 stainless steel alloy with one end pinned and the other fixed end using (K = 0.7). The numerical results of critical buckling under dynamic increasing load without factor of safety (F. S.), as (P_{cr}= 11237,10216), (received, after 60day) respectively.
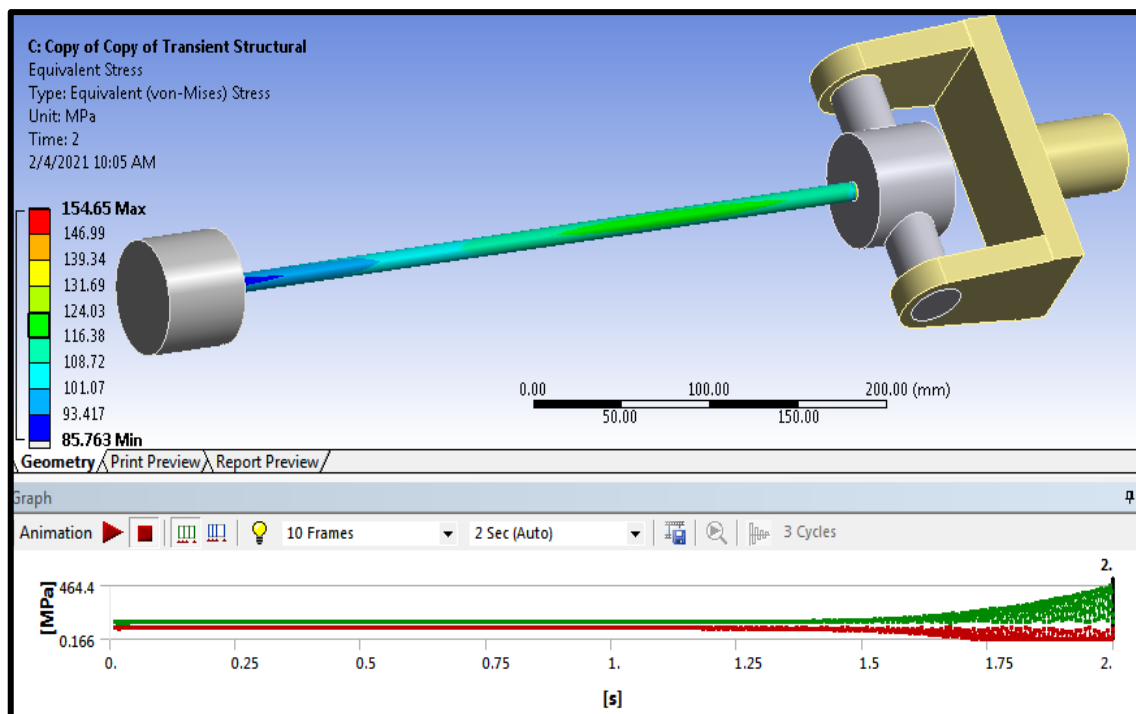

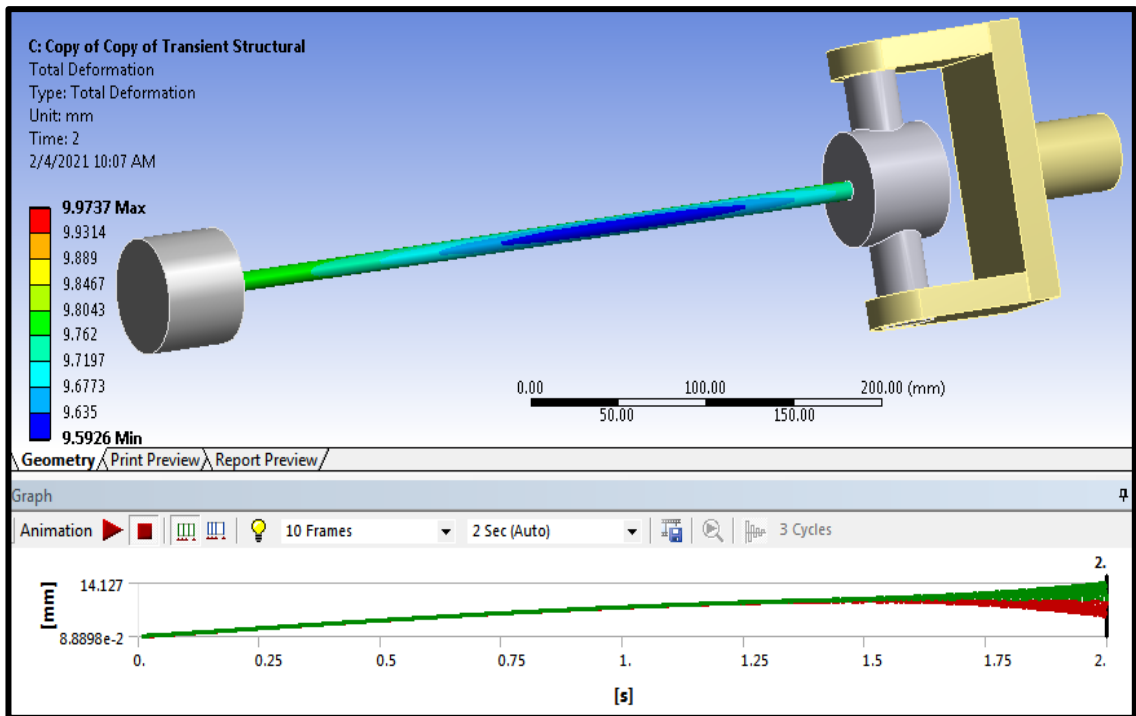**Figure (4-9): buckling mode of equivalent stress (500mm).**

Figure (4-10): buckling mode of total deformation (500mm).
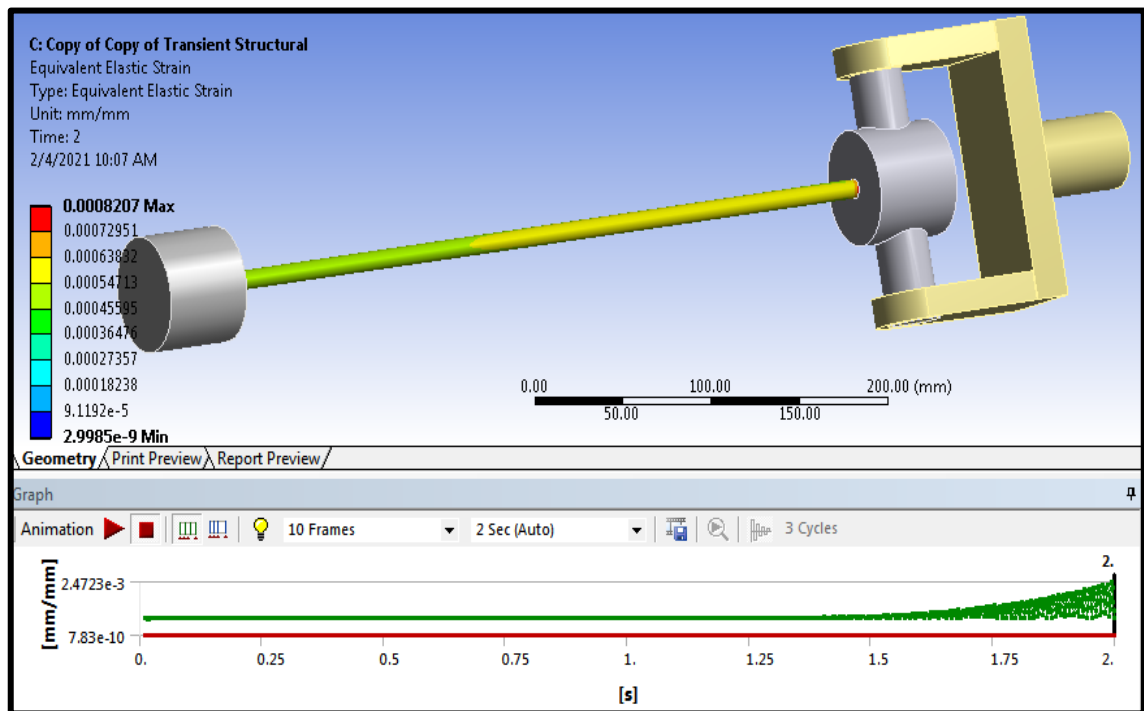

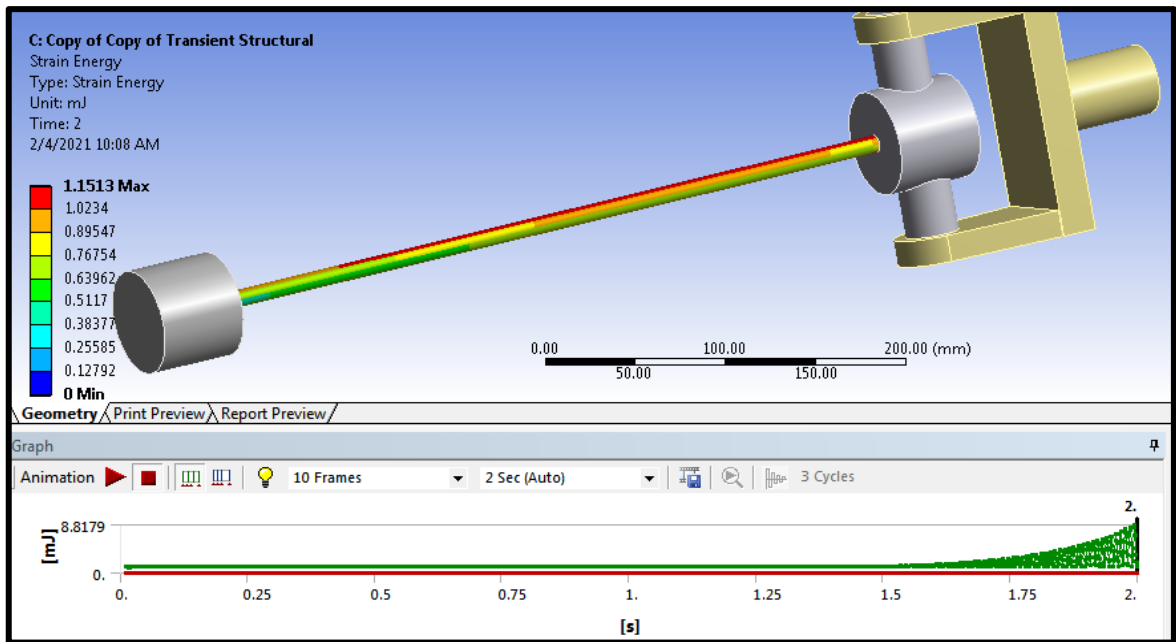**Figure (4-11): buckling mode of equivalent elastic strain (500mm).**

Figure (4-12): buckling mode of strain energy (500mm).

figures (4-13), (4-14), (4-15) and (4-16) show the numerical results of critical buckling under dynamic increasing load without safety factor (F. S.). If a factor of safety of (2) has to be applied then the figures (4-13), (4-14), (4-15), (4-16) and appendix (2) rustles give Equivalent between the Stress, total deformation, elastic strain and strain.

the ANSYS package outcomes are displaying the relation of stress at failure and the Equivalent Stress, total deformation, Equivalent elastic strain and strain energy of 304 stainless steel alloy with one end pinned and the other fixed end using (K = 0.7). The numerical results of critical buckling under dynamic increasing load without factor of safety (F. S.), as (P_{cr}= 12389,11262), (received, after 60day) respectively.
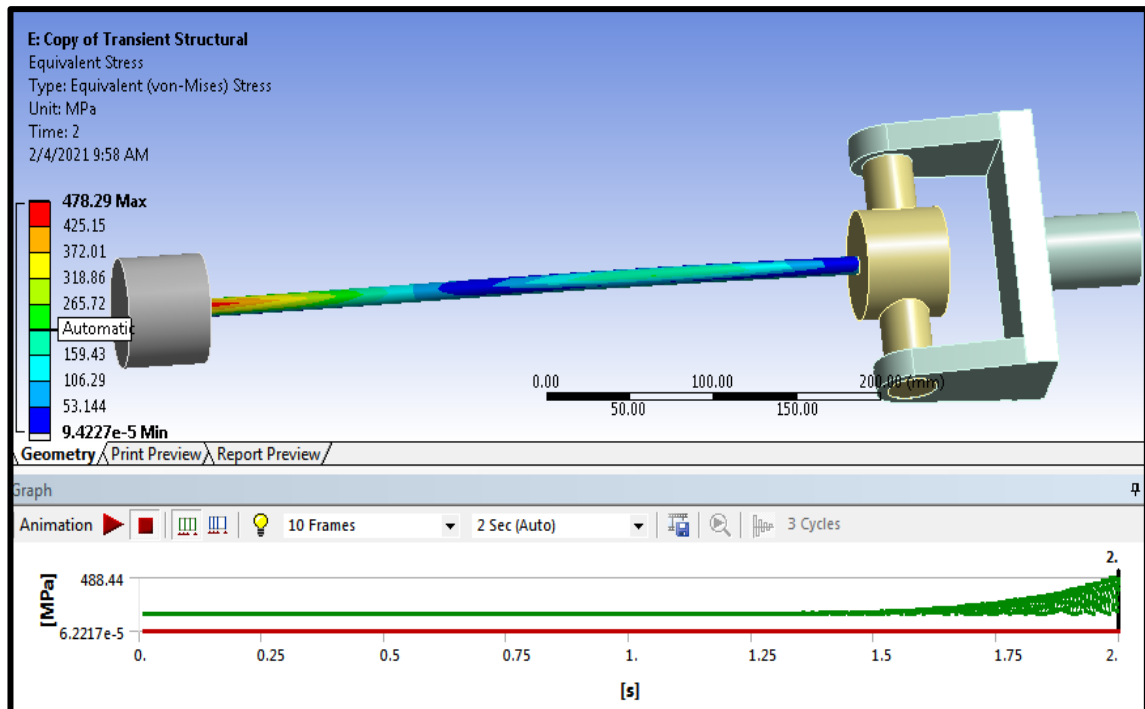
Figure (4-13): buckling mode of equivalent stress (480mm).

Figure (4-14): buckling mode of total deformation (480mm).

Figure (4-15): buckling mode of equivalent elastic strain (480mm).
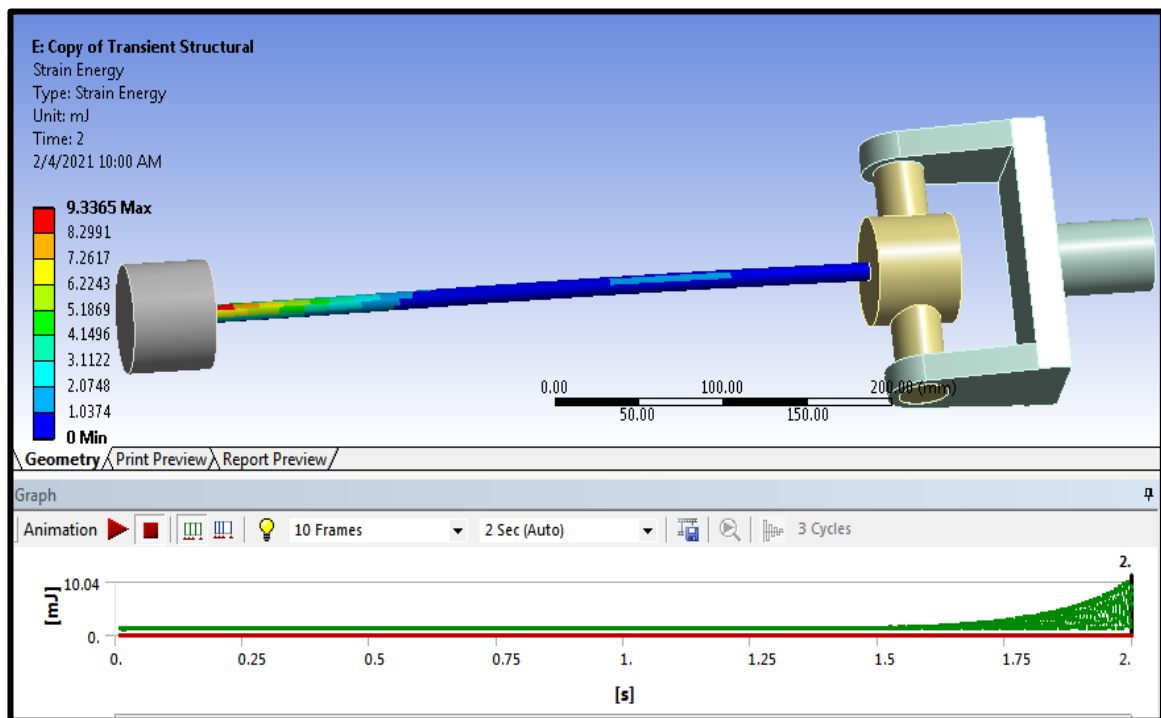
Figure (4-16): buckling mode of strain energy (480mm).

Figures (4-17), (4-18), (4-19) and (4-20) show the numerical results of critical buckling under dynamic increasing load without safety factor (F. S.). If a factor of safety of (2) has to be applied then the figures (4-17), (4-

18), (4-19), (4-20) and appendix (3) rustles give on a per between the Stress, total deformation, elastic strain and strain.

the ANSYS package outcomes are displaying the relation of stress at failure and the Equivalent Stress, total deformation, Equivalent elastic strain and strain energy of 304 stainless steel alloy with one end pinned and the other fixed end using (K = 0.7). The numerical results of critical buckling under dynamic increasing load without factor of safety (F. S.), as (P_{cr}= 13727,10216), (received, after 60day) respectively.

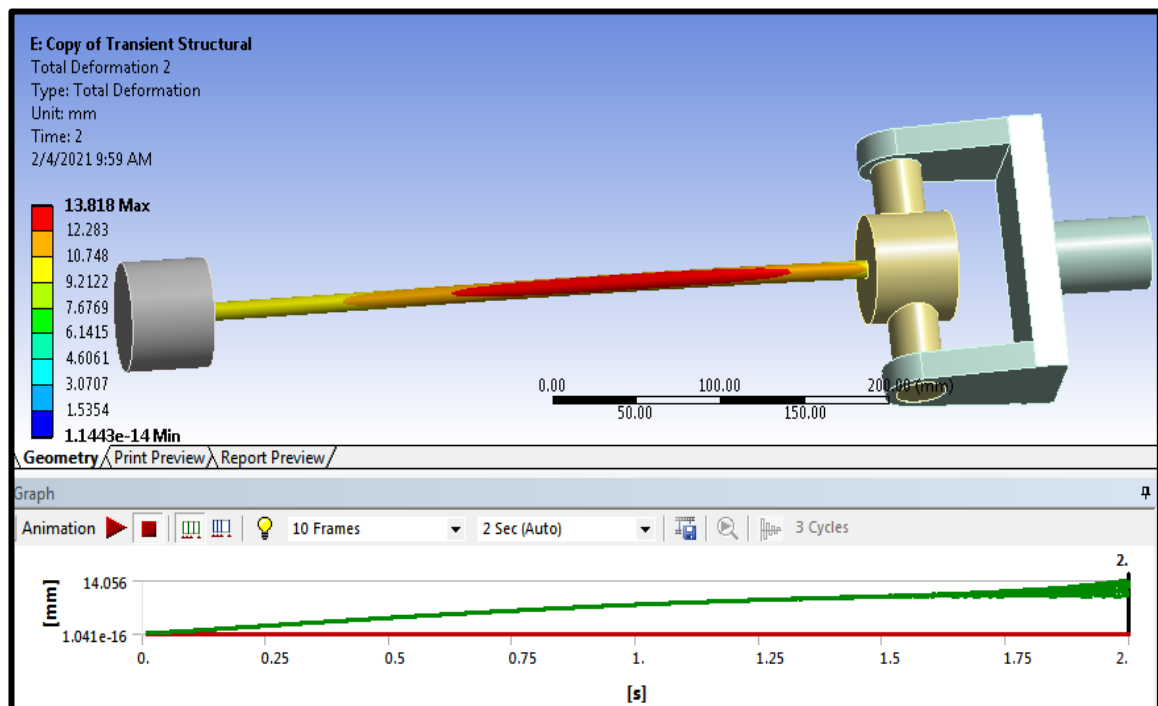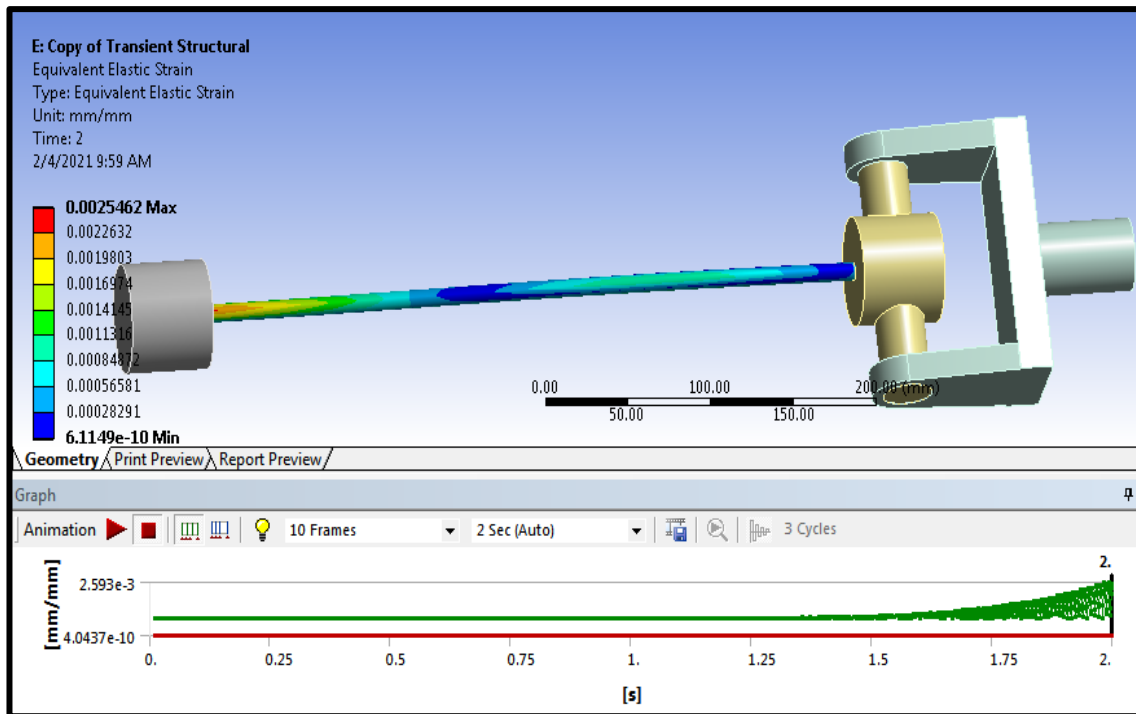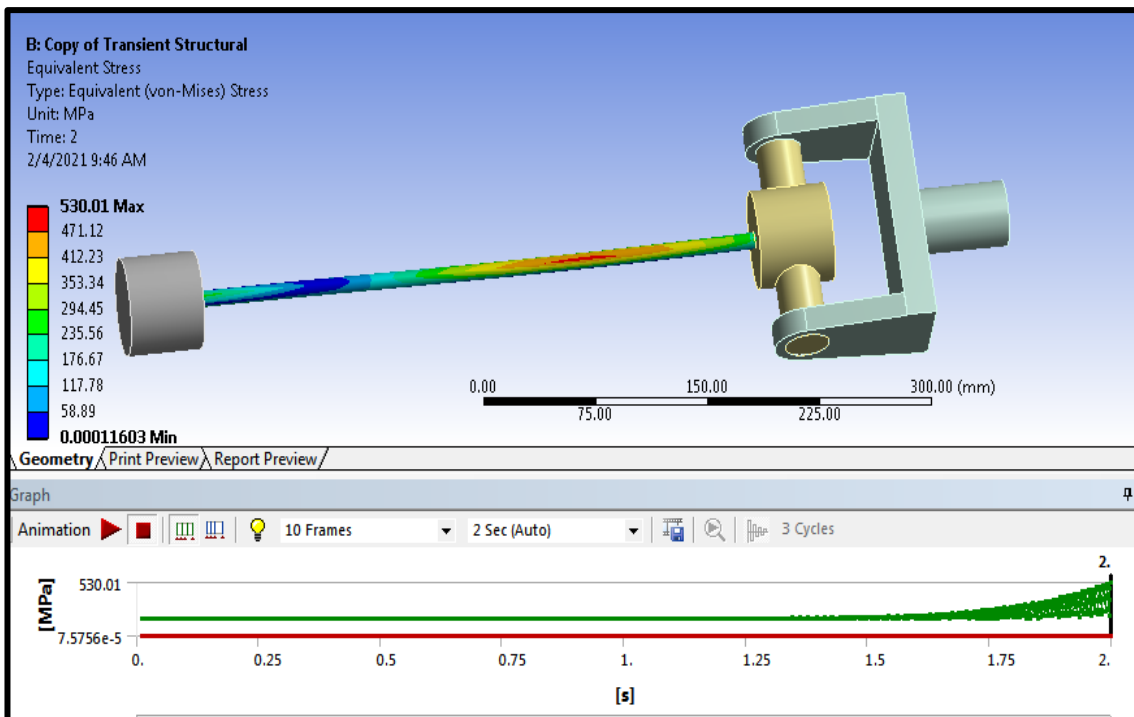**Figure (4-17): buckling mode of equivalent stress (460mm).**

Figure (4-18): buckling mode of total deformation (460mm).

Figure (4-19): buckling mode of equivalent elastic strain (460mm).

Figure (4-20): buckling mode of strain energy (460mm).

fingers (4-21), (4-22), (4-23) and (4-24) show the numerical results of critical buckling under dynamic increasing load without safety factor (F. S.). If a factor of safety of (2) has to be applied. The fingers (4-21), (4-22), (4-23) and (4-24) and appendix (4) rustles give between the Equivalent Stress, total deformation, Equivalent elastic strain and strain.

The ANSYS package outcomes are displaying the relation of stress at failure and the Equivalent Stress, total deformation, Equivalent elastic strain and strain energy of 304 stainless steel alloy with one end pinned and the other fixed end using (K = 0.7). Numerical results of critical buckling under increased dynamic load without safety factor (F. S.) recorded (P_cr = 14295) for the samples as extracted from the factory and the ones were buried for 60 days recorded (P_cr = 12995), respectively.

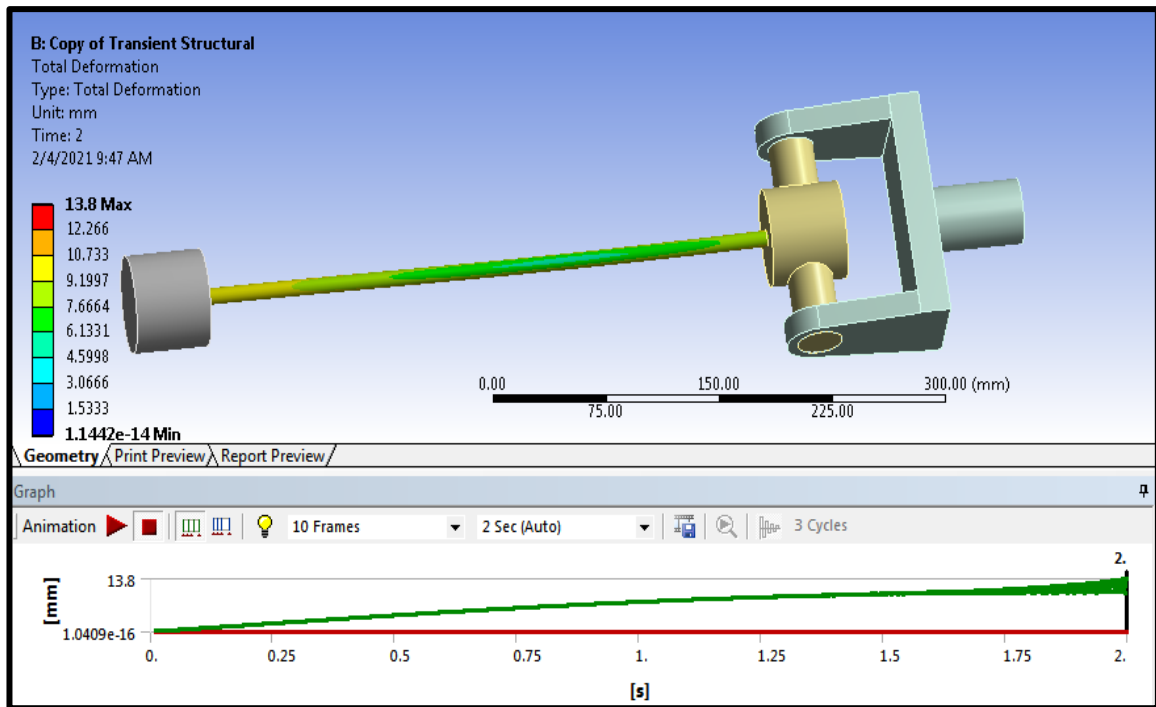**Figure (4-21): buckling mode of equivalent stress (440mm).**

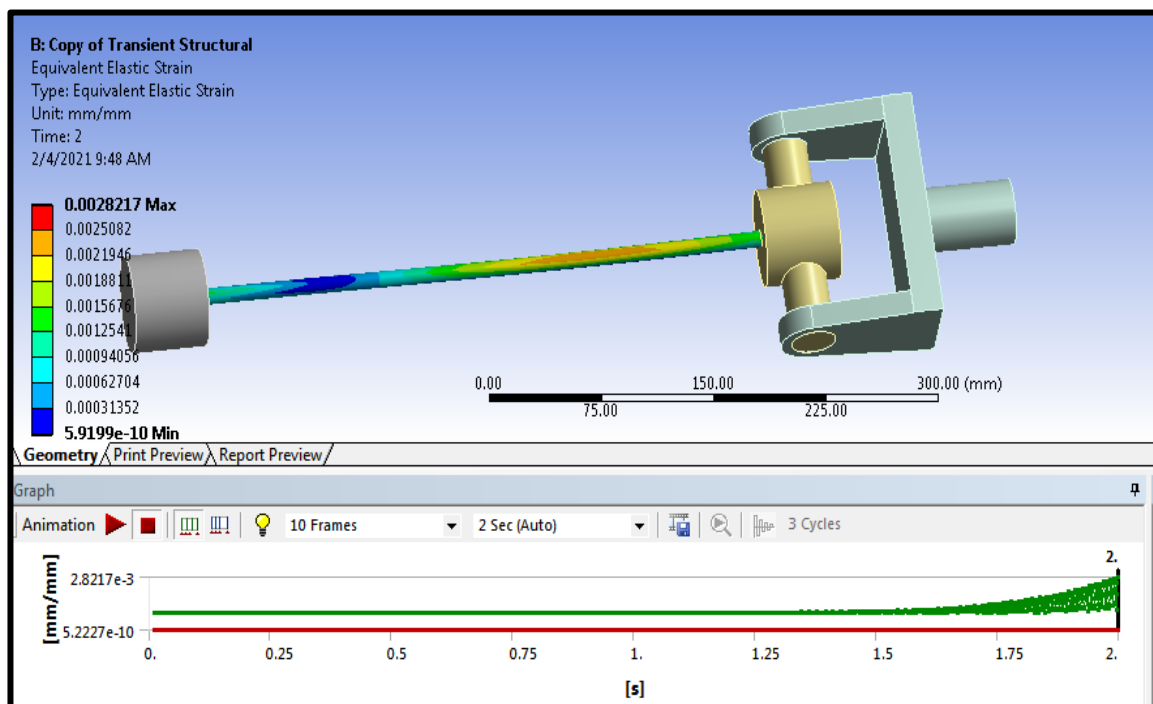**Figure (4-22): buckling mode of total deformation (440mm).**

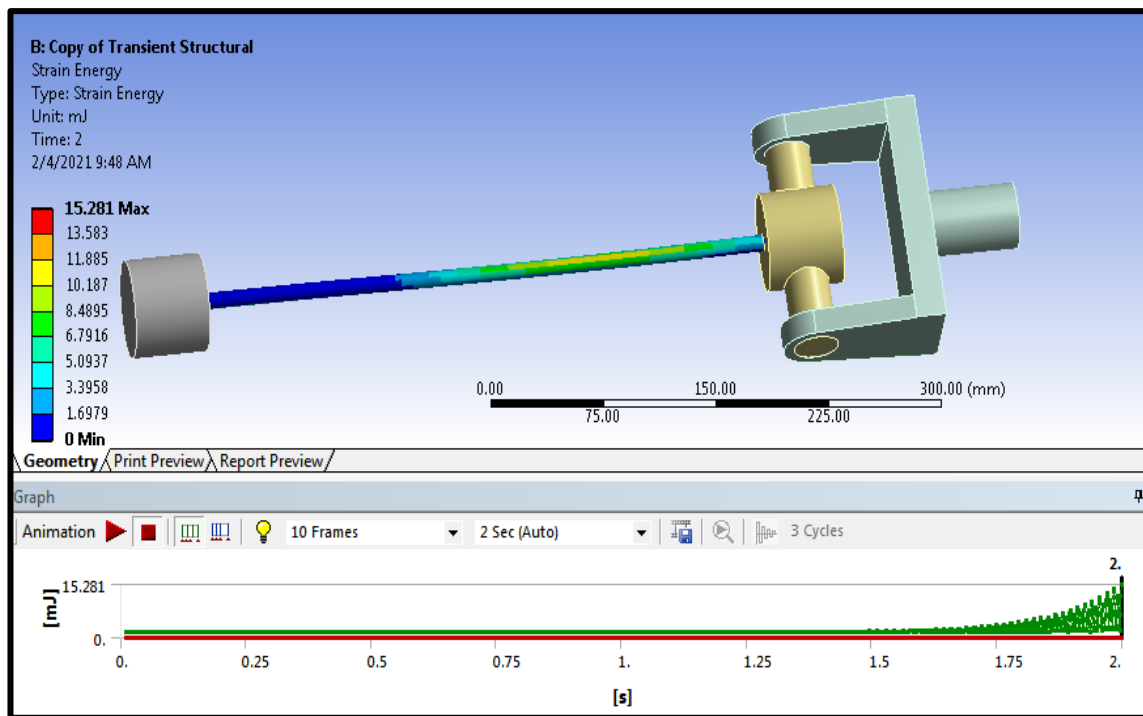**Figure (4-23): buckling mode of equivalent elastic strain (440mm).**

Figure (4-24): buckling mode of strain energy (460mm).

figures (4-25), (4-26), (4-27) and (4-28) show the numerical results of critical buckling under dynamic increasing load without safety factor (F. S.). If a factor of safety of (2) has to be applied. The figures (4-25), (4-26),

(4-27), (4-28) and appendix (5) rustles give valent between the Stress, total deformation, elastic strain and strain.

The ANSYS package outcomes are displaying the relation of stress at failure and the Equivalent Stress, total deformation, Equivalent elastic strain and strain energy of 304 stainless steel alloy with one end pinned and the other fixed end using (K = 0.7). Numerical results of critical buckling under dynamic load increase without safety factor (F. S.) recorded (P_cr = 13289) were recorded for the samples as extracted from the factory and the ones were buried for 60 days recorded (P_cr = 12080), respectively.
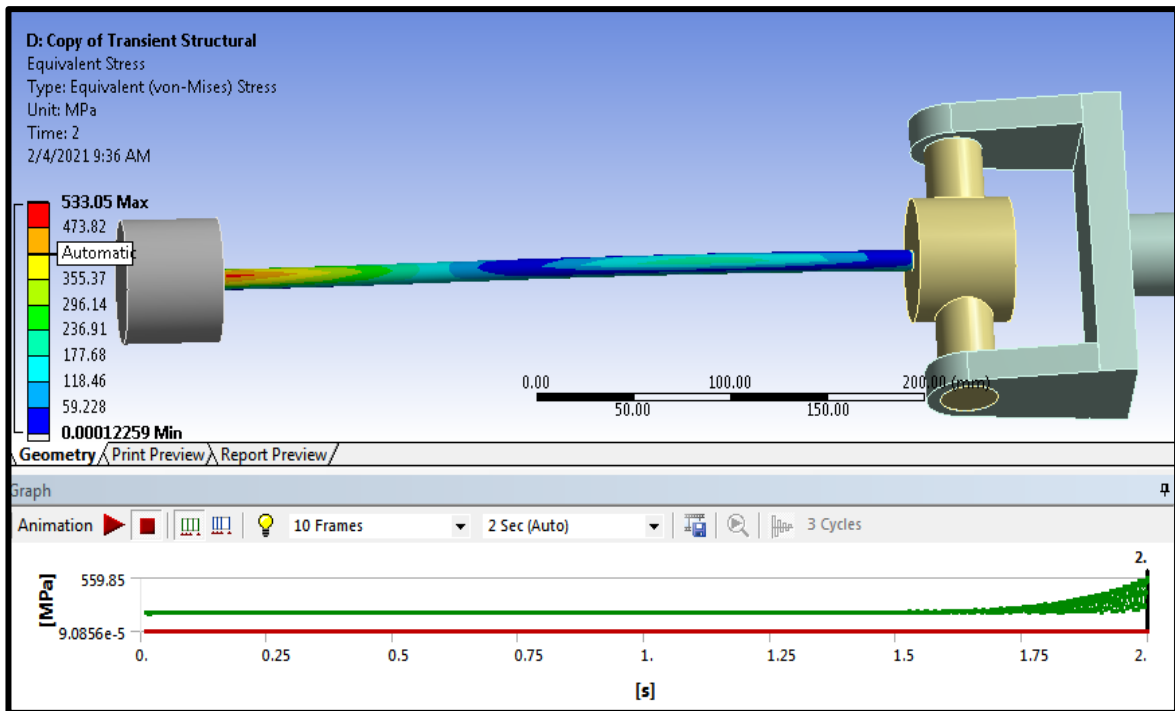

Figure (4-25): buckling mode of equivalent stress (400mm).

Figure (4-26): buckling mode of total deformation (400mm).

Figure (4-27): buckling mode of equivalent elastic strain (400mm).
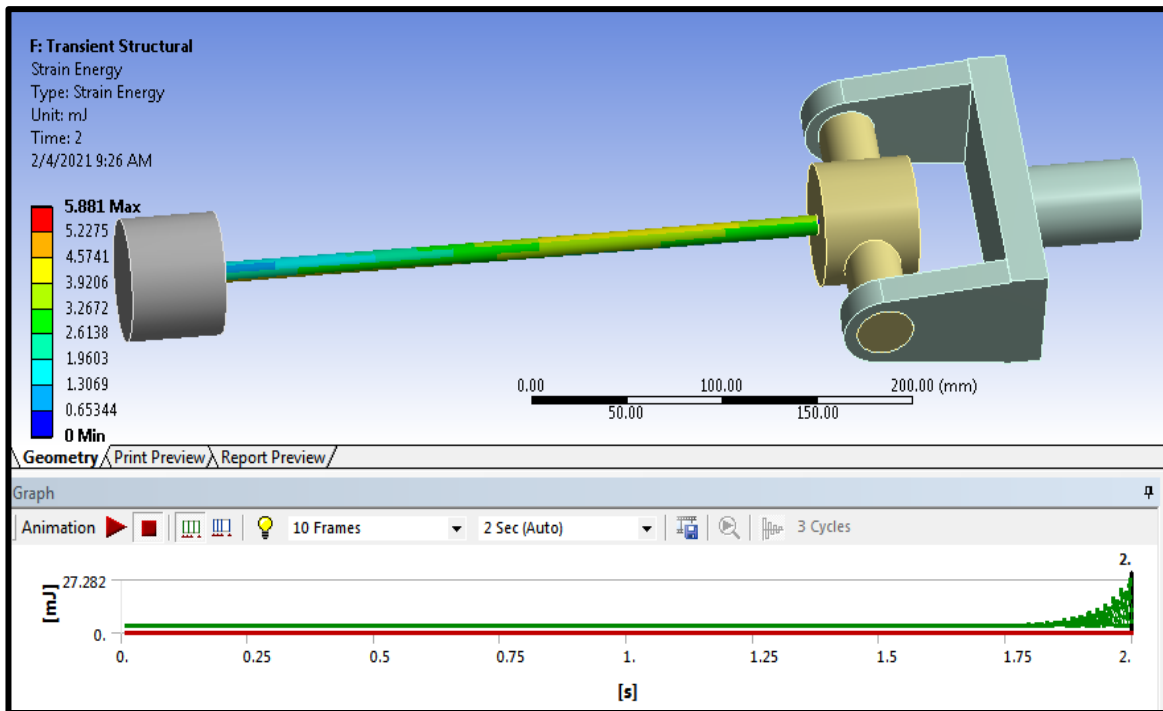
Figure (4-28): buckling mode of strain energy (400mm).

figures (4-29), (4-30), (4-31) and (4-32) show the numerical results of critical buckling under dynamic increasing load without safety factor (F. S.). If a factor of safety of (2) has to be applied. The figures (4-29), (4-30), (4-31), (4-32) and appendix (6) rustles give Equivalent between the Stress, total deformation, elastic strain and strain.

The ANSYS package outcomes are displaying the relation of stress at failure and the Equivalent Stress, total deformation, Equivalent elastic strain and strain energy of 304 stainless steel alloy with one end pinned and the other fixed end using (K = 0.7). Numerical results of critical buckling under increased dynamic load without safety factor (F. S.) recorded (P_cr = 15190) for the samples as extracted from the factory and the ones were buried for 60 days recorded (P_cr = 13809), respectively.

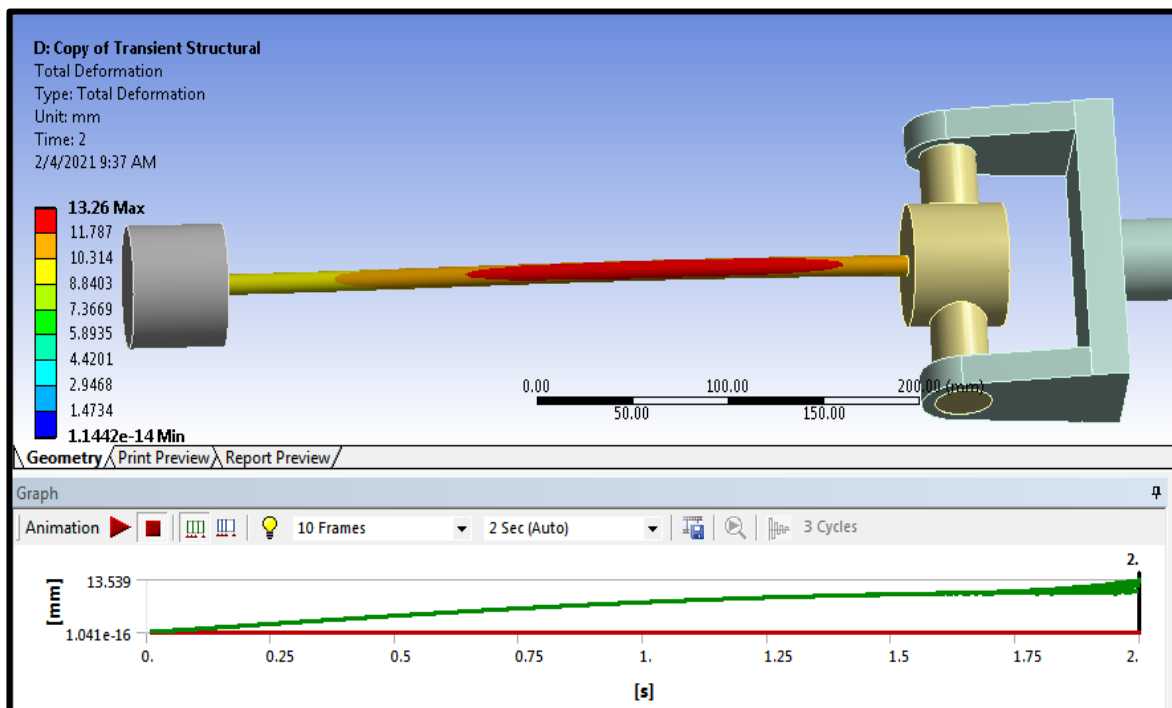**Figure (4-29): buckling mode of equivalent stress (380mm).**

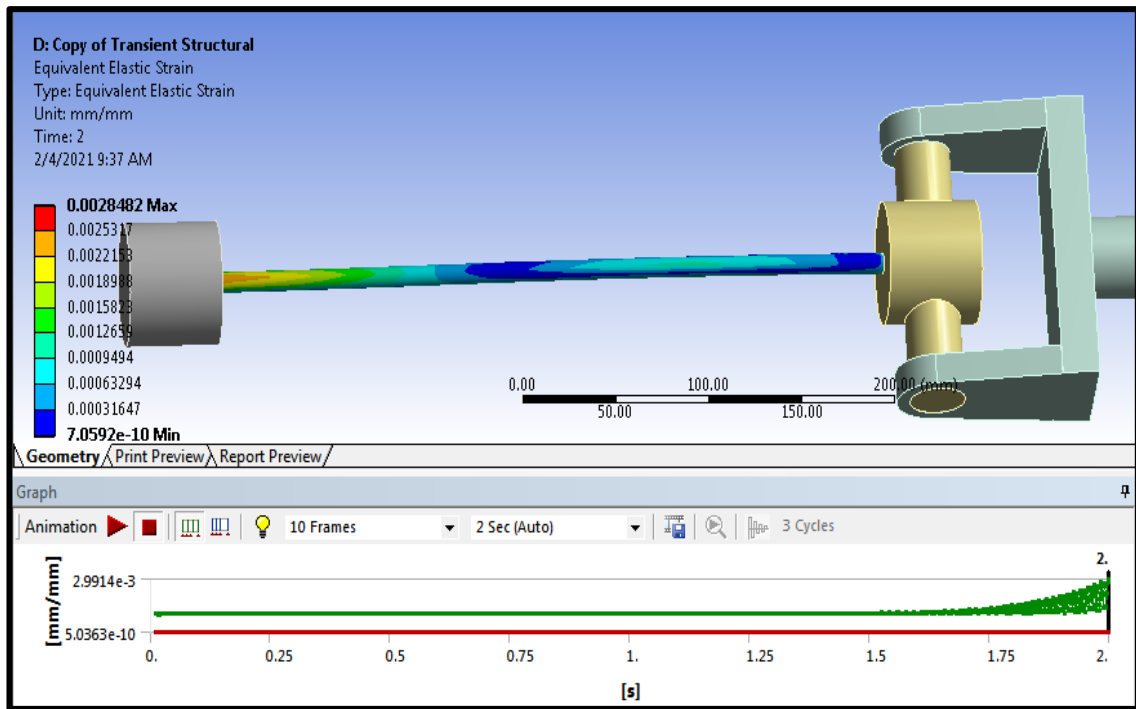**Figure (4-30): buckling mode of total deformation (380mm).**

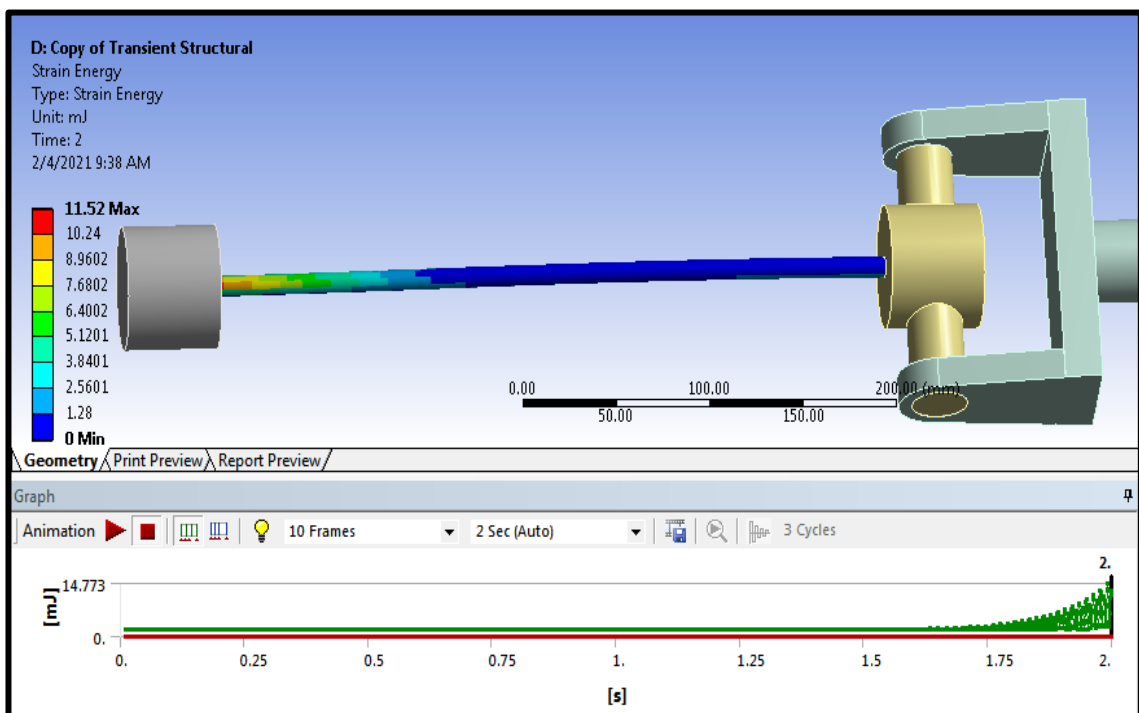**Figure (4-31): buckling mode of equivalent elastic strain (380mm).**
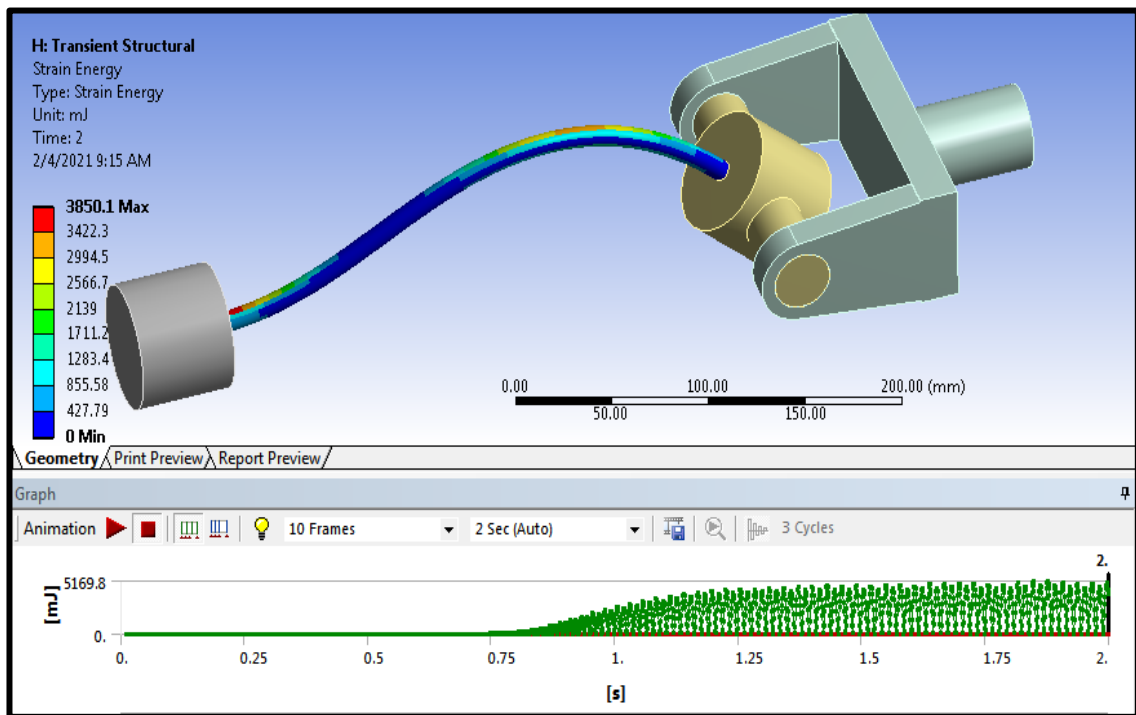
Figure (4-32): buckling mode of strain energy (380mm).

figures (4-33), (4-34), (4-35) and (4-36) show the numerical results of critical buckling under dynamic increasing load without safety factor (F. S.). If a factor of safety of (2) has to be applied. The figures (4-33), (4-34), (4-35), (4-36) and appendix (7) rustles give amounting between the Stress, total deformation, elastic strain and strain.

The ANSYS package outcomes are displaying the relation of stress at failure and the Equivalent Stress, total deformation, Equivalent elastic strain and strain energy of 304 stainless steel alloy with one end pinned and the other fixed end using (K = 0.7). Numerical results of critical buckling under increased dynamic load without safety factor (F. S.) recorded (P_cr = 15472) for the samples as extracted from the factory and the ones were buried for 60 days recorded (P_cr = 14065), respectively.
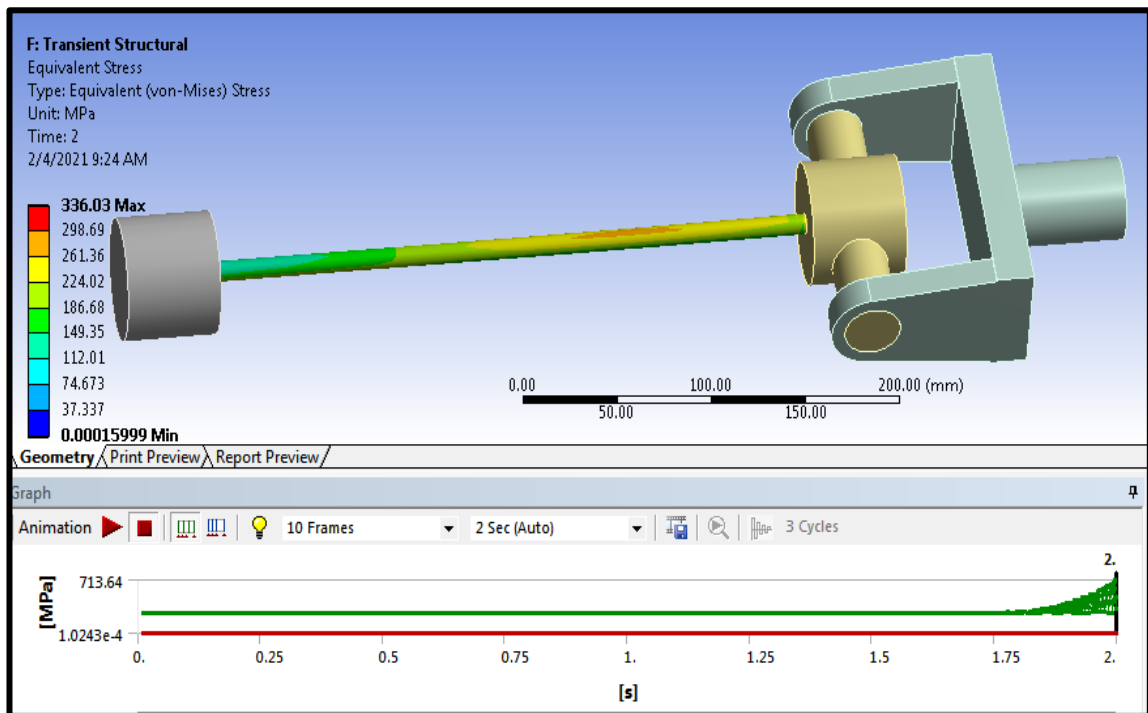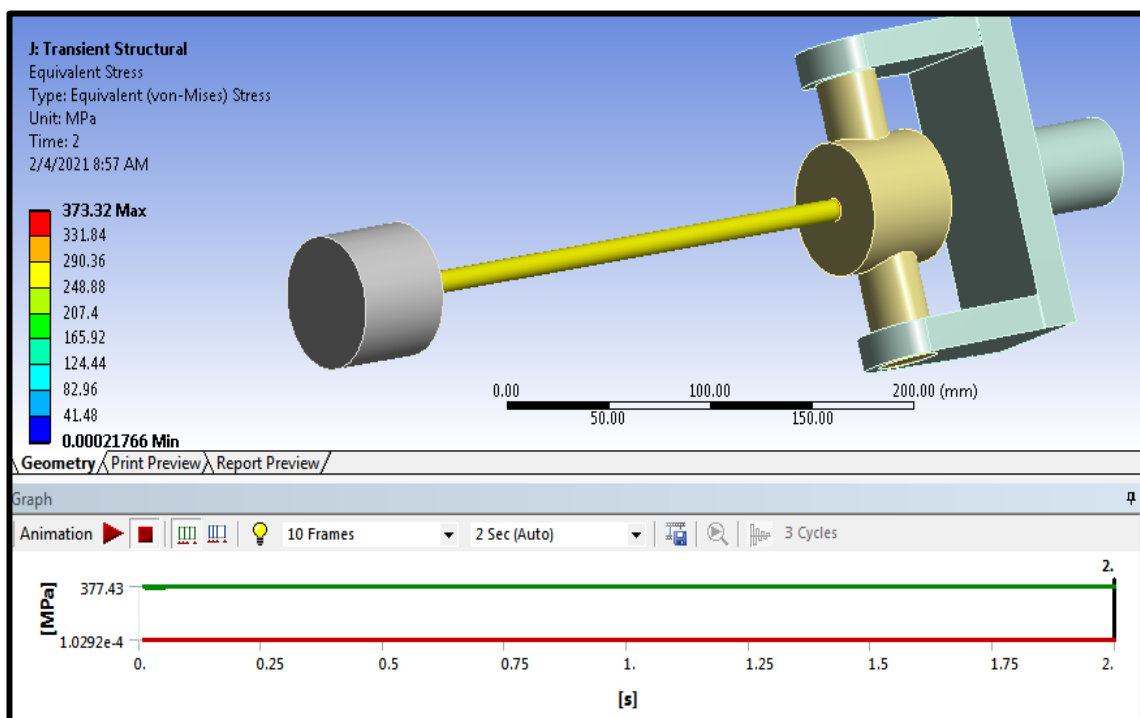

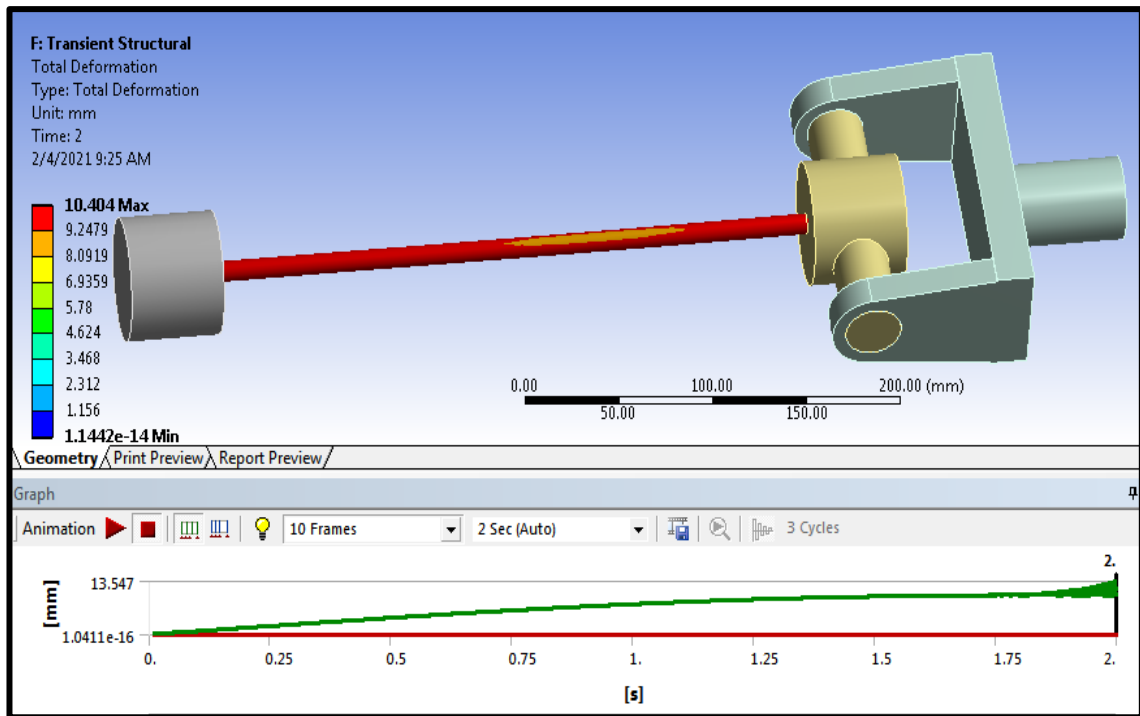**Figure (4-33): buckling mode of equivalent stress (360mm).**
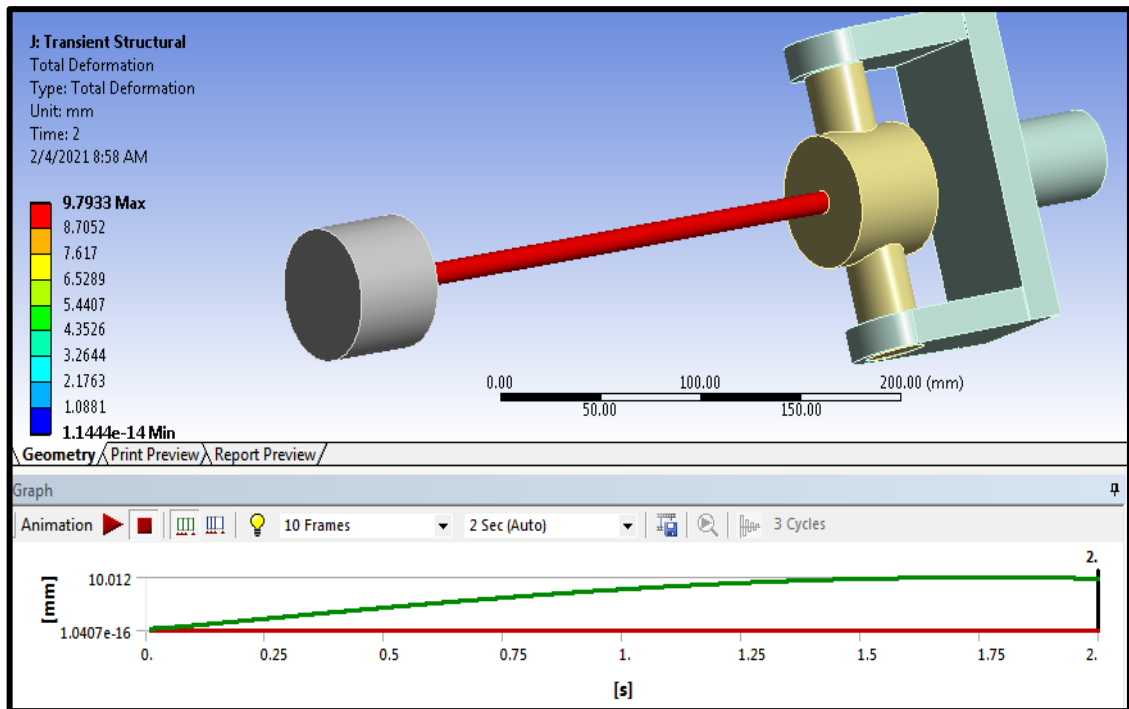
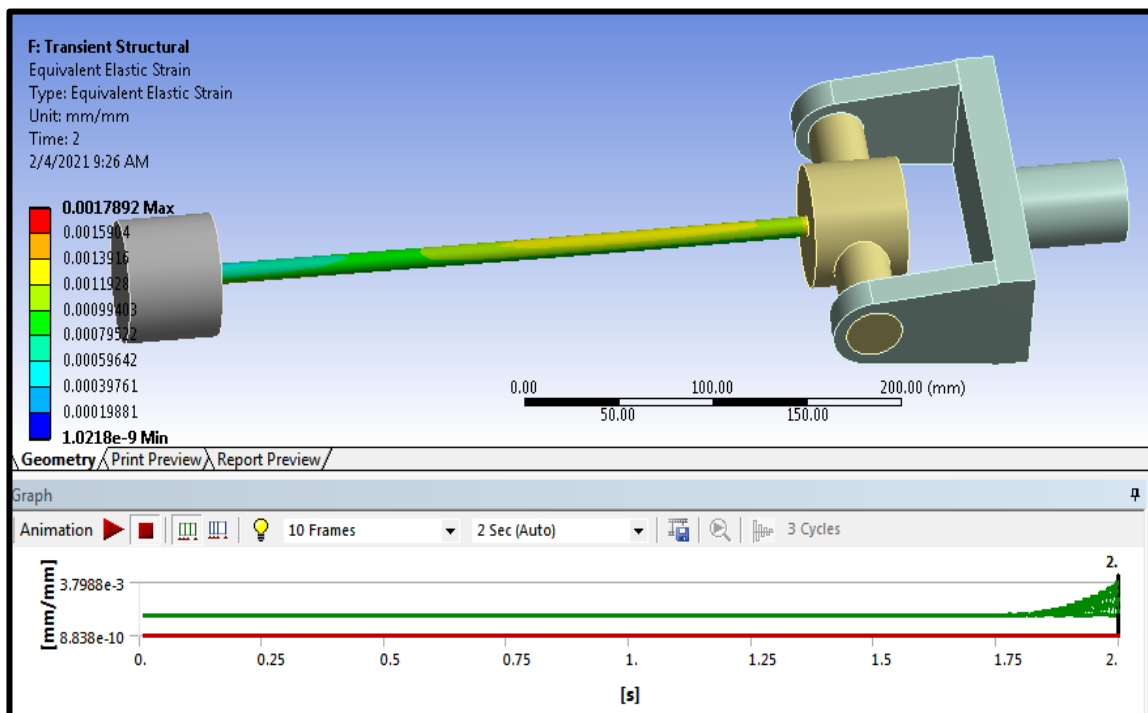**Figure (4-34): buckling mode of total deformation (360mm).**
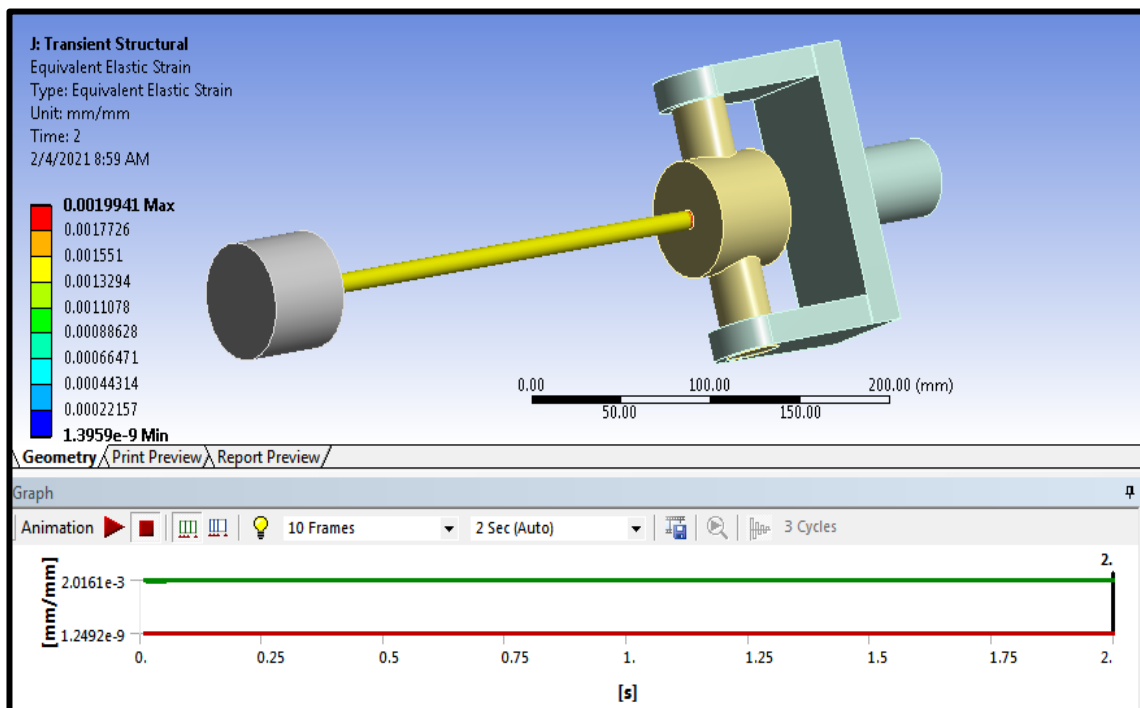
**Figure (4-35): buckling mode of equivalent elastic strain (360mm).**
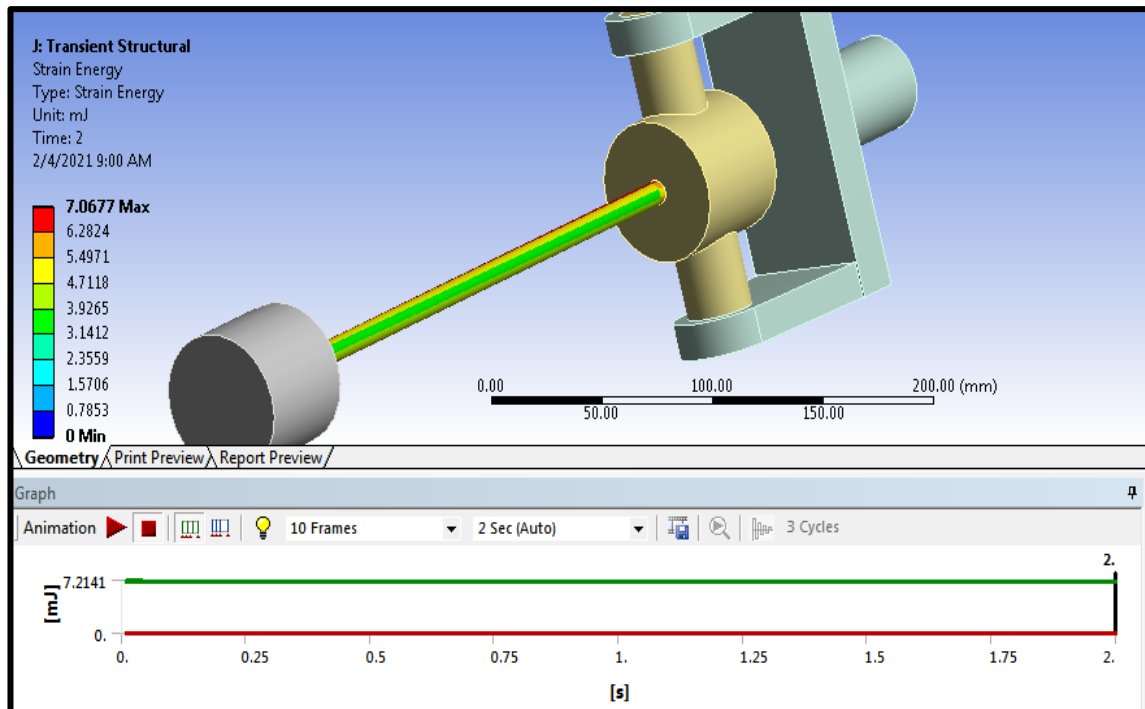
Figure (4-36): buckling mode of strain energy (360mm).

fingers (4-37), (4-38), (4-39) and (4-40) showed the numerical results of critical buckling under dynamic increasing load without safety factor (F. S.). If a factor of safety of (2) has to be applied. The fingers (4-41), (4-42), (4-43) and (4-44) and appendix (7) rustles give between the Equivalent Stress, total deformation, Equivalent elastic strain and strain.

the ANSYS package outcomes are displaying the relation of stress at failure and the Equivalent Stress, total deformation, Equivalent elastic strain and strain energy of 304 stainless steel alloy with one end pinned and the other fixed end using (K = 0.7). The numerical results of critical buckling under dynamic increasing load without factor of safety (F. S.), as (P_{cr}= 16967,15424), (received, after 60day) respectively.
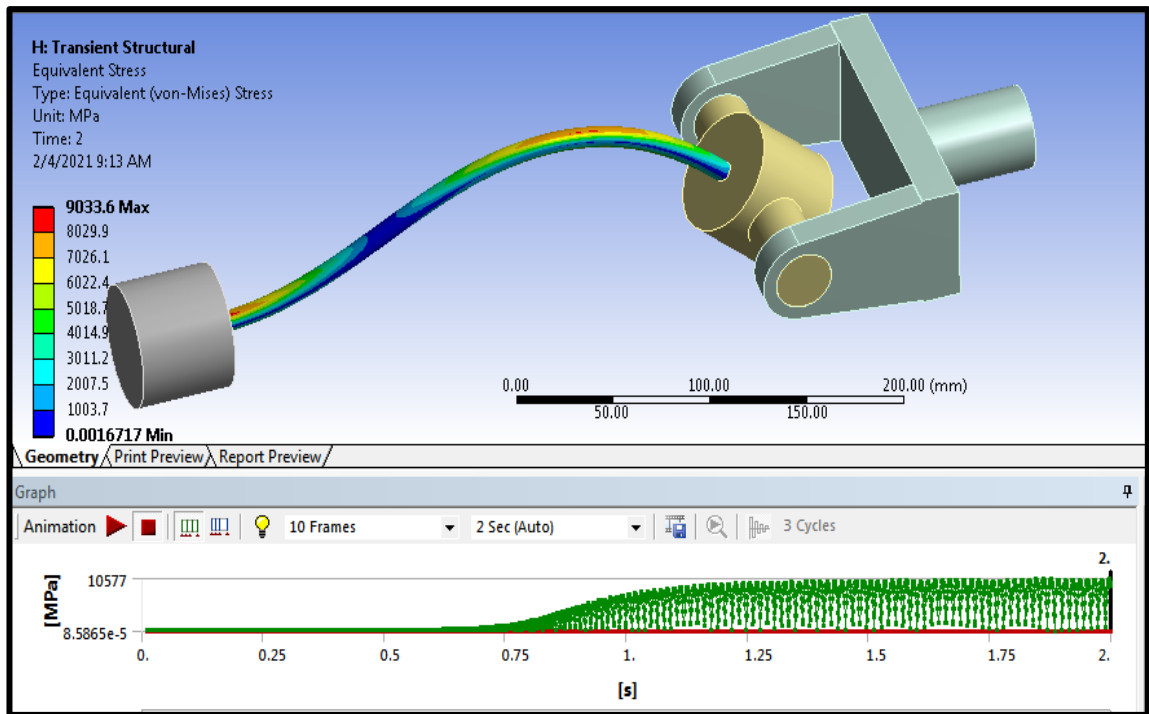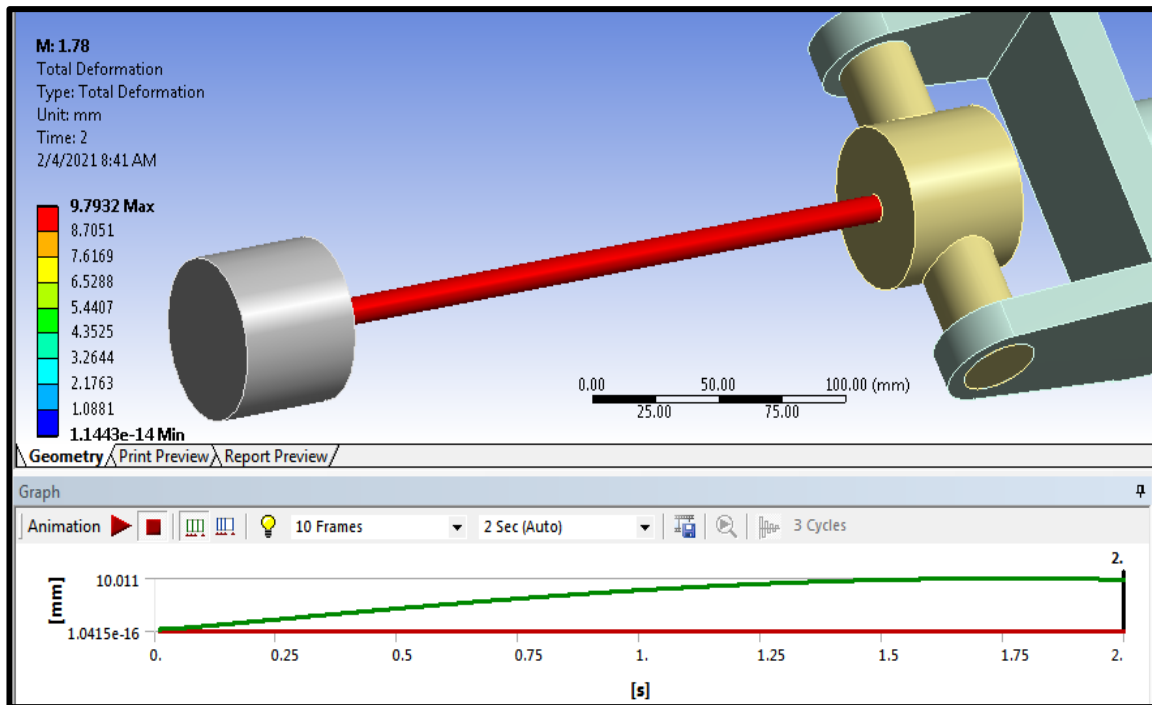
Figure (4-37): buckling mode of equivalent stress (340mm).
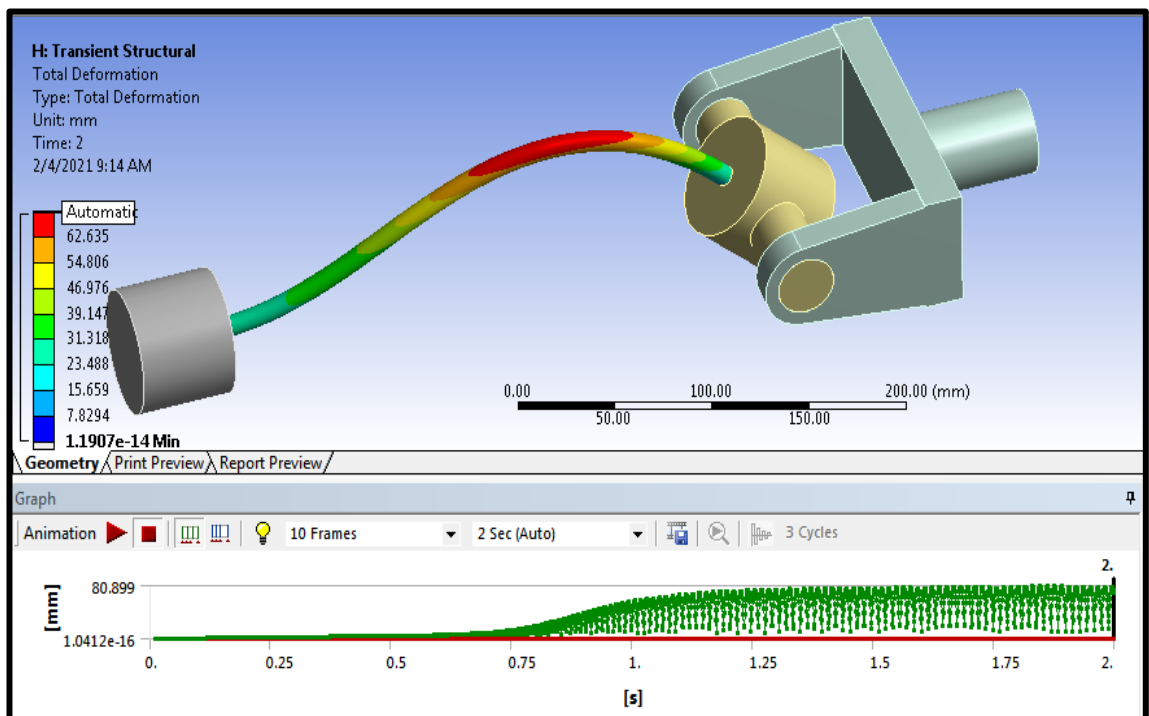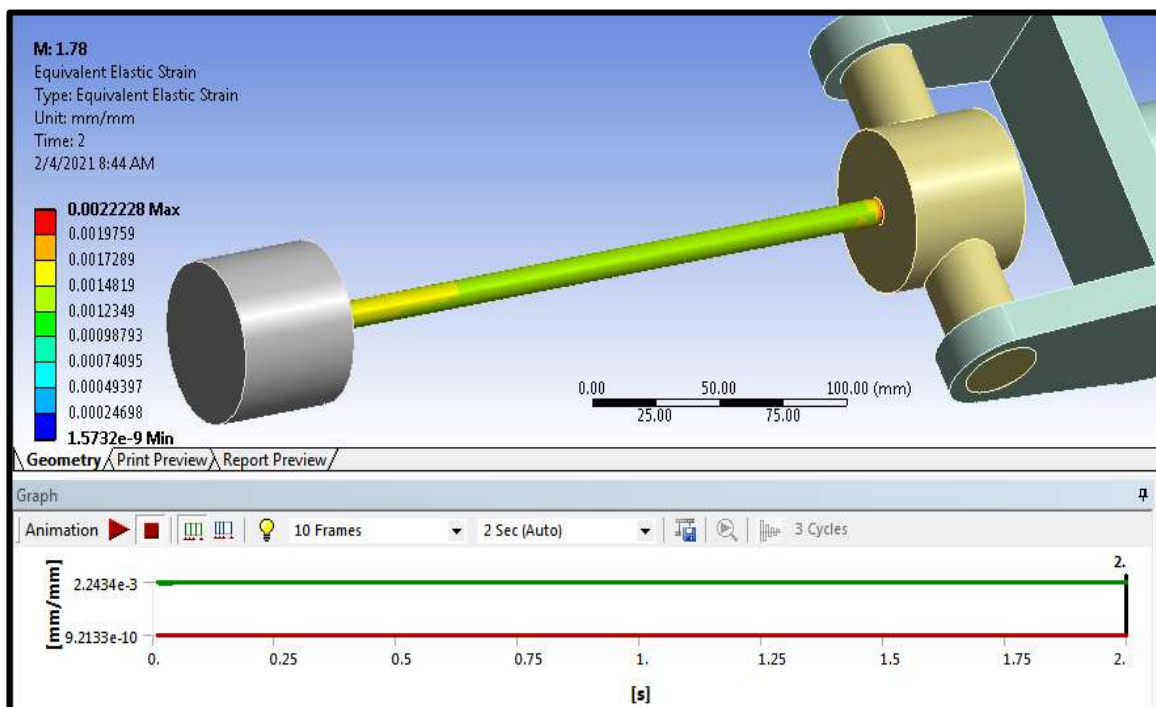

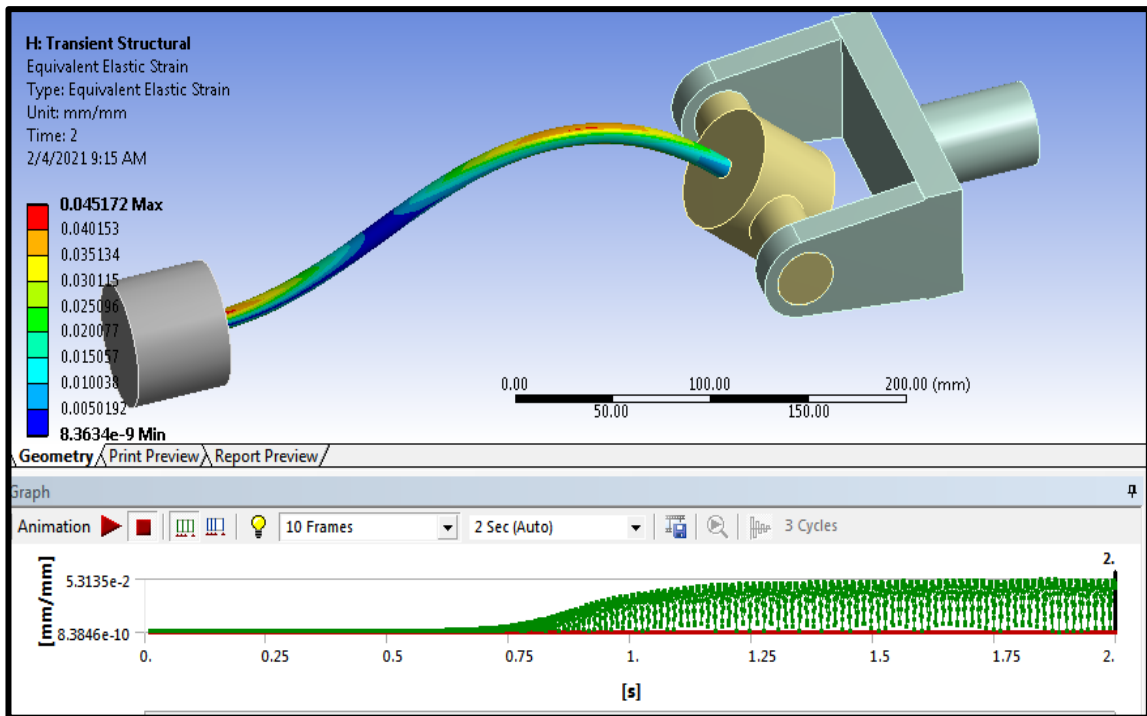**Figure (4-38): buckling mode of total deformation (340mm).**
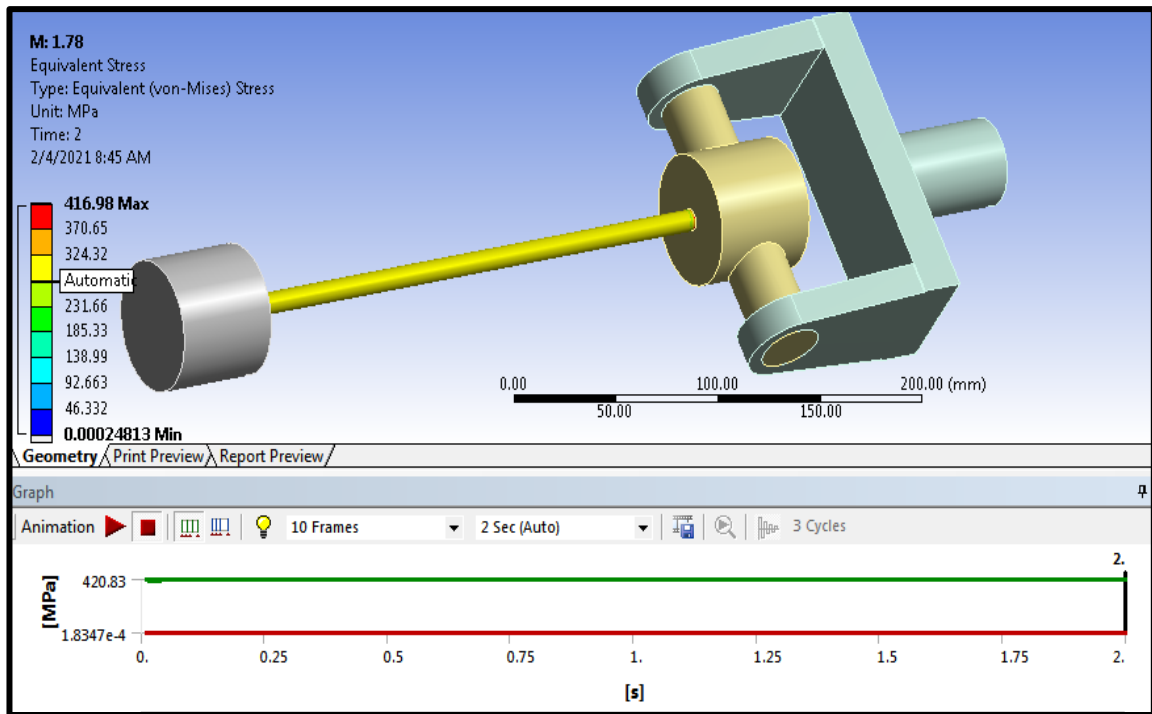
**Figure (4-38): buckling mode of equivalent elastic strain (340mm).**
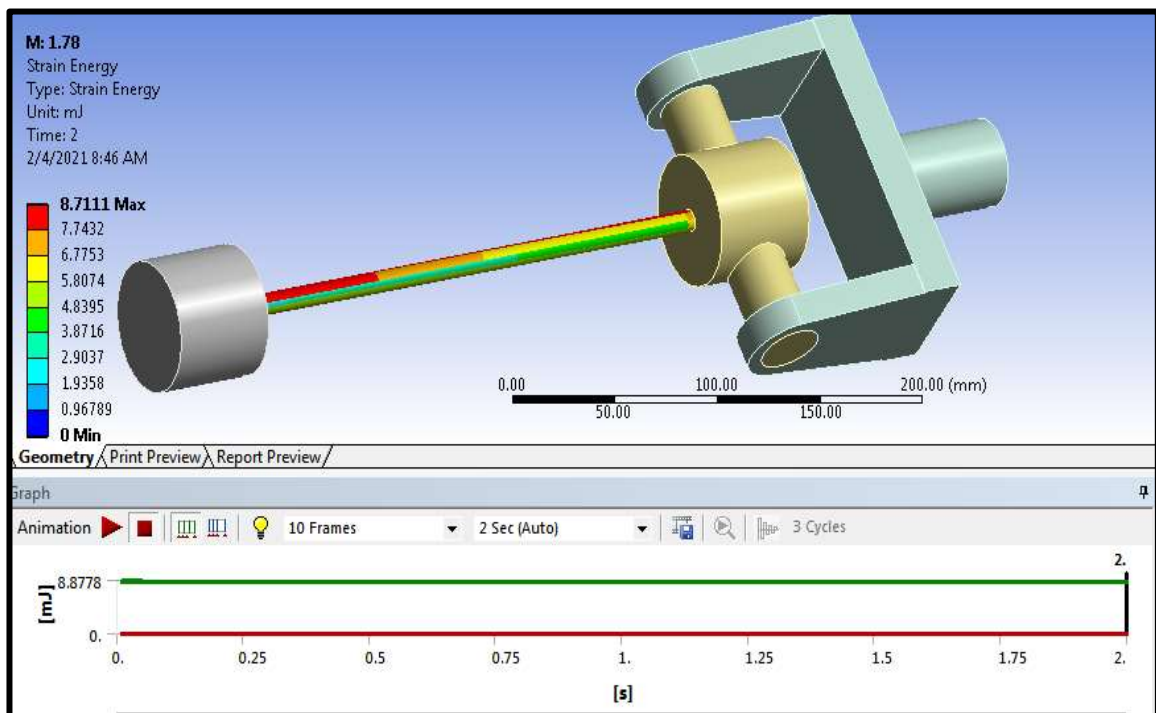
Figure (4-39): buckling mode of strain energy (340mm).

Chapter Five

Conclusions and Suggestions

Chapter Five

Conclusions and Suggestions

5.1 Conclusions

The effect of the buckling behavior was investigated for 304 stainless steel alloy columns by testing new columns as well and as other corroded by burial. The following conclusions can be drawn:-

The critical load (Pcr) for long column is not affected by the strength of the material (i.e. strength is not a factor) when applying Euler's formula but stiffness or elasticity modulus (E) of material is taken a major factor for calculating (Pcr)

The critical load (Pcr) for intermediate columns is affected by strength in addition to its stiffness or elasticity (E) when applying Johnson formula.

Before and after applying (SP + LASER) to the eroded columns in both conditions (dry) and (corroded), the experimental results showed a good agreement in the output with (Euler, Johnson, Perry Robertson) formulas after adding the safety factor (3), (3), and (1.3), but for ANSYS the safety factor was (2).

The electrical laser alarm system worked successfully for controlling the critical buckling load and assessment the buckling failure which was defined as 1% of effective length.

Corrosion leads to reduce the surface mechanical properties. The specimens of 60 days corroded have approximately 4.1 % reduction in ultimate strength compared to the non-corroded specimens.

The time that the shaft is buried reduces the critical load value and its range, for example reducing the range from 1.92% to 7.62% for 60

days for long corroded shafts and from 2.2% to 4.67% for 60 days for intermediate corroded shafts.

The Perry-Robertson formula gives an approximation of the experimental results but with a safety factor of (1.3) that gives more satisfied expectations.

The Euler equation for the long columns and Jonson for the short and intermediate columns give unsatisfying results compared with the experimental results for the critical buckling but with a safety factor of (3) it is gives accurate results.

ANSYS 17 program used in calculating the buckling stresses showed good agreement in comparison with the analytical and experimental results, with a (2) factor of safety.

The results of practical and analytical experiments indicate that the overturning load of long and medium corroded columns has been reduced by (28%) and (19.6%) respectively compared to the receiving conditions, which facilitates operations inside the oil well and reduces maintenance operations.

5.2 Suggestions for future work

The following suggestions may be taken into consideration for future wok:

1- Study the behavior of buckling of 304 stainless steel alloy under increasing combined load with high-speed rotation.

2- Study the effect of the laser treatment and shot peening on non-corroded columns and corroded columns.

3- Study the effect of corrosion time on the critical buckling loads of long and intermediate columns of other materials such as aluminum alloy, copper alloy and others and compare them with 304 stainless steels.

4- Study the effect of corrosion time on the critical buckling load of the seawater submerged columns.

5- Use other programs to calculate critical buckling load such as the SOLDWORK.

References

A. H. Al-Jelehawy, 2012, "Reducing the tensile residual stresses induced from spot welding using shot peening process, MSc.Thesis, University of Technology, Department of Mechanical Engineering, Bagdad, Iraq.

Ak steel Report, 2007, "304/304L stainless steel, UNS S30400/UNS S30403, www.aksteel.com.

Al-Alkawi H. J., Al-Khazraji A. N., Essam Zuhier Fadhel, 2013, "Determination the optimum shot peening time for improving the buckling behavior of medium carbon steel, Eng. and Tech. Journal, Vol.32, No.3, Iraq.

Al-Alkawi H. J. M., Al-Khazraji A. N. Z. F., 2015, "Effect of shot peening on dynamic buckling critical load parameter produced for carbon steel columns, Journal of Babylon University/ Engineering Sciences, Vol.23, No.2, Bagdad, Iraq.

Al-Alkawi H. J., Talal A. A., Safaa H. A., Selman B. A., Khengab A. Y., 2012, "The effects of dry and wet shot peening on the mechanical and fatigue properties of 7075-T$_6$ Al- alloy, International J. of Multidisp1. Research and Advcs. in Eng. (IJMRAE), Vol.4, No.2, pp.343-356, Iraq.

Ali A. Ali, Esam A. Ebrahim, Mohammed H. Sir, Barazan A. Hamah Said, 2013, "Effect of shot peening time on mechanical properties of aluminium alloys AA 2017-T and AA 6063-T$_5$, Diyala Journal of Engineering Sciences, Vol.6, No.2, pp.1-8, Iraq.

Al-Alkawi H. J. M., Ekbal H. Ali, Firas A. Jasim, 2016, "Buckling behavior for 304 stainless steel using electrical laser alarm system, Eng. And Tech. Journal, Vol.34, No.11, PP.2036-2046, Iraq.

A. L. D. Ricardo, 2005, "Fatigue behavior and structural integrity of scratch damaged shot peened surfaces at elevated temperature, PhD. Thesis, University of Portsmouth, UK.

Amir Javiddinejad, Zodiac Aerospace, 2012, "Buckling of Beams and Columns under Combined Axial and Horizontal Loading with Various Axial Loading Application Locations, Journal of Theoretical and Applied Mechanics, Sofia, Vol.42, No.4, pp19 – 30, USA.

Arnold Mukuvare, 2013, "Euler buckling, University of Surrey, UK.

Barry Dupen, 2012, "Applied strength of materials for engineering technology, Associate Professor, Mechanical Engineering Technology, Indiana University – Purdue University Fort Wayne, Vol.2, Indiana, USA.

B. C. Nakra, K. K. Chauhry, 2006, "Instrumentation, Measurement and Analysis″ , 2nd Ed., Tata Mc Graw- Hill Education, USA.

B. Han, D. Y. Ju and W. P. Jia, 2007, "Influence of water cavitation peening with aeration on fatigue behavior of SAE1045 Steel, Applied Surface Sciene, Vol.253, pp.9342 – 9346, China.

Breck Hitz, J. J. Ewing, Jeff Hecht, 2001, "Introduction to Laser Technology, 3^{ed} Edition, IEEE Press, USA.

Charles E. Riley, (2003), "Elastic buckling loads of slender columns with variable cross section by the newmark meyhod, M.SC. Thesis, Colorado state University, Department of Civil Engineering, Colorado, USA.

Chhabra Nitish, Bhardwaj Sudeep, 2011, "Laser basic principles and Classification, International Journal of Research in Ayurveda and Pharmacy, Vol.2, No.1, pp.132 – 141, Poland.

C. Yang, P. D. Hodgson, Q. Liu and L. Ye, 2008, "Geometrical effects on residual stresses in 7050 – T7451 aluminum alloy rods subject to Laser shock peening, Journal of Materials Processing Technology, Vol.201, pp.303 – 309, Netherland.

Derci Felix da Silva, Daniel Acosta-Avalas, 2006, "Light dependent resistance as a sensor in spectroscopy setups using pulsed light and compared with electret microphones, Sensors, ISSN 1424-8220, PP.514-525, Switzerland.

Diponkar Paul, Md. Shohel Rana, Md. Mokarram Hossain, 2012, "A preview on experimentation on laser security system, International Journal of Engineering Science and Technology, Vol.2, No.2, pp.359-366, Malaysia.

Dongming Wei, Alejandro Sarria, Mohamed Elgindi, June-2013, "Critical buckling loads of the perfect Hollomon's Power – Law columns, ar Xiv : 1306 . 4762 v1 [cond – mat . mtrl – sci], USA.

D. Y. Ju and B. Han, 2009, "Investigation of water cavitation peening – induced microstructures in the near – surface layer of pure titanium, Journal of Materials Processing Technology, Vol.209, pp.4789 – 4794, Netherland.

E. J. Barbero, 2000, "Prediction of Buckling – Mode Interaction in Composite Columns, Journal of Mechanics of Composite Materials and Structures, Vol.7, pp.269 – 284, USA.

E. Z. Fadhel, 2014, "Effect of shot peening on the buckling behavior of steel CK35 under combined loading, PhD. Thesis, University of Technology, Mechanical Engineering Department, Bagdad, Iraq.

Guido Giuliani, Michele Norgia, Silvano Donati and Thierry Bosch, 2002, "Laser diode self-mixing technique for sensing applications, Journal of optics A: pure and applied optics, Pll:S1464-4258(02)40129-8, UK.

H. A. Hussein, March-2010, "Buckling of square columns under cycling loads for nitriding steel din (ck45, ck67, ck101), PhD. Thesis, University of Technology, Mechanical Engineering Department, Bagdad, Iraq.

Husam Al-Qablan, Hasan Katkhuda, Hazim Dwairi, 2009, "Assessment of the buckling behavior of square composite plates with circular cutout subjected to in – plane shear, Jordan Journal of Civil Engineering, Vol.3, No.2, Jordan.

Hussain Abdulziz A., H. J. M. Al –Alkawi, 2009, "An appraisal of Euler and Johnson buckling theories under dynamic compression buckling loading, The Iraqi Journal for Mechanical and Material Engineering, Vol.9, No.2, pp.173-181, Bagdad, Iraq.

K. H. Al-Jubori, March-2005, "Column lateral buckling under combined dynamic loading, PhD. Thesis, University of Technology, Technical Education Department, Bagdad, Iraq.

James M. Gere, Barry J. Goodno, 2009, "Mechanics of materials, Seventh Edition, USA.

J. Dutta Majumdar, I. Manna, 2003, "Laser processing of materials, Sadhana Journal, Vol.28, Parts 3 and 4, pp.495 – 562, India.

J. M. Gere, 2004, "Mechanics of material, 6th Ed, Thomson Learning Academic Resource Centre, Stanford University, Stanford, USA.

Jorge H.B. Sampaio Jr., Joan R. Hundhausen, 1998, "A mathematical model and analytical solution for buckling of inclined beam-columns, Applied Mathematical Modelling, Vol.22, pp.405-421, UK.

M. Arif Gurel, Murat Kisa, 2005, "Buckling of slender prismatic columns with a single edge crack under concentric vertical loads, Turkish J. Eng. Env. Sci., Vol.29, pp: 185 – 193, Turkey.

Mehmet Avcar, 2014, "Elastic buckling of steel columns under axial compression", Amerian Journal of Civil Engineering, Vol.2, No.3, pp.102 – 108, (2014).

Mikell P. Groover, 2010, "Fundamentals of Modern Manufacturing, John Wiley and Sons Press, USA.

M. N. James, 2010, "Residual stress influences in Mechanical Engineering, XVIII Congreso Nacional de Ingcnieria Mecanica, UK.

Mohamad K. Alwan, Naseem Sabah Abrahim, 2014, "Experimental and numerical study of buckling for carburized low carbon steel columns, Journal of Engineering and Development, Vol.18, No.2, ISSN1813-7822, Jordan.

Mott Robert L., 1996, "Applied Strength of Materials, 3rd Ed., Prentice Hall, Englewood Cliffs, New Jersey, USA.

M. Kobayashi, T. Matsui and Y. Murakami, 1998, "Mechanism of creation of compressive residual stress by shot peening, International Journal of Fatigue, Vol.20, No.5, pp.351-357, UK.

Nashwa Abdul – Hammied Saad, Aathraa Husian Hashim, 2014, "Geath of aluminium alloy AA 2024- T, The Iraqi Journal for Mechanical and Material Engineering, Vol.14, No.1, Bagdad, Iraq.

N. Barry, S. V. Hains worth and M. E. Fitzpatrick, 2009, "Effect of shot peening on the fatigue behavior of cast magnesium A8, Material Science and Engineering, Vol.507, No.(1-2), pp.50-57, UK.

P. Arker, J. Lu, J. Flavenot, 1990, "Effect of glass beads nature and ageing on the behavior of shot peened aeronautical materials presented at the 4th international Conf. on shot peening (ICSP -4), Tokyo, Japan.

P. S. Prevey and J. T. Cammett, September-2002, "The effect of shot peening coverage on residual stress, cold work and fatigue in a Ni – Cr –Mo low alloy steel, Proceedings International Conference on Shot Peening, Garmisch – Partenkirchen, Germany.

R. C. Hibbler, 2005, "Mechanics of materials, Second Edition, Prentice Hall, New Jersey, USA.

Rekha M. Bhoi, L.G.Kalurkar, 2014, "Study of buckling behavior of beam and column, IOSR Journal of Mechanical and Civil Engineering, Vol.11, Issue 4, pp.36-40, Australia.

Robert L. Mott, 2004, "Machine elements in mechanical design, 4th Edition, Pearson Prentice Hall, USA.

Robert D. Cook and Warren C. Young, 1985, "Adanced mechanics of materials, Macmillan Publishing Company, London, UK.

R. Wathins, John Shaw, October-2013, "Shape memory alloy column buckling: An experimental study, ICAST 2013: 24th International conference on adaptive structures and technology, Aruba.

S. H. Alokaidi, January-2012, "Fatigue behavior of shot peened aluminum alloys under variable stress conditions, PhD. Thesis, University of Technology, Ectromechanical Engineering Department, Bagdad, Iraq.

Solis Romero, E. R. Delos Rios, Y. H. Fam, A. Levers, 1999, "Optimization of shot peening process in terms of fatigue resistance, 7th International Conference on shot peening (ICSP – 7), Warsaw, Poland.

Timoshenko S. P. and Gere, J. M, 1961, "Theory of elastic stability, Mc Graw Hill Book Company Inc, Toronto.

Thomas H. K. Kang, Kenneth A. Biggs, Chris Ramseyer, 2013, " Buckling Modes of Cold – Formed Steel Columns, IACSIT International Journal of Engineering and Technology, Vol.5, No.4, pp.447-451, Malaysia.

Toe-Wan Kim, 2007, "Continuum damage mechanics-based creep-Fatigue-Intracted life prediction of nickel-based superalloy at high temperature, Scripta Materiallia, Vol.57, pp.1149-1152, Elsevier, USA.

Uros Zupanc, Janez Grum, 2010, "Surface integrity of shot peened aluminium alloy 7075-T651, Journal of Mechanical Engineering, Vol.57, No.5, pp.79-384, Slovenia.

Vladislav Gerginov, Brian Laughman, Diana DiBerardino, Robert J. Rafac, Steven T. Ruggiero, Carol E. Tanner, 2001, "Diode lasers for fast-beam laser experiments', Optics Communications, Vol.187, pp.219-230, UK.

W. H. Duan, C. M. Wang, 2008, "Exact Solution for Buckling of Columns Including Self – Weight, Journal of Engineering Mechanics, Constant Volume. Mathematics 2021, 9, 657, PP 233-240, USA.

William T. Silfvast, 2005, "Fundamentals of Photonics', University of Central Florida Orlando, pp. 42-65 Florida, USA.

Y. Fouad, Mostafa M. Elmetwally, 2011, "Effect of shot peening on high cycling fatigue of Al 2024-T4, International Conference on Advanced Materials Engineering IPCSIT, Vol.15, pp. 95-104, Singapore.

Y. Pekbey, A. Ozdamar and O. Sayman, 2007, "Buckling optimization of composite columns with variable thickness, Journal of Reinforced Plastics and Composites, Vol.26, No.13, pp. 1337- 1356, USA.

Young, B., Lui, W. M., 2005, "Behavior of cold-formed high strength stainless steel section, J. Struct. Eng., ASCE, Vol.13, No.11, pp.1738-1745, USA.

Young B., 2005, "Local buckling and shift of effective centroid of cold-formed stainless-steel columns, Steel and Composite Structures, Vol.5, No.(23), pp.235-246, USA.

Z. P. Bazat, 2000, "Structural stability, International Journal of Solids and Structures", Vol.37, pp.55 – 67, USA.

Appendices

Appendix (1) 340-260 mm
Model (P4) > Transient (P5) > Solution (P6) > Results

Object Name	Total Deformation	Equivalent Elastic Strain	Equivalent Stress	Strain Energy
State	Solved			
Scope				
Scoping Method	Geometry Selection			
Geometry	All Bodies			
Definition				
Type	Total Deformation	Equivalent Elastic Strain	Equivalent (von-Mises) Stress	Strain Energy
By	Time			
Display Time	Last			
Calculate Time History	Yes			
Identifier				
Suppressed	No			
Results				
Minimum	1.1444e-014 mm	1.8761e-009 mm/mm	3.0097e-004 MPa	0. mJ
Maximum	9.7931 mm	2.2224e-003 mm/mm	412.73 MPa	8.6205 mJ
Minimum Occurs On	3	2		1
Maximum Occurs On	2			
Minimum Value Over Time				
Minimum	1.0455e-016 mm	9.275e-010 mm/mm	1.8285e-004 MPa	0. mJ
Maximum	1.1698e-014 mm	1.4242e-008 mm/mm	2.3763e-003 MPa	0. mJ
Maximum Value Over Time				
Minimum	0.39579 mm	2.2015e-003 mm/mm	408.85 MPa	8.4572 mJ

Maximum	10.011 mm	2.2427e-003 mm/mm	416.5 MPa	8.7844 mJ
Information				
Time	2. s			
Load Step	1			
Substep	487			
Iteration Number	1949			
Integration Point Results				
Display Option		Averaged		
Average Across Bodies		No		

Appendix (2) 360-280 mm
Model (J4) > Transient (J5) > Solution (J6) > Results

Object Name	*Equivalent Stress*	*Total Deformation*	*Equivalent Elastic Strain*	*Strain Energy*
State	Solved			
Scope				
Scoping Method	Geometry Selection			
Geometry	All Bodies			
Definition				
Type	Equivalent (von-Mises) Stress	Total Deformation	Equivalent Elastic Strain	Strain Energy
By	Time			
Display Time	Last			
Calculate Time History	Yes			
Identifier				
Suppressed	No			
Integration Point Results				
Display Option	Averaged		Averaged	
Average Across Bodies	No		No	

Results				
Minimum	2.1766e-004 MPa	1.1444e-014 mm	1.3959e-009 mm/mm	0. mJ
Maximum	373.32 MPa	9.7933 mm	1.9941e-003 mm/mm	7.0677 mJ
Minimum Occurs On	2	3	2	1
Maximum Occurs On	2			
Minimum Value Over Time				
Minimum	1.0292e-004 MPa	1.0407e-016 mm	1.2492e-009 mm/mm	0. mJ
Maximum	1.4576e-003 MPa	1.1699e-014 mm	7.7009e-009 mm/mm	0. mJ
Maximum Value Over Time				
Minimum	369.53 MPa	0.38844 mm	1.9739e-003 mm/mm	6.9284 mJ
Maximum	377.43 MPa	10.012 mm	2.0161e-003 mm/mm	7.2141 mJ
Information				
Time	2. s			
Load Step	1			
Substep	568			
Iteration Number	2266			

Appendix (3) 380-300 mm
Model (F4) > Transient (F5) > Solution (F6) > Results

Object Name	*Equivalent Stress*	*Total Deformation*	*Equivalent Elastic Strain*	*Strain Energy*
State	Solved			
Scope				
Scoping Method	Geometry Selection			
Geometry	All Bodies			
Definition				

Type	Equivalent (von-Mises) Stress	Total Deformation	Equivalent Elastic Strain	Strain Energy
By	Time			
Display Time	Last			
Calculate Time History	Yes			
Identifier				
Suppressed	No			
Integration Point Results				
Display Option	Averaged		Averaged	
Average Across Bodies	No		No	
Results				
Minimum	1.5999e-004 MPa	1.1442e-014 mm	1.0218e-009 mm/mm	0. mJ
Maximum	336.03 MPa	10.404 mm	1.7892e-003 mm/mm	5.881 mJ
Minimum Occurs On	2	3	2	1
Maximum Occurs On	2			
Minimum Value Over Time				
Minimum	1.0243e-004 MPa	1.0411e-016 mm	8.838e-010 mm/mm	0. mJ
Maximum	1.8711e-004 MPa	1.1698e-014 mm	1.1249e-009 mm/mm	0. mJ
Maximum Value Over Time				
Minimum	262.35 MPa	0.31718 mm	1.3991e-003 mm/mm	3.5341 mJ
Maximum	713.64 MPa	13.547 mm	3.7988e-003 mm/mm	27.282 mJ
Information				
Time	2. s			
Load Step	1			

Substep	619
Iteration Number	2710

Appendix (4) 400-320 mm
Model (F4) > Transient (F5) > Solution (F6) > Results

Object Name	*Equivalent Stress*	*Total Deformation*	*Equivalent Elastic Strain*	*Strain Energy*
State	Solved			
Scope				
Scoping Method	Geometry Selection			
Geometry	All Bodies			
Definition				
Type	Equivalent (von-Mises) Stress	Total Deformation	Equivalent Elastic Strain	Strain Energy
By	Time			
Display Time	Last			
Calculate Time History	Yes			
Identifier				
Suppressed	No			
Integration Point Results				
Display Option	Averaged		Averaged	
Average Across Bodies	No		No	
Results				
Minimum	1.5999e-004 MPa	1.1442e-014 mm	1.0218e-009 mm/mm	0. mJ
Maximum	336.03 MPa	10.404 mm	1.7892e-003 mm/mm	5.881 mJ
Minimum Occurs On	2	3	2	1
Maximum Occurs On	2			
Minimum Value Over Time				

Minimum	1.0243e-004 MPa	1.0411e-016 mm	8.838e-010 mm/mm	0. mJ
Maximum	1.8711e-004 MPa	1.1698e-014 mm	1.1249e-009 mm/mm	0. mJ
Maximum Value Over Time				
Minimum	262.35 MPa	0.31718 mm	1.3991e-003 mm/mm	3.5341 mJ
Maximum	713.64 MPa	13.547 mm	3.7988e-003 mm/mm	27.282 mJ
Information				
Time	2. s			
Load Step	1			
Substep	619			
Iteration Number	2710			

Appendix (5) 440-360 mm
Model (D4) > Transient (D5) > Solution (D6) > Results

Object Name	*Equivalent Stress*	*Total Deformation*	*Equivalent Elastic Strain*	*Strain Energy*
State	Solved			
Scope				
Scoping Method	Geometry Selection			
Geometry	All Bodies			
Definition				
Type	Equivalent (von-Mises) Stress	Total Deformation	Equivalent Elastic Strain	Strain Energy
By	Time			
Display Time	Last			
Calculate Time History	Yes			
Identifier				
Suppressed	No			
Integration Point Results				

Display Option	Averaged		Averaged	
Average Across Bodies	No		No	
Results				
Minimum	1.2259e-004 MPa	1.1442e-014 mm	7.0592e-010 mm/mm	0. mJ
Maximum	533.05 MPa	13.26 mm	2.8482e-003 mm/mm	11.52 mJ
Minimum Occurs On	2	3	2	1
Maximum Occurs On	2			
Minimum Value Over Time				
Minimum	9.0856e-005 MPa	1.041e-016 mm	5.0363e-010 mm/mm	0. mJ
Maximum	3.44e-004 MPa	1.1697e-014 mm	1.8484e-009 mm/mm	0. mJ
Maximum Value Over Time				
Minimum	188.46 MPa	0.26488 mm	1.0073e-003 mm/mm	1.84 mJ
Maximum	559.85 MPa	13.539 mm	2.9914e-003 mm/mm	14.773 mJ
Information				
Time	2. s			
Load Step	1			
Substep	776			
Iteration Number	3335			

Appendix (6) 460-380 mm
Model (B4) > Transient (B5) > Solution (B6) > Results

Object Name	*Equivalent Stress*	*Total Deformation*	*Equivalent Elastic Strain*	*Strain Energy*
State	Solved			
Scope				
Scoping Method	Geometry Selection			

- 104 -

Geometry	All Bodies			
Definition				
Type	Equivalent (von-Mises) Stress	Total Deformation	Equivalent Elastic Strain	Strain Energy
By	Time			
Display Time	Last			
Calculate Time History	Yes			
Identifier				
Suppressed	No			
Integration Point Results				
Display Option	Averaged		Averaged	
Average Across Bodies	No		No	
Results				
Minimum	1.1603e-004 MPa	1.1442e-014 mm	5.9199e-010 mm/mm	0. mJ
Maximum	530.01 MPa	13.8 mm	2.8217e-003 mm/mm	15.281 mJ
Minimum Occurs On	2	3	2	1
Maximum Occurs On	2			
Minimum Value Over Time				
Minimum	7.5756e-005 MPa	1.0409e-016 mm	5.2227e-010 mm/mm	0. mJ
Maximum	2.7132e-004 MPa	1.1697e-014 mm	1.46e-009 mm/mm	0. mJ
Maximum Value Over Time				
Minimum	168.86 MPa	0.24827 mm	9.0078e-004 mm/mm	1.4741 mJ
Maximum	530.01 MPa	13.8 mm	2.8217e-003 mm/mm	15.281 mJ
Information				

Time	2. s
Load Step	1
Substep	830
Iteration Number	3514

Appendix (7) 480-400 mm
Model (E4) > Transient (E5) > Solution (E6) > Results

Object Name	Total Deformation	Equivalent Stress	Equivalent Elastic Strain	Strain Energy
State	Solved			
Scope				
Scoping Method	Geometry Selection			
Geometry	All Bodies			
Definition				
Type	Total Deformation	Equivalent (von-Mises) Stress	Equivalent Elastic Strain	Strain Energy
By	Time			
Display Time	Last			
Calculate Time History	Yes			
Identifier				
Suppressed	No			
Results				
Minimum	1.1443e-014 mm	9.4227e-005 MPa	6.1149e-010 mm/mm	0. mJ
Maximum	13.818 mm	478.29 MPa	2.5462e-003 mm/mm	9.3365 mJ
Minimum Occurs On	3	2		1
Maximum Occurs On	2			
Minimum Value Over Time				
Minimum	1.041e-016 mm	6.2217e-005 MPa	4.0437e-010 mm/mm	0. mJ

Maximum	1.1698e-014 mm	1.8746e-004 MPa	1.0124e-009 mm/mm	0. mJ
Maximum Value Over Time				
Minimum	0.24174 mm	152.63 MPa	8.1481e-004 mm/mm	1.2125 mJ
Maximum	14.056 mm	488.44 MPa	2.593e-003 mm/mm	10.04 mJ
Information				
Time	2. s			
Load Step	1			
Substep	857			
Iteration Number	3552			
Integration Point Results				
Display Option		Averaged		
Average Across Bodies		No		

Appendix (8) 500-420 mm
Model (C4) > Transient (C5) > Solution (C6) > Results

Object Name	*Equivalent Stress*	*Total Deformation*	*Equivalent Elastic Strain*	*Strain Energy*
State	Solved			
Scope				
Scoping Method	Geometry Selection			
Geometry	1 Face		All Bodies	
Definition				
Type	Equivalent (von-Mises) Stress	Total Deformation	Equivalent Elastic Strain	Strain Energy
By	Time			
Display Time	Last			
Calculate Time History	Yes			
Identifier				

Suppressed	No			
Integration Point Results				
Display Option	Averaged		Averaged	
Average Across Bodies	No		No	
Results				
Minimum	85.763 MPa	9.5926 mm	2.9985e-009 mm/mm	0. mJ
Maximum	154.65 MPa	9.9737 mm	8.207e-004 mm/mm	1.1513 mJ
Minimum Occurs On			2	1
Maximum Occurs On			2	
Minimum Value Over Time				
Minimum	0.16595 MPa	8.8898e-002 mm	7.83e-010 mm/mm	0. mJ
Maximum	98.292 MPa	9.9766 mm	3.5342e-009 mm/mm	0. mJ
Maximum Value Over Time				
Minimum	142.29 MPa	0.23726 mm	7.5965e-004 mm/mm	1.0568 mJ
Maximum	464.37 MPa	14.127 mm	2.4723e-003 mm/mm	8.8179 mJ
Information				
Time	2. s			
Load Step	1			
Substep	802			
Iteration Number	3356			